Hydrocracking Catalysts

For

Vacuum Gas Oil and De-Metallized Oil

Blend

by
Walid A. Al-Naeem

A Thesis Presented to the
DEANSHIP OF GRADUATE STUDIES

In Partial Fulfillment of the Requirements for
the Degree
MASTER OF SCIENCE
IN
CHEMICAL ENGINEERING
King Fahd University of Petroleum & Minerals
January, 2004

King Fahd University of Petroleum & Minerals

DHAHRAN 31261, SAUDI ARABIA

DEANSHIP OF GRADUATE STUDIES

This thesis, written by Walid A. Al-Naeem under the direction of his thesis advisor and approved by his thesis committee, has been presented to and accepted by the Dean of Graduate Studies, in partial fulfillment of the requirements for the degree of MASTER OF SCIENCE IN CHEMICAL ENGINEERING.

Thesis Committee

Prof. M. A. Al-Shalabi
(Thesis Advisor)

Prof. H. H. Redhwi
(Co-Advisor)

Prof. Mohamed B. Amin
(Department Chairman)

Prof. M. A. Al-Saleh
(Member)

Prof. Osama Ahmed Jannadi
(Dean of Graduate Studies)

Dr. D. Al-Harbi
(Member)

Dr. Shakeel Ahmed
(Member)

Date _____

DEDICATION

This work is dedicated to my parents and my family

ACKNOWLEDGMENT

I sincerely acknowledge the support provided by King Fahd University of Petroleum & Minerals (KFUPM). My deep gratitude is extended to the Center of Refining and Petroleum (CRP), KFUPM-RI for their support to make this research happen.

With deep sense of gratitude and appreciation, I would like to express my sincere thanks to my thesis advisor, Prof. Mazen A. Al- Shalabi for his inspiring guidance and excellent cooperation in supervising this research work. I am also very grateful to Prof. Mohammad A. Al-Saleh, manager of CRP, and Prof H. H. Redhwi, my co-advisor, for facilitating this research, continuous encouragement and several discussions.

I owe special thanks to Dr. Shakeel Ahmed, Research Engineer III and a member of my thesis committee for his continuous guidance and assistance during the course of my work. I would like to offer my sincere thanks to my thesis committee member Dr. D. Al-Harbi for his interest and useful comments during the committee meetings.

Finally and humbly, I offer my sincere thanks to my parents and other family members for their encouragement, supports and prayers.

(Walid A. Al-Naeem)

CONTENTS

LIST OF TABLES

LIST OF FIGURES

ABSTRACT

Name: **WALID A. AL-NAEEM**

Title: **HYDROCRACKING CATALYSTS FOR VACUUM GAS OIL AND DE-METALLIZED OIL BLEND**

Degree: **MASTER OF SCIENCE**

Major field: **CHEMICAL ENGINEERING**

Date of degree: **JANUARY 2004**

At present, the objective of Hydrocracking is to convert medium and heavy vacuum gas oil (VGO) and possibly deasphalted oil (DAO) or demetallized oil (DMO) into gasoline lines, jet fuels and diesel oils according to geographical and seasonal variations in demand. In some specific cases one can try to get Liquefied Petroleum Gas (LPG) and lubricating bases. The challenges that are posed on refiners are to employ the most suitable catalyst system that is capable of handling large hydrocarbon molecules and heavy poly-aromatic molecules. That certainly necessitates having large pores catalyst that can accommodate these large molecules and perform the desired reactions. As a result, various catalyst types were prepared throughout this work, at the same Nickel-Molybdenum metals loadings and zeolite to alumina binder compositions. This is an attempt to spot the appropriate catalyst support that can process VGO/DMO feed blend. The nature of the VGO/DMO is the real challenge in this work since not many people has done research in this area. From the literature survey, many scientists have only attempted to study catalysts performance using VGO feed not VGO/DMO feed blend, since DMO oil is only produced in very few refineries in the world one of them is in Riyadh Refinery at the Kingdom of Saudi Arabia.

Master of Science Degree

King Fahd University of Petroleum & Minerals

Dhahran, Saudi Arabia

January 2004

ملخص الرسالة

الإسم: وليدعبد اللطيف عبدالله النعيم

العنوان: المواد الحافزة للتكسير الهيدروجيني لمزيج VGO و DMO

الدرجة: ماجستير

التخصص: هندسة كيميائية

التاريخ: يناير 2004

في الوقت الحاضر, الغاية من عمليات التكسير الهيدروجيني هو تحويل الزيوت الثقيلة المتمثلة بمادتي VGO و DMO إلى مواد صالحة لأن تكون وقودا للسيارات والمحركات بحسب الحاجة الجغرافية و الفصلية لكل بلد. و في بعض الحالات الأخرى هناك قدرة على الحصول على غازات مسالة وزيوت تشحيم من خلال مادتي VGO و DMO. إن التحديات المطروحة أمام العاملين في مصافي النفط هي في توظيف المواد الحافزة المناسبة التي تستطيع التعامل بشكل فعال مع الزيوت الثقيلة وتحويلها إلى مواد خفيفة. هذا بالتأكيد يحتم إستخدام مواد حافزة تتمتع بمسامات واسعة لها القدرة على إيواء المواد الهيدروكربونية الثقيلة والقيام بالتفاعلات اللازمة. إستنادا لذلك, من خلال هذا البحث تم تحضير عدد من المواد الحافزة التي تحتوي على نفس النسب من معدني النيكل و المولبد ينم ولكن في المقابل تختلف في نوعية الزيوليت. هذا العمل إنما هو محاولة للحصول على مادة حافزة قادرة على التعامل مع مادتي VGO و DMO. إن طبيعة مادتي VGO و DMO هي التحدي الحقيقي في هذا البحث حيث أن قلة قليلة من الباحثين قاموا بالبحث في هذا المجال. من خلال البحث في ما كتب في هذا الموضوع تبين أن كثيرا من الباحثين درسوا التفاعلات الناجمة عن مادة VGO فقط وهذا يعزى إلى أن مادة DMO لا تنتج إلا في أماكن قليلة من العالم ومثالا على ذلك مصفاة الرياض الكائنة بالمملكة العربية السعودية.

درجة الماجستير

جامعة الملك فهد للبترول والمعادن

الظهران, المملكة العربية السعودية

يناير 2004

Introduction and History

1.1 Introduction

Catalysis plays a fundamental role in the evolution of industrial technology, whether looking for scientific, technical or practical point of view. The growing constraints imposed by requirements of energy saving and environmental protection will accelerate these trends. Material science is a prime driver for innovation or field of catalytic processes. Developments on material science, particularly in the last decade have yielded a broad range of porous solids, which have found application in the industrially important area of catalysis[1].

In catalytic reactions, the reactants must diffuse through the pores to reach the catalyst surface for reaction. Transport through these pores occurs mainly by diffusion and often affects or even controls the overall reaction rate of the process. The mechanisms by which diffusion may proceed are highly affected by the nature of the diffusing molecules and their interactions with the surroundings[2]. The following in-series steps can occur during a heterogeneous reaction:

(a) Diffusion of reactants to the exterior of the crystal surface (external diffusion) from the flowing stream.

(b) Diffusion of the reactants through the crystal pores (internal diffusion).

(c) Adsorption of the reactants on the crystal active sites, which is the result of the collision between the reactant molecules and active sites.

(d) Chemical reaction at the active sites.

(e) Desorption of the products.

(f) Diffusion of the products through the crystal pores to the external surface of the crystal.

(g) Transfer of the product from the external surface of the zeolite crystal to the bulk stream.

1.2 Need for Hydrocracking Catalyst

The flexibility of hydrocracking as a process for refining petroleum has resulted in its phenomenal growth during the past 15 years. Feedstocks that can be converted to lower boiling or more desirable products range from residue to naphtha. Products include such widely diverse materials such as gasoline, kerosene, middle distillates, lubricating oils, fuel oils, and various chemicals.

Commercial Hydrocracking is carried out in a single (Figure 1-1) or in two stages in series. Numerous hydrocracking catalysts have been developed and the more recent of these have exceptionally long lives even at severe operating conditions. The choice of catalysts and of the particular process scheme will depend on many factors such as feed properties, desired products properties, size of the hydrocracking unit, and various other economic considerations.

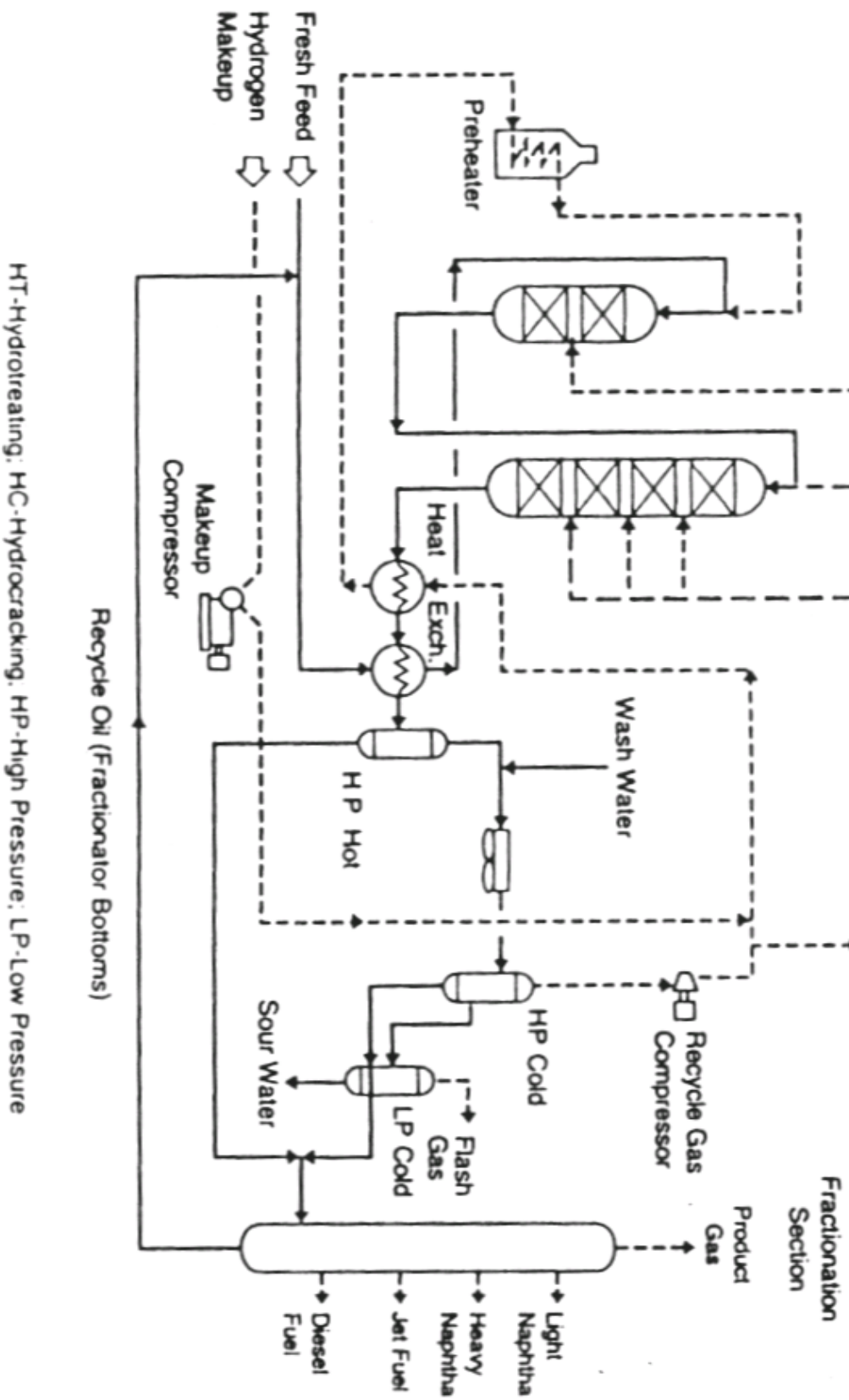

FIGURE 1-1 Single stage dual catalyst hydrocracking process with recycle oil [3]

1.3 Hydrocracking Chemistry

The reactions that occur during the Hydrocracking process take three major routes:

1. Non-catalytic thermal cleavage of C-C bonds via hydrocarbon radicals, with hydrogen addition (hydropyrolysis).
2. Monofunctional C-C bond cleavage with hydrogen addition over hydrogenation components consisting of metals (Pt, Pd, Ni, Mo, Co), oxides, or sulfides (hydrogenolysis).
3. Bifunctional C-C bond cleavage with hydrogen addition over bifunctional catalysts consisting of a hydrogenation component dispersed on a porous, acidic support. In petroleum refining, most hydrocracking reactions follow this route.

In addition to the above reactions, there are other reactions that take place during the hydrocracking processes. These reactions are called hydrotreating, which include hydro-desulfurization (HDS), hydro-denitrofication (HDN), hydro-deoxigenation (HDO), olefin hydrogenation, and partial aromatics hydrogenation.

In an attempt to better understand the reaction chemistry of the hydrocracking process for various industrial feedstocks, a series of kinetic studies were carried out for individual hydrocarbons (Model Compounds) [4, 5, 6, 7]. Kinetic models have been developed for hydroisomerization and hydrocracking of model compounds, such as n-heptane, n-octane, n-decane, and n-dodecane over zeolite or amorphous catalysts. These kinetic models can be satisfactorily described by using Langmuir-Hinshelwood models; such models are difficult to apply to petroleum fractions. The kinetic study of reactions occurring during hydrocracking of petroleum feedstocks is considerably difficult because the process involves a network of complex reactions and numerous components.

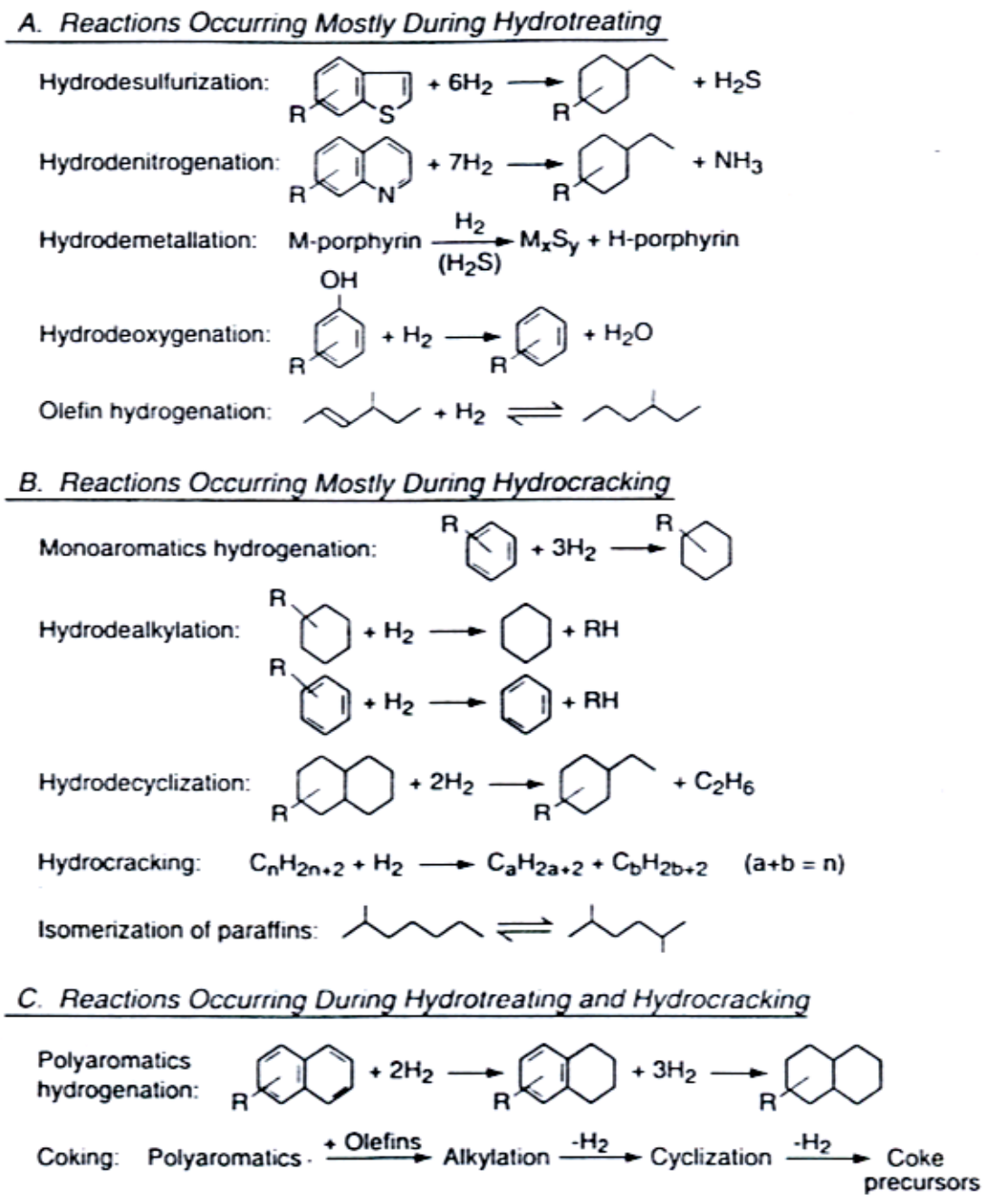

FIGURE 1-2 Typical hydrocracking reactions [3]

1.4 Need for Hydrotreating Catalyst

Hydrotreating is a catalytic process that simultaneously dehydrogenates, cracks and hydrogenates the feedstocks, removing nitrogen, sulfur, oxygen, metal and aromatic constituents. Hydrotreating is a part of a complex process to remove undesirable impurities and lower the molecular weight of heavy petroleum feed stocks in presence of hydrogen and suitable catalyst. Technique of removing sulfur is known as hydrodesulfurization. Analogous procedure for nitrogen and metal removal are hydrodenitrogenation and hydrodemetalization respectively.

1.4.1 Hydrodesulfurization Chemistry

Sulfur is the most abundant heteroatom in crude oils. Sulfur is in the form of thiols (mercaptanes), sulfides, disulfides, thiophene and thiophene derivatives.

The reactivity of thiophene decreases in the order of

Thiophene> benzothiophene>dibenzothiophene> thiophene derivatives.

Group 1 Benzothiophene with no substituents in the 2 or 7

relative K=1

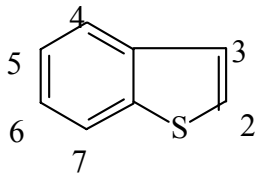

Group 2 Dibenzothiophenes with no substituents in 4 & 6

relative K=0.23

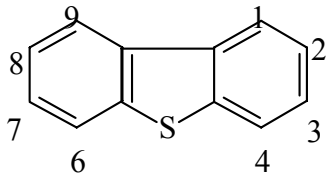

Group 3 Dibenzothiophenes with one substituent in the 4

relative K=0.08

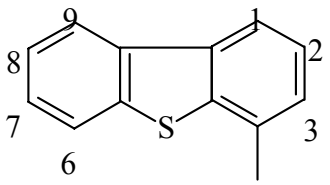

Group 4 Dibenzothiophenes with two substituents in the 4 & 6

relative K=0.028

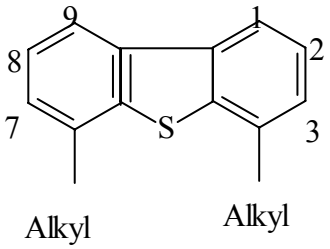

FIGURE 1-3 HDS relativity groups (Whitehurst *et al.*[8] in 1998)

1.4.1.1 The HDS Mechanism

Thiols and sulfides react to form hydrogen sulfides and hydrocarbon[9].

Sulfur Class	Reaction
Mercaptanes	$R\text{-}SH + H_2 \longrightarrow RH + H_2S$
Sulfides	$R\text{-}S\text{-}R + 2\ H_2 \longrightarrow 2\ RH + H_2S$
Disulfides	$R\text{-}S\text{-}S\text{-}R + 3H_2 \longrightarrow 2\ RH + H_2S$
Thiophene	$+\ 4\ H_2 \longrightarrow CH_3(CH_2)_2CH_3 + H_2S$
Benzothiophene	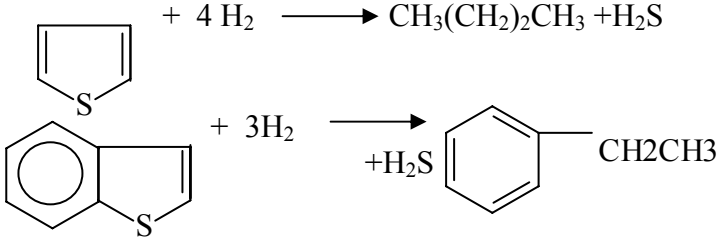

Figure 1-3 provides the structure of thiophene derivatives with their relative HDS rate constants. For highly substituted dibenzothiophene, ring dissociation prior to sulfur

extrusion is the major route to hydrocarbon production as, relative to the parent molecules, aliphatic constituents on aromatic ring carbons adjacent to the sulfur atom impose severe steric hindrance towards bonding to the catalyst surface and to the production of appropriate intermediate species.

1.4.1.2 The HDS catalytic active phase

Hydrodesulfurization is carried out over sulfides of molybdenum or tungsten, and promoted with cobalt or nickel. Hydrodesulfurization represents a number of different reactions, which are discussed in previous sections.

Molybdenum sulfide alone shows high activity for direct sulfur extrusion from sulfur compounds such as thiophene[10]. Molybdenum sulfide has graphite-like stacked lamellar structure. Molybdenum sulfide can be visualized as a sandwich of the metal between two sulfur layers. The chemical reactivity of molybdenum sulfide is attributed to molybdenum cations. Sulfur anions in the basal planes of molybdenum sulfide are more difficult to remove than anions at corners and edges. Therefore, there will be a greater number of exposed molybdenum ions at the edges and corners of the molybdenum sulfide sandwich. The sulfur atom of the sulfur-containing compound adsorbs to the exposed molybdenum ion at a sulfur vacancy through a one-point attachment. This is followed by hydrogen transfer and sulfur elimination to complete desulfurization. the addition of small amounts of the sulfides of a second metal such as cobalt or nickel enhances activity of molybdenum sulfide was established in as early as 1928 [8]. The monolayer model, attributing activity to highly dispersed molybdenum oxy-sulfides bound strongly to the support, was the first explanation offered by Lipsch and Schuit[11]and Massoth[12]. The monolayer model suggests that cobalt is located deep inside the support. This was followed by the pseudo-intercalation model which

believed that cobalt when intercalated at the edges of the layers of molybdenum sulfide created the active phase[13] .

The most widely accepted model of the HDS active phase, now, is the Co-Mo-S model postulated on the basis of Mossbaauer spectroscopic experiments by Topsoe *et. al.*[14] and Wivel[15]. The catalytically active Co-Mo-S phase consists of small stacks of molybdenum sulfide with cobalt atoms decorating the edges of the layered molybdenum sulfide structures. It may also contain cobalt ions firmly bound to the support and crystallites of Co_9S_8 which has a lower activity for HDS. Depending on the relative proportions of cobalt and molybdenum and on the pretreatment, a sulfided catalyst contains either a relatively large amount of Co_9S_8 or a large amount of the Co-Mo-S phase[16]. Notwithstanding debate on the role of the promoter, molybdenum sulfide is widely accepted as the basic active phase for HDS catalysis.

A hydrogenolysis catalytic circle during HDS over sulfided Co-Mo catalysts is proposed by Hensen *et. al.*[17], which is as shown in figure 1-4. The mechanism briefly describes the possible reaction steps involved on the local sites. It is assumed that gaseous hydrogen adsorbs dissociatively on the surface of the catalysts and that the hydrogen species consumed in the reaction are supplemented by means of spillover on the surface. Similarly, the HDS reaction mechanism over Mo/MCM41 is as shown in figure 1-5. The cleavage and formation of bonds take place between the edged Mo atom and its neighboring Mo atom. Since the strength of Mo-S bond is higher than the Co-S bond, Mo-S attached to the edged Mo atom is more difficultly cleaved than the Co-S bond. Consequently, the HDS reaction rate over Mo catalyst is lower than that over Co promoted Mo catalyst.

Nagai[18] proposed a mechanism for Ni-Mo sulfides in figure 1-6, which briefly describes the possible reaction steps involved on the local site. It was assumed that gaseous hydrogen adsorbed dissociatively on the surface of catalysts and that the hydrogen species consumed in the reaction were supplemented by means of spillover on the surface.

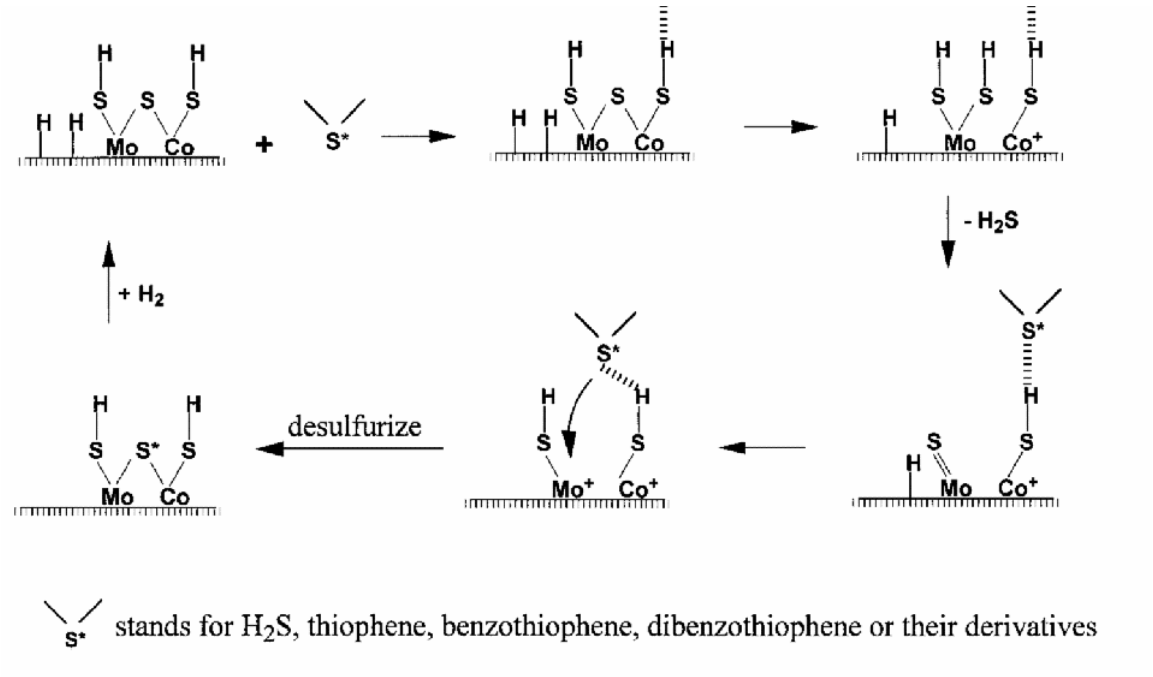

FIGURE 1-4 Mechanism of hydrodesulfurization of DBT over sulfided Co-Mo catalysts[1].

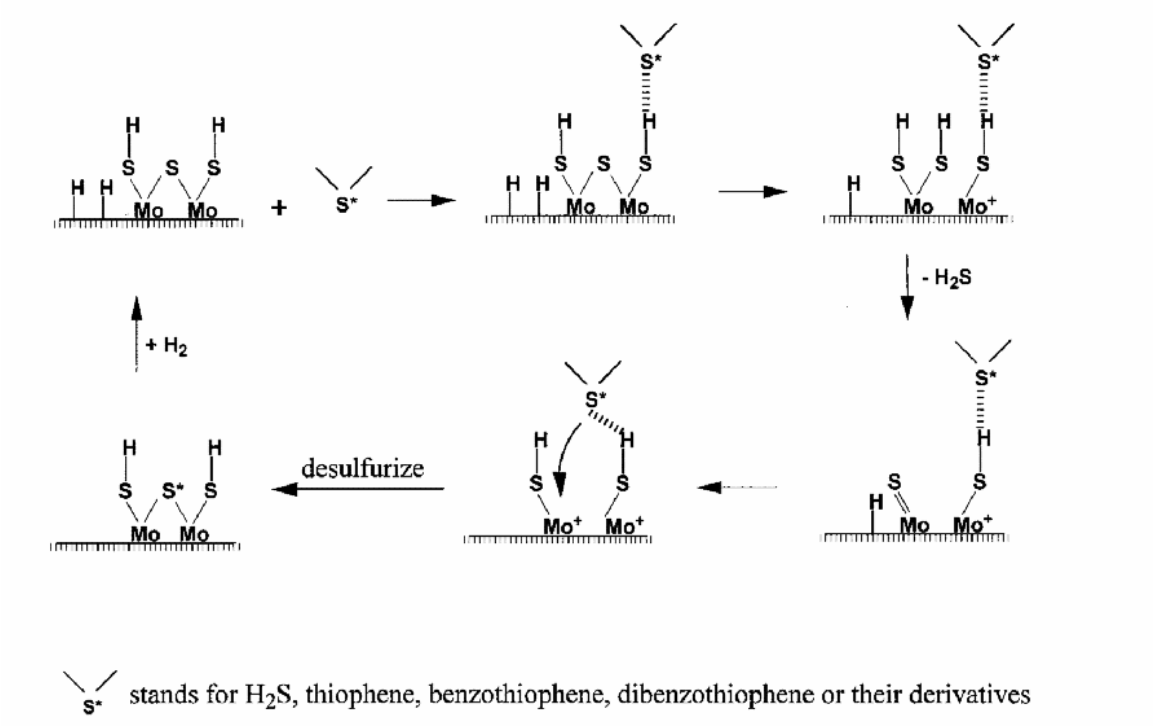

FIGURE 1-5 Mechanism of hydrodesulfurization of DBT over sulfided Mo catalysts[1].

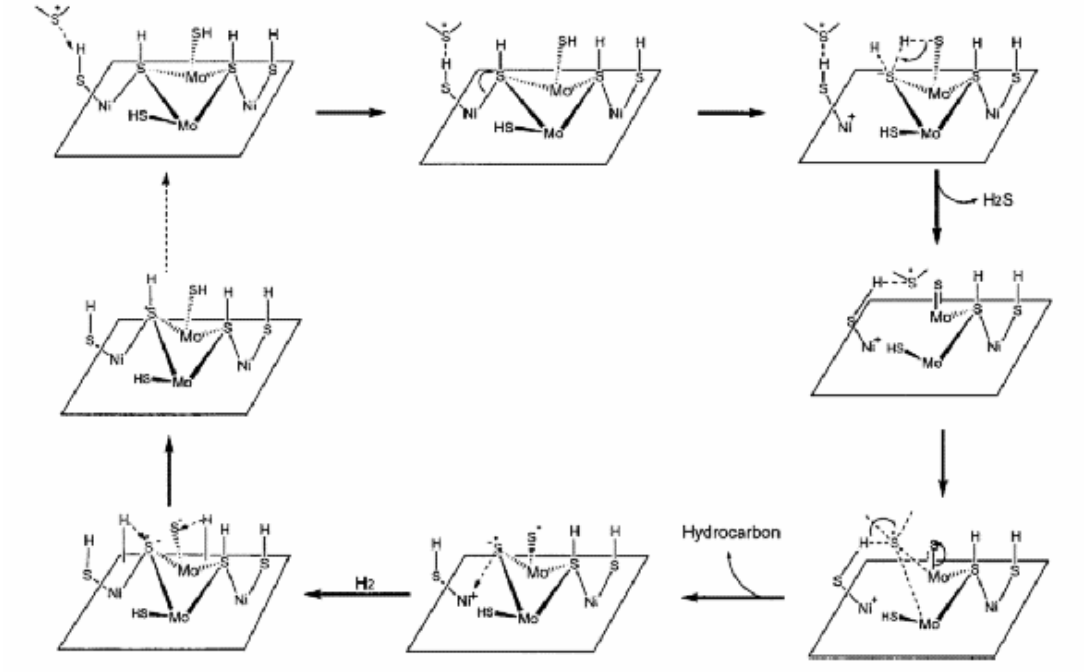

FIGURE 1-6 Mechanism of hydrodesulfurization of DBT over sulfided Ni-Mo sulfides[1].

1.5 Objective

The intent of this research work is summarized as follows:

1. Prepare hydrocracking catalysts based on four different supports that vary in terms of porosity and acidity. These supports are:
    - Ultra Stable Y (USY) zeolite.
    - β zeolite.
    - MCM-41 material.
    - Amorphous Silica Alumina (ASA).
2. Synthesize MCM-41 to be used as a support for hydrocracking catalysts since this is not commercially available.
3. Test the prepared catalysts with a heavy feed composed of vacuum gas oil (VGO) and demetallized oil (DMO) blend. The blend ratio will be 85/15 volume % of VGO and DMO respectively.
4. Compare the prepared catalysts with a reference commercial catalyst with the same feed and operating conditions.
5. Identify the catalyst that is competitive to the commercial catalyst and has potential to function in commercial hydrocracking units with the above feed blend.

Literature Survey

Most of the hydrocracking catalysts of commercial interest are dual functional in nature, consisting of both a hydrogenation-dehydrogenation component and an acidic support. The reactions catalyzed by the individual components are quite different. In specific catalysts, the relative strengths of the two components can be varied. The reactions occurring and the products formed depend critically upon the balance between these two components [3].

The acidic function of the catalyst is supplied by the support. The acidic support consists of (a) amorphous oxides (e.g. silica alumina) (b) a crystalline zeolites (mostly modified Y zeolites) plus binder (e.g. alumina) or (c) a mixture of crystalline zeolites and amorphous oxides. Moreover, among the supports are silica-alumina, silica-zirconia, silica-magnesia, alumina-boria, silica-titania, acid-treated clays, acidic metal phosphates, alumina, and other such solid acids.

The metals providing the hydrogenation-dehydrogenation functions can be noble metals (palladium, platinum), or non-noble metal sulfides from group VIA (molybdenum, tungsten) and group VIIIA (cobalt, nickel). These metals catalyze the hydrogenation of the feedstock, making it more reactive for cracking and heteroatom removal, as well as reducing the coking rate [19]. They also initiate the cracking by forming a reactive olefin intermediate via dehydrogenation.

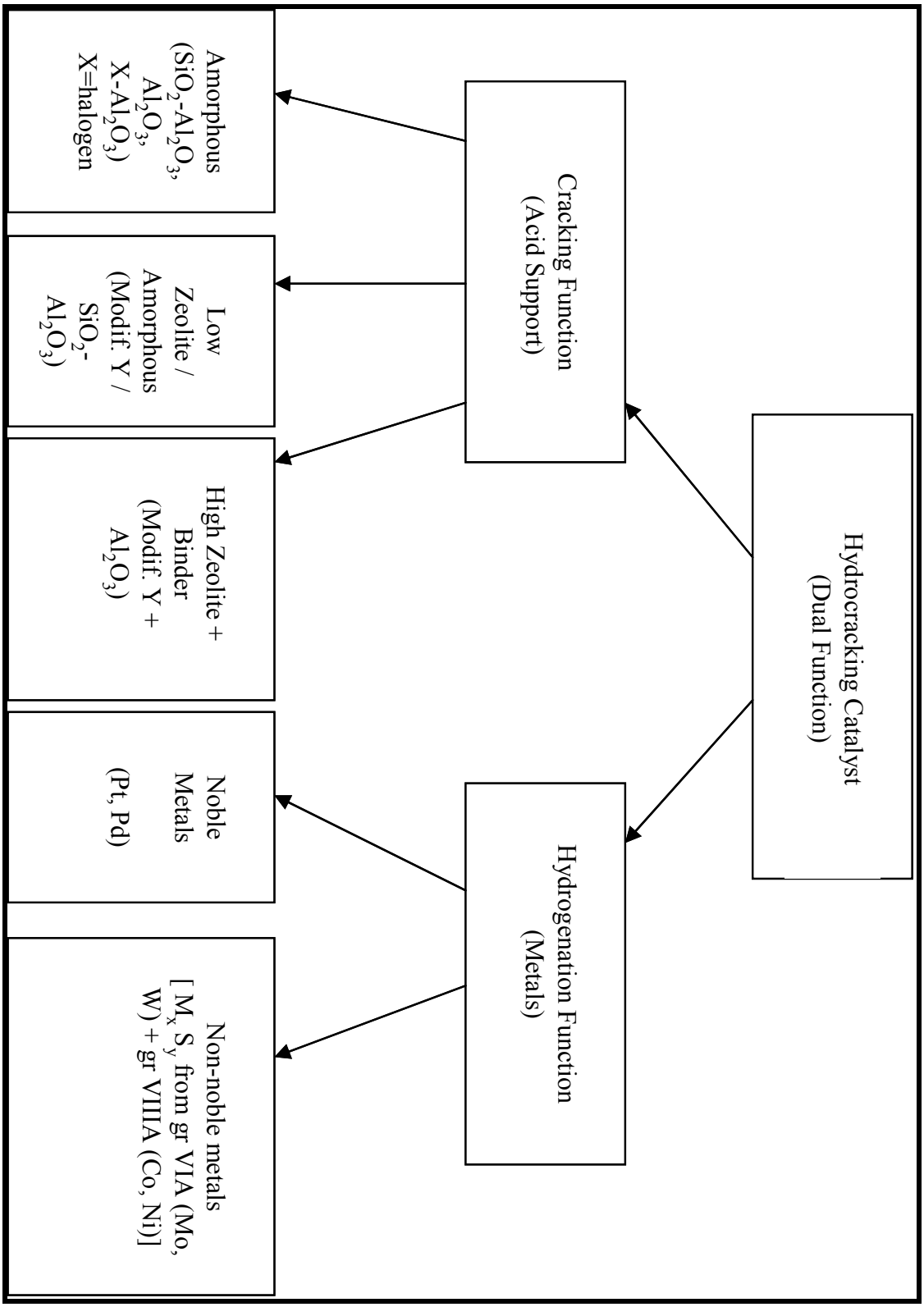

FIGURE 2-1 Composition of Hydrocracking Catalysts [3]

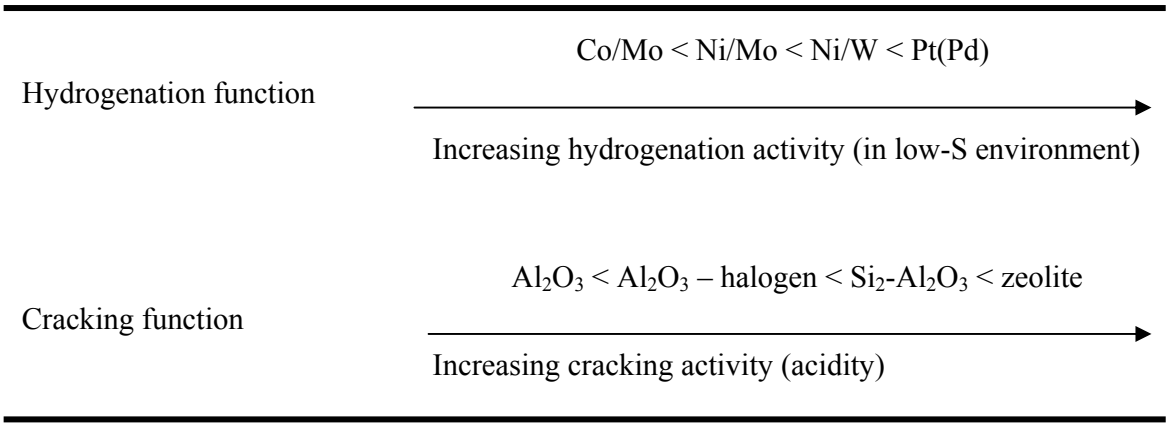

FIGURE 2-2 Strength of Hydrogenation and Cracking Functions in Bi-functional Catalysts [3]

Since hydrocracking of industrial feedstocks is to be carried in presence of hydrogen sulfide and organic sulfur compounds, the metal site has to be in a metal sulfide form of the VIA group promoted by a nickel or cobalt sulfide. Figure 2-3 presents the results obtained when toluene is used as a model molecule in the presence of hydrogen sulfide. It can be inferred from this figure that for every couple of sulfides, the activity passes through a maximum when the atomic ratio $\rho \approx 0.25$ [20]. The atomic ratio is the Ni or Co wt-% by the total wt-% of Ni (or Co) & Mo (or W). *Gary et al.* has found out that the addition of Ni and more Mo to the support had surprisingly little effect on catalyst activity [21].

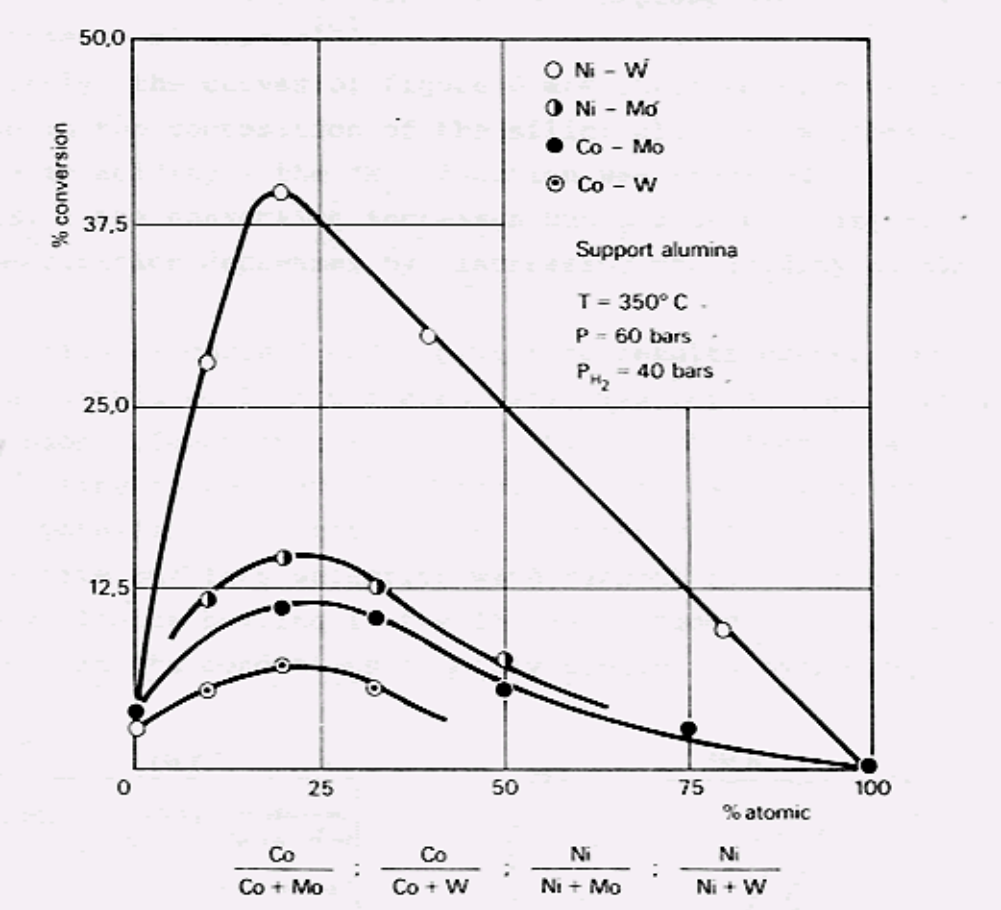

FIGURE 2-3 Optimum metal pairs atomic ratio [20]

The ratio between the catalyst's cracking function and hydrogenation function can be adjusted in order to optimize activity and selectivity. For hydrocracking catalysts to be effective, there should be a rapid molecular transfer between the acid sites and hydrogenation sites in order to avoid undesirable secondary reactions. Rapid molecular transfer can be achieved by having the hydrogenation sites located in the proximity of the cracking acid sites [20].

Khorasheh et al. [21] analyzed the gas oil and found evidence for sequential hydrogenation and cracking to yield more 4- and 6-carbon products. At high temperatures, the thermal reactions would also compete with the catalytic reactions for the local supply of dissolved

hydrogen. Moreover, he and his colleagues have conducted experimental work on hydrocracking of residues from Alberta Bitumens. They concluded that Ni-Mo catalyst was the most active material for most indices of performance, e.g. hydrodesulfurization (HDS), residue conversion, etc. They observed that Ni-Mo catalyst had very significant effect to boost the yield of gas oil around 10% higher than Mo on γ-alumina catalyst. This finding signifies the importance of Nickel promoter to achieve more activity and selectivity towards gas oil.

Shakeel et al. [19] had prepared zeolite based hydrocracking catalysts on two different supports by mixing the steam modified Y-zeolite with commercial γ-alumina CP-100 in ratios of 50:50 and 30:70 respectively. On these mixtures of zeolite and alumina, Ni-Mo and Ni-W were sequentially impregnated. It was observed that catalysts containing Molybdenum have higher surface area as compared with those having tungsten as base metal. This could be explained on the basis of ionic radii of these metals. The other major finding that was observed is that Ni-Mo catalysts showed relatively better HDS activity as compared with Ni-W catalysts. Moreover, the Ni-Mo catalyst on the 30:70 zeolite to γ-alumina ratio showed a slightly higher VGO conversion and gas oil production than the 50:50 ratio support. Besides, having more zeolite means more acidity. Too high an acidity, results in too strong an adsorption of the heaviest species and then in a formation of coke deposits [20].

The above finding is in-line with *Franck et al.* [20] who found that Ni-Mo has relatively similar activity to Ni-W and at the same time is a lot cheaper and is generally selected for commercial catalyst production.

A. Hassan et al. [22] have studied the effects of the metals co-impregnation and successive impregnation on various β and USY zeolite based catalysts. One of their findings is that the co-impregnation of Ni-W on the various supports showed higher surface area, m2/g, and pore volume, cm3/g, than the successive impregnation.

M. A. Ali et al. [23] have studied various support compositions composed of USY zeolite, β zeolite, and Amorphous Silica Alumina (ASA). They found that the β-zeolite based catalysts produced higher amounts of naphtha and lower amounts of kerosene and gas oil fractions while USY based catalysts produced higher amounts of gas oil and lower amounts of kerosene and naphtha.

In light of the above, it is apparent that there are numerous support alternatives that can be used for preparing hydrocracking catalysts. These supports vary in terms of pore sizes and acidity. ASA has the biggest pores which makes it attractive support for heavy hydrocarbon molecules. Whereas, β and USY zeolites, have more acidity and products selectivity in terms of gas oil and naphtha. Additionally, MCM-41 material which was recently discovered by Mobil researchers became an attractive alternative in the area of hydrodesulfurization of heavy petroleum distillates. This is due to the fact that the size of the pores in these materials can be varied according to the synthesis procedure between 20 to 100 A^0 [24]. MCM-41 also has mild surface acidity compared to β and USY zeolites. The mesoporous feature of this zeolite can be used to accommodate very large hydrocarbon molecules such VGO and DMO with little fear of mouth-plugging of the catalyst pores.

In addition, the research institute (RI) of King Fahd University of petroleum and minerals (KFUPM) has successfully attempted to synthesize MCM-41 material. This material was

used as a catalyst support for several metals and tested against VGO feed. Complete details can be found in *R. Ahmed Khan* master thesis [1].

In conclusion, scientists are continually conducting research to optimize the zeolite porosity to accommodate large molecules. It has been always the interest of researchers to come up with zeolites that have mesoporous property especially in the area of Hydrocracking. This is obvious from the research that was conducted by *Y. Hashimoto et al.* [25] where they tried to modify a commercial zeolite with titanium sulfate to generate a zeolite with mild acidity, mesoporous property, and high hydrogenation activity.

3

Experimental Approach

3.1 Experimental Design

This section describes the design of the experiments that will be conducted throughout this work. Table 3-1 specifies all variables and conditions that will be taken into consideration during this study. Table 3-2 shows the properties of the feedstock that will be used to test the catalyst. In addition, figure 3-1 shows the flowchart and the scenario of the experimental work of this study. Table 3-1, table 3-2 and figure 3-1 represent the domain and scope of this research work.

TABLE 3-1 Experimental Design

		Catalyst Systems				
Catalyst Preparation	-	**Commercial**	**NiMo-MCM-41**	**NiMo-USY**	**NiMo-β**	**NiMo-ASA**
γ-alumina binder, wt%			70	70	70	70
Support, wt%			30	30	30	30
NiO, wt%			2.5	2.5	2.5	2.5
MoO3, wt%			12	12	12	12
Ni, wt%			2	2	2	2
Mo, wt%			8	8	8	8
Atomic Ratio			0.2	0.2	0.2	0.2
Catalyst Characterization						
Surface Area, m^2/g			324	300	313	186
Pore Vol., cm^3/g			0.4	0.35	0.41	0.33
Pore Size, Angstrom			25	23	26	36
Acidity, mmol/gm			0.33	0.59	0.56	0.5
Catalyst Evaluation						
Batch Reactor	-	-				
No. of Runs		5	1	1	1	1
Temperatures, deg. C		410	410	410	410	410
Pressures, kg/cm^2		150	150	150	150	150
Feed weight, g		100	100	100	100	100
Catalyst weight, g		3	3	3	3	3

TABLE 3-2 Feedstock Definition

Feedstock Properties	VGO	DMO	VGO/DMO 85% / 15%
Specific Gravity	0.92-0.93	0.96-0.97	0.93-0.94
Total Nitrogen, wt ppm	700-900	1300-2100	1100-1200
Total Sulfur, wt%	2-3	3-3.5	2.6-2.8
ASTM Distillation, D2887			
5%, ^{0}C	279	402	
50%, max ^{0}C	472	596	495
90%, max ^{0}C	543	678	615
Ni + V wt. ppm	< 1	8.0-13.5	2-3

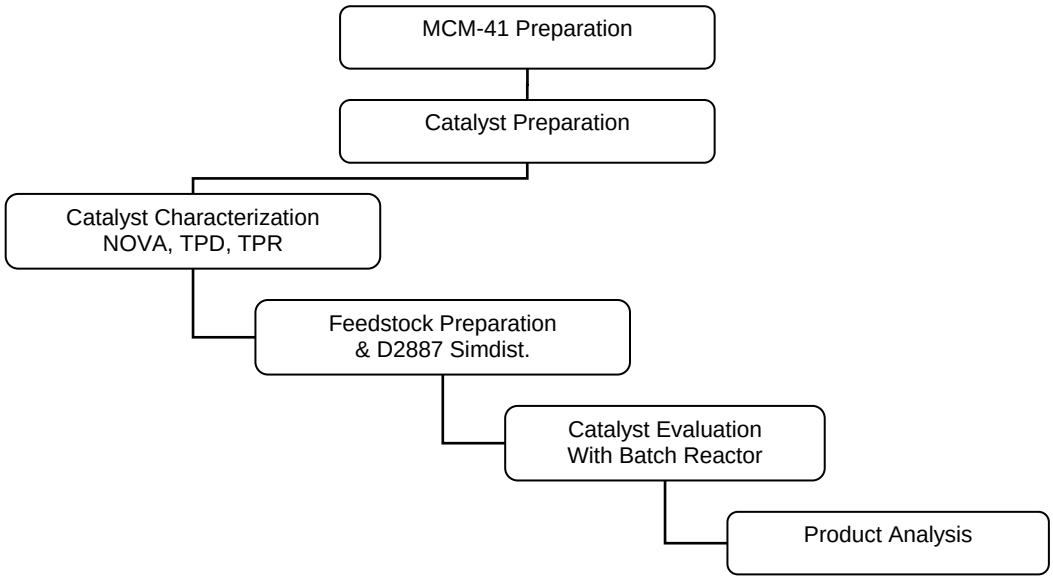

FIGURE 3-1 Experimental Flow Chart

3.2 Synthesis of MCM-41

3.2.1 Synthesis

Synthesis of MCM41 based molecular sieves is done in alkaline medium. One of the main steps in preparing molecular sieves is preparation of the gel i.e. mixture of inorganic species, template and metal. A number of parameters in a gel preparation process can affect the resultant phases. These include pH, molar ratio of reactants, aging, stirring, addition sequence of reactants, etc [26].

After the preparation of the homogeneous gel, it needs to be transferred to an oven that is maintained at 370^{o}K temperature for 4 days. During these 4 days pH is maintained at 10.5. Upon the completion of the 4 days, the mixture will be separated normally by filtration with extensive washing in order to remove any unwanted species such as sodium ions, chloride, nitrate etc.

3.2.2 Drying

After the solution is filtered we will get a cake, which should be dried in an oven at 370^{o}K at atmospheric pressure, overnight. Prolonged drying of MCM-41 based materials might result in partial removal of the template molecules.

3.2.3 Template Removal

Template removal will be done by calcination. The procedure for calcination of as-synthesized sample is as follows:

1. Temperature is increased from room temperature to 120 ^{0}C at 10 ^{0}C /min and maintained for 30 minutes.
2. Temperature is increased from 120 ^{0}C to 250 ^{0}C at 2 ^{0}C /min and maintained for 30 minutes.

3. Temperature is increased from 250 ^{0}C to 550 ^{0}C at 10^{0}C /min and maintained for 6 hours.

3.2.4 Ion Exchange

To activate MCM-41, it should be ion exchanged with 0.1 M ammonium nitrate solution. Ion exchange process is as follows:

1. Add catalyst to ammonium nitrate solution in a beaker and solution is stirred continuously. For every 10 gm of catalyst, 150 ml of ammonium nitrate is used.
2. Change ammonium nitrate solution after every 24 hours. Keep stirring.
3. After 3 days filter the sample and dry it in the oven overnight.
4. Calcine the sample with temperature program similar to template removal except that temperature will be decreased to 500 ^{0}C only instead of 550 ^{0}C.

3.3 Characterization of MCM-41

3.3.1 X-Ray Diffraction

The various samples of MCM41, being crystalline, have characteristic X-ray powder diffraction patterns, which are used for their identification. X ray diffraction patterns of as-synthesized and calcined mesoporous samples show characteristic peaks of 100, 110 and 210. X-ray diffraction patterns from typical catalyst powders give information about interplanar lattice spacing through Bragg's equation.

$$2*d*\sin\theta=n\lambda$$

Where

d is interplanar spacing.

Θ is angle between lattice plane and both the incident and diffracted X ray beam.

n is order of Bragg's reflection.

Λ is the wavelength of the X-rays.

Combined with fact that intensities of diffraction lines depend on the arrangement of atoms in unit cell of crystal lattice, this information in principle provides an almost unique description of nature of the crystalline phases present. However in practice the interpretation of diffraction patterns may not always be trivial as catalysts often contain many different phases. The equipment is used to measure the crystalline pattern of the synthesized sample by step measurement method. The diffraction pattern is generated by a 2-theta/ theta scanning diffractometer.

The operating conditions of XRD analysis is:

Cu broad focus tube at 40 Kv and 30ma.

Scanning speed and interval of data collection was 0.01 degree two theta/sec.

Angle scanned: 1 to 10 two theta.

3.3.2 XRD Setup

X ray Diffraction (XRD) experiments were done on system supplied by *Jeol Ltd.*, (model JDX-3530) employing a multicomputer system, 32-bit engineering workstation as a core of the system, for improving the data processing capability. The multi-task and multi-window allows parallel execution of measurement and data processing, and serial execution of measurement, data processing and result output. Measured results are displaced on the high-resolution color CRT for easy observation of measurement results. Outline of diffraction optics is given in figure comprising of arrangement of X ray source, X ray source side soller slit, divergence slit, receiving slit, scattering slit, X ray detector. A picture of XRD setup is given in figure 3-3.

FIGURE 3-3 XRD Setup

3.4 Catalyst Preparation

Hydrocracking catalysts can be prepared by variety of methods. Although there is a relationship between the catalyst formulation, preparation procedure, and catalytic properties, the details of that relationship are not always well understood due to the complex nature of catalytic systems [3].

3.4.1 Selection of Catalyst Supports

Shakeel et al.[29] observed in his study that Ni-Mo catalysts had relatively better HDS activity as compared with Ni-W catalysts. Moreover, the Ni-Mo catalyst on the 30:70 zeolite to γ-alumina ratio showed a slightly higher VGO conversion and gas oil production than the 50:50 ratio support. Besides, having more zeolite means more acidity. Too high an acidity, results in too strong an adsorption of the heaviest species and then in a formation of coke deposits [20].

In addition, it is apparent that there are numerous support alternatives that can be used for preparing hydrocracking catalysts. These supports vary in terms of pore sizes and acidity. ASA has the biggest pores which makes it attractive support for heavy hydrocarbon molecules. Whereas, β and USY zeolites, have more acidity and products selectivity in terms of gas oil and naphtha. Also, MCM-41 which was recently discovered by Mobil researchers became an attractive alternative in the area of hydrodesulfurization of heavy petroleum distillates.

In light of the above, it was decided to use the above mentioned supports as basis of our research work. Moreover, 30:70 support to γ-alumina binder ratio as catalyst supports will be used for all of the catalyst preparations trials that will be carried out. Four supports will be mixed with the γ-alumina binder and will be used throughout this work. These supports are USY, β, MCM-41, and amorphous silica alumina.

3.4.2 Selection of Impregnated Metals

In reference to figure 2-3, it can be inferred that for every couple of sulfides, the activity passes through a maximum when the atomic ratio $\rho \approx 0.20$ [15]. The atomic ratio is the Ni or Co wt-% by the total wt-% of Ni (or Co) & Mo (or W). *Gary et al.* has found out that the addition of Ni and more Mo to the support had surprisingly little effect on catalyst activity [21]. Moreover, Khorasheh and his colleagues [21] have conducted experimental work on hydrocracking of residues from Alberta Bitumens. They concluded that Ni-Mo catalyst was the most active material for most indices of performance, e.g. hydrodesulfurization (HDS), residue conversion, etc. They observed that Ni-Mo catalyst had very significant effect to boost the yield of gas oil around 10% higher than Mo on γ-alumina catalyst. This finding signifies the importance of Nickel promoter to achieve more activity and selectivity towards

gas oil. The above findings have led to the decision to use atomic ratio (ρ) of 0.20 by impregnating 2.0 wt% Nickel and 8.0 wt% Molybdenum.

3.4.3 Preparation Technique

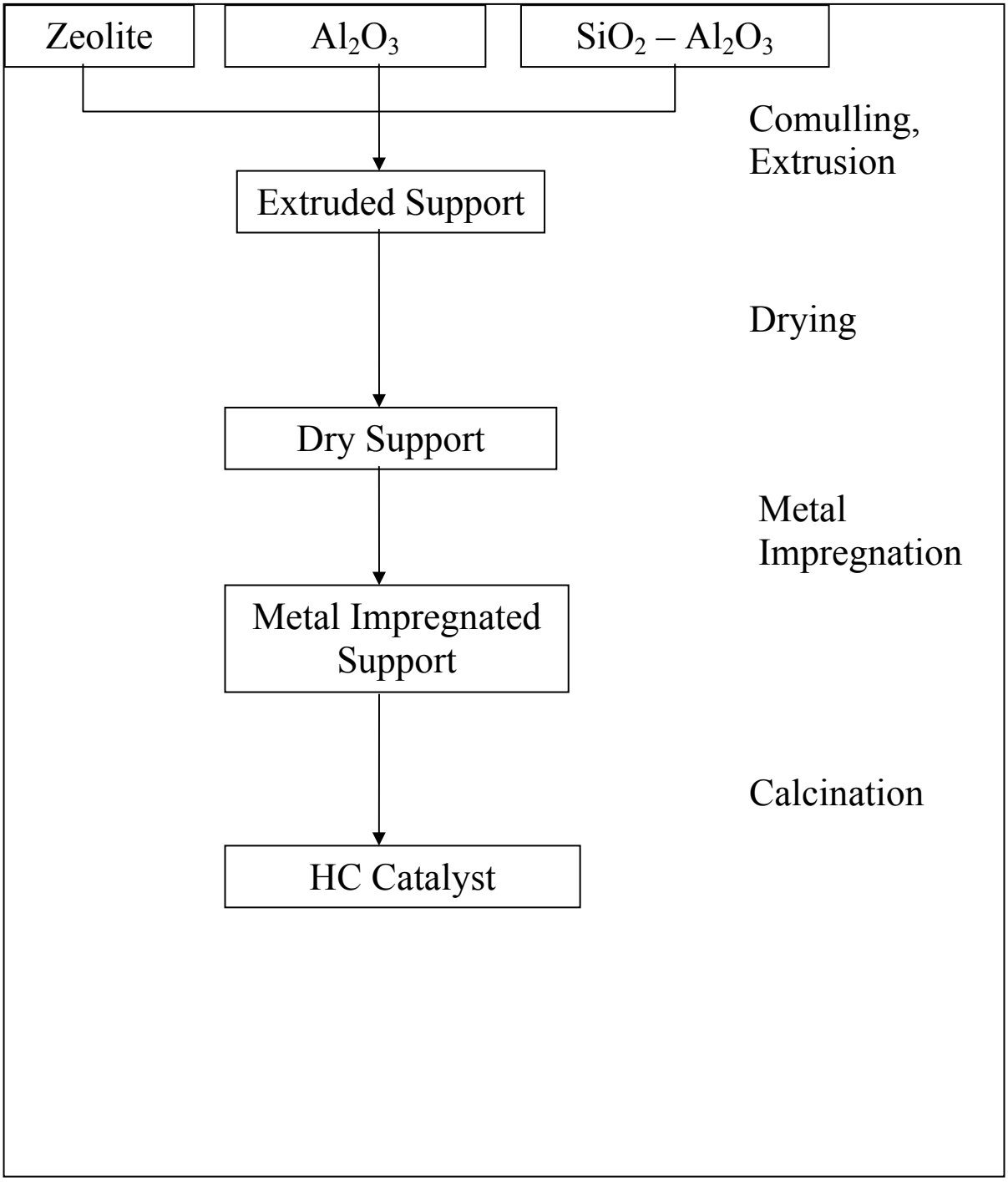

FIGURE 3-4 Flow diagram for a typical Hydrocracking Catalyst Preparation using Comulling and Impregnation [3]

1. Comulling and Extrusion—30-wt% of the support will be physically mixed with 70-wt% alumina binder until homogeneity is achieved. Distilled water will be added to this homogenous mixture to form dough which will be then extruded using a syringe. The metal support can be either zeolites or amorphous.
2. Drying—the extruded catalyst will be dried overnight in the oven at 110 ^{0}C to reduce the moisture level on the catalyst support.
3. Calcination—this step is applied before and after metal impregnation of the catalyst formed. This step is to eliminate water, volatile and unstable cations or anions as well as organic compounds. This step is crucial since it determines the physical and the catalytic properties of the catalyst. Moreover, surface area, pore size distribution, stability, attrition resistance, crushing resistance, as well as catalytic activity are affected by the drying and calcinations conditions. Excessive calcinations conditions may result in structural collapse of the support, loss in surface area, loss of smaller pores, and destruction of active sites. The procedure for calcination of prepared samples is as follows:
    1. Temperature is increased from room temperature to 120 ^{0}C at 10 ^{0}C /min and maintained for 30 minutes.
    2. Temperature is increased from 120 ^{0}C to 250 ^{0}C at 2 ^{0}C /min and maintained for 30 minutes.
    3. Temperature is increased from 250 ^{0}C to 550 ^{0}C at 10^{0}C /min and maintained for 4 hours.
4. Impregnation—this step is to incorporate a metal component into a performed catalyst support. This method is the most common method for manufacturing

hydrocracking catalysts. In addition, several impregnation methods can be applied: (a) Dipping (b) Incipient Wetness (c) Evaporative Impregnation. The last two methods are the common ones for manufacturing industrial hydrocracking catalysts[27]. In our work, we will use the incipient method.

3.5 Catalyst Characterization

3.5.1 Gas Sorption Analyzer (NOVA)

Accurate sorption measurements of a gas on solids surface will be carried out in NOVA-1200 system supplied by *Quanta chrome Corporation*. A schematic flow diagram of apparatus is given. NOVA is an acronym for NO VOID ANALYSIS which measure multipoint BET surface area, single point BET surface area, total pore volume, average pore radius, sample volume, density, twenty five point adsorption isotherms, twenty five points desorption isotherms.

3.5.1.1 NOVA Operational Procedure

Procedure for pretreatment and subsequent experiment is as follows:

0.25 gm of catalyst sample is weighed and is placed in a sample cell assembly which is heated to 90^{o}C in 10 min and temperature is maintained for 1 hr then the temperature is raised to 350^{o}C and is maintained for 2 hr. Adsorbate source used is Nitrogen as it serves to be most common adsorbate source and well characterized one. All measurements are done as it is programmed (fully automated).

Mesopore size calculations are done assuming cylindrical pore geometry using the Kelvin equation.

$$r_k = \frac{-2\gamma V_m}{RT \ln(P/P_0)}$$

Where γ is the surface tension of nitrogen at its boiling point (8.85 ergs/cm^2 at 77K).

V_m is molar volume of liquid nitrogen (34.65cm^3/mol).

R is gas constant (8.314x10^{7}ergs/deg mol).

T is boiling point of nitrogen.

P/P_0 is relative pressure of nitrogen.

r_k is the Kelvin radius of the pore.

Kelvin radius r_K is the radius of pore in which condensation occurs at a relative pressure of P/P_o. Since prior to condensation some adsorption has taken place on the walls of the pore r_K is not actual pore radius. Actual pore radius is given by

$r_p = r_K + t$

t is the thickness of the adsorbed layer.

t is given by

$$t(A^0) = 3.54\left[\frac{5}{2.303\log(P_0/P)}\right]^{1/3}$$

Total pore volume is derived from the amount of vapor adsorbed at a relative pressure by assuming that pores are filled with liquid adsorbate. Most common method in determining the total surface area of the catalyst that is developed by Braunner, Emmet and Teller (called BET method).

BET equation is given by

$$\frac{P}{V_a(P_o - P)} = \frac{1}{V_m C} + \frac{c-1}{V_m C}\left(\frac{P}{P_o}\right)$$

V_a is the quantity of gas adsorbed at a relative pressure P/P_0.

V_m is the quantity of adsorbate constituting a monolayer of surface coverage.

C (BET constant) is related to energy of adsorption in the first adsorbed layer and indicates the magnitude of the adsorbate /adsorbent interactions. In this technique, amount of nitrogen adsorbed at equilibrium at its normal boiling point (-195.8^{o}C) is measured over a range of partial pressure below 1 atmosphere. The volume of gas adsorbed is calculated by measuring pressure variation resulting from adsorption of known volume of N_2 gas by test sample.

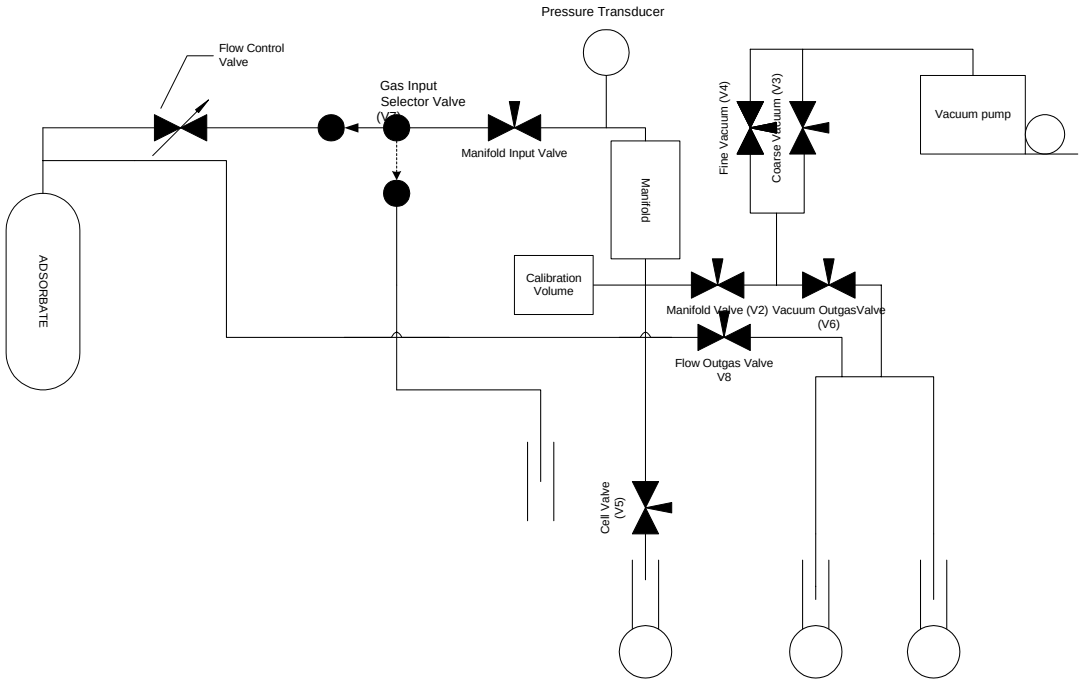

FIGURE 3-5 Schematic flow diagram of Nova sorption analyzer

3.5.2 Temperature Programmed Reduction (TPR)

TPR is used to monitor metal support interactions. It also provides useful information about the temperatures needed for the complete reduction of a catalyst. For bimetallic catalysts, TPR patterns often indicate whether two components are mixed or not.

Reduction is an inevitable step in the preparation of metallic catalysts. The reduction of metal oxide MO_n by H_2 is described by the equation.

$$MO_n + nH_2 \longrightarrow M + n\,H_2O$$

Reaction of metal oxides by hydrogen, start with dissociative adsorption of H_2, which is a much more difficult process on oxides than on metals. Rate expression for the reduction reaction under conditions where the reverse reaction from metal to oxide can be ignored, is

$$-\frac{d[MO_n]}{dt} = k_{red}[H_2]^p f([MO_n])$$

In which

[MO_n] is the concentration of metal oxide.

[H_2] is the concentration of hydrogen gas.

k_{red} is the rate constant of the reduction reaction.

p is the order of the reaction in hydrogen gas.

f is the function, which describes the dependence of the rate of reduction on the concentration of metal oxide.

t is the time

3.5.2.1 Setup of TPR

Temperature programmed reduction (TPR) experiments were carried out in a system supplied by *Ohkura Riken Co. Ltd.*, (model TP-200). A schematic flow diagram of apparatus

is given in figure 3-6. The equipment is developed to enable user to obtain data related to reduction and sulfiding characteristics of metal oxides or catalysts containing metals.

3.5.2.2 Operational Procedure for TPR

The operational procedure can be divided into two parts:

3.5.2.2.1 Pretreatment

150 mg of catalyst sample (particle size 600-212 μm) is weighed and placed in a quartz tube (8 mm O.D.) reactor in such a way that it is close to the thermocouple with the help of quartz wool plugs. Temperature is raised to 400^{o} C at a rate of 10^{o} C for 2 hr, then cooled to ambient temperature. Air is purged by flowing dry air (22 cm^3/min) for 30 min at ambient temperature.

3.5.2.2.2 Reduction

Gas mixture used for reduction was 5 % H_2 in Argon at a flow rate of 30 cm^3/min. Temperature of the reactor is programmed to increase linearly from room temperature to 1030^{o}C at a heating rate of 10^{o}C/min and then retained at this temperature for 15 minutes. A 5A molecular sieve is used to trap the water formed either by reduction or from dehydration process. The hydrogen concentration is determined with a thermal conductivity detector (TCD). The temperature of the catalyst and the TCD current response is monitored and recorded continuously on a personal computer (NEC Model PC9821-Xe10).

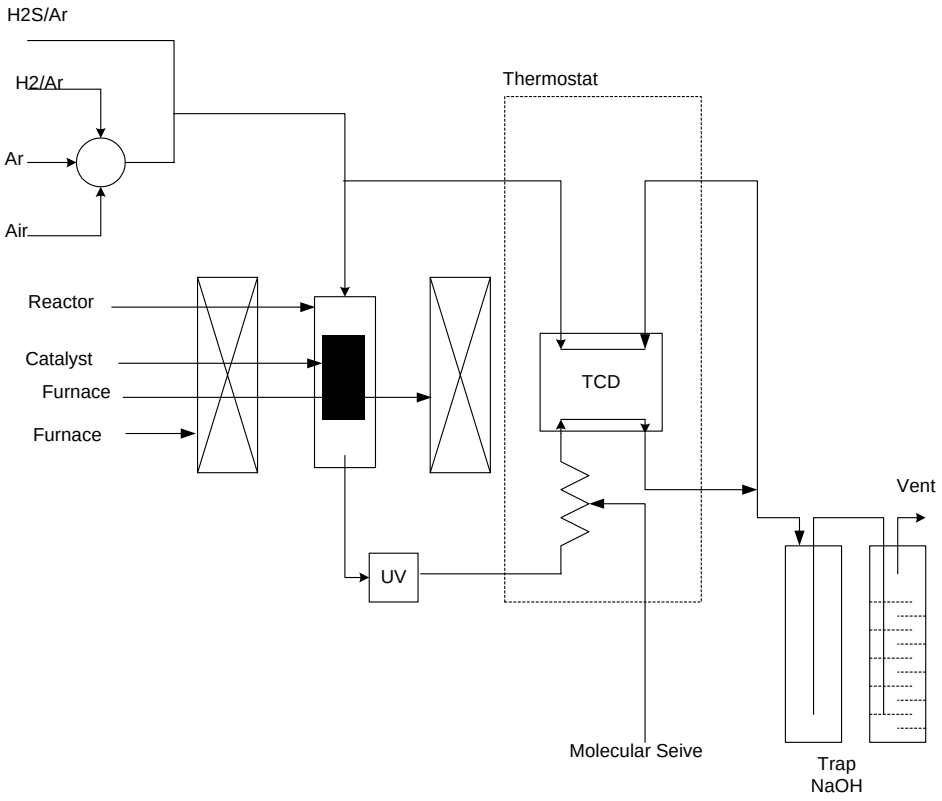

FIGURE 3-6 Temperature programmed reduction apparatus

3.6 Catalyst Evaluation

3.6.1 Batch Autoclave Reactor

Batch autoclave reactor is suitable for studying high exothermic hydrocracking reactions. With advantage of excellent fluid contacts, isothermicity within reactor, simple to operate, it also provides information about cracking activity of catalyst and kinetic data that can be used to determine the intrinsic reaction order and activation energy.

The size of autoclave reactor is 300 ml. The reactor is housed in furnace. There is programmed control system for controlling temperature, speed of the stirrer. Pressure and flows is controlled manually. A schematic flow diagram of this system is shown in figure 3-7.

In addition, the feed that was used to evaluate the various prepared catalysts along with the reference catalyst is a blend of VGO and DMO at 85-% to 15-% respectively.

It has to be born in mind that the commercial catalyst that is used as our reference in this work is very well known catalyst and used broadly in many refineries that process very heavy Hydrocracker feedstock since many years. Our attempt is to prepare a catalyst that can relatively compete or have close catalytic properties to this broadly used catalyst. Having catalyst with similar features to the reference catalyst is a very challenging task and requires very extensive work and number of years to accomplish.

3.6.2 Batch Reactor Operational Procedure

An amount of 100 gm of feed and 3 gm of sulfided catalyst is loaded inside the reactor. Reactant and catalyst is purged in N_2 and H_2 and leak is checked by H_2 detector. The system is allowed to react for 3 ½ hours. System is allowed to cool down to room temperature and then it is purged by N_2 after removing the product gas sample. Liquid product is analyzed by simulated distillation techniques.

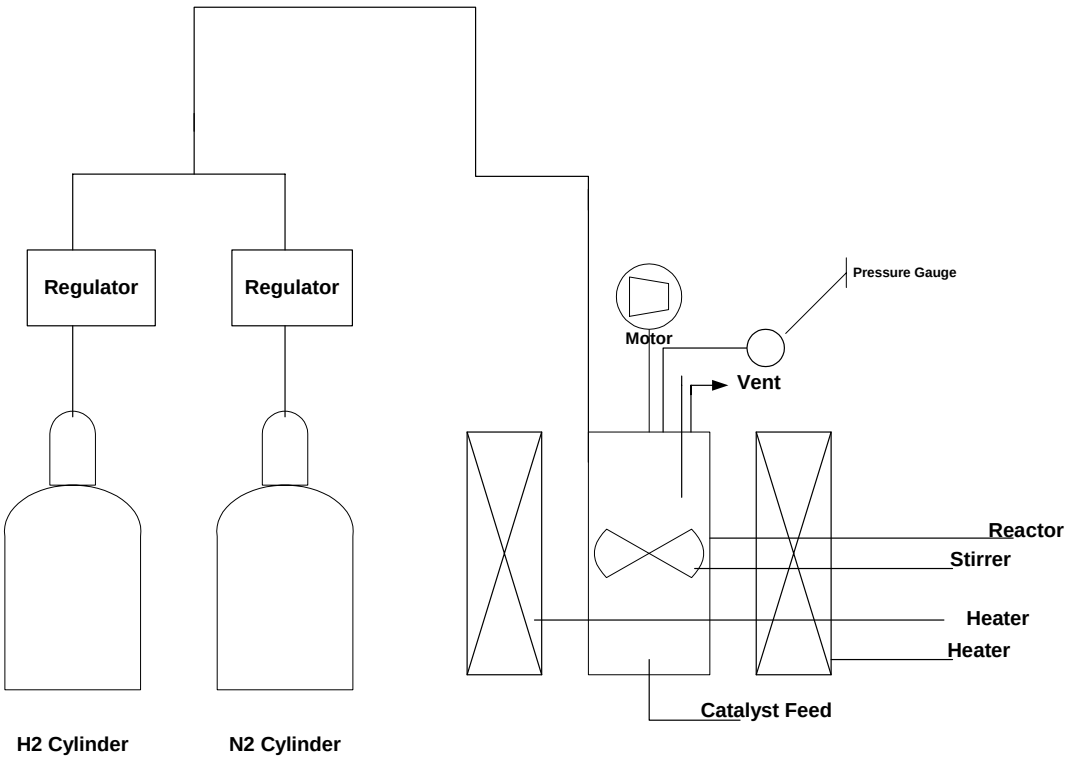

FIGURE 3-7 Experimental setup of batch autoclave reactor

Results and Discussion

4.1 MCM-41 X-Ray Diffraction (XRD)

Figure 4-2 presents the typical powder diffractogram of calcined MCM-41 sample. From figure 4-3, It can be seen that our prepared MCM-41 sample shows similar XRD pattern with well-defined 100, 110, and 210 reflection peaks. After synthesizing MCM41 sample, the measurements were carried out in order to confirm that the mesoporous material has been crystallized as MCM41.

From d_{100}, calculation of parameter a_o in a hexagonal lattice was done by using the formula

$$a_o = 2*d_{100}/\sqrt{3}$$

As shown in figure 4-1, unit cell parameter a_o and d_{100} is clear.

Framework thickness D can be calculated from the formula given below

$$D = a - 2*r$$

Where r is pore radius.

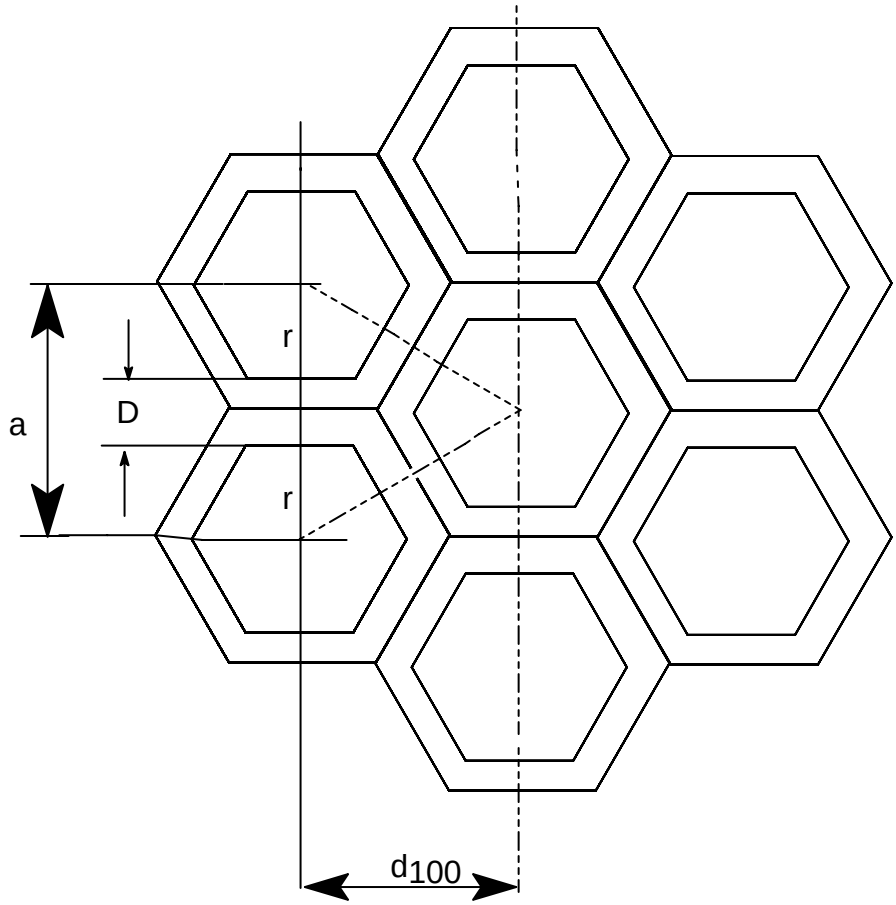

FIGURE 4-1 showing d_{100}, a (unit cell size), D (Framework thickness), r (radius of the pore) and 2*r represents the pore size.

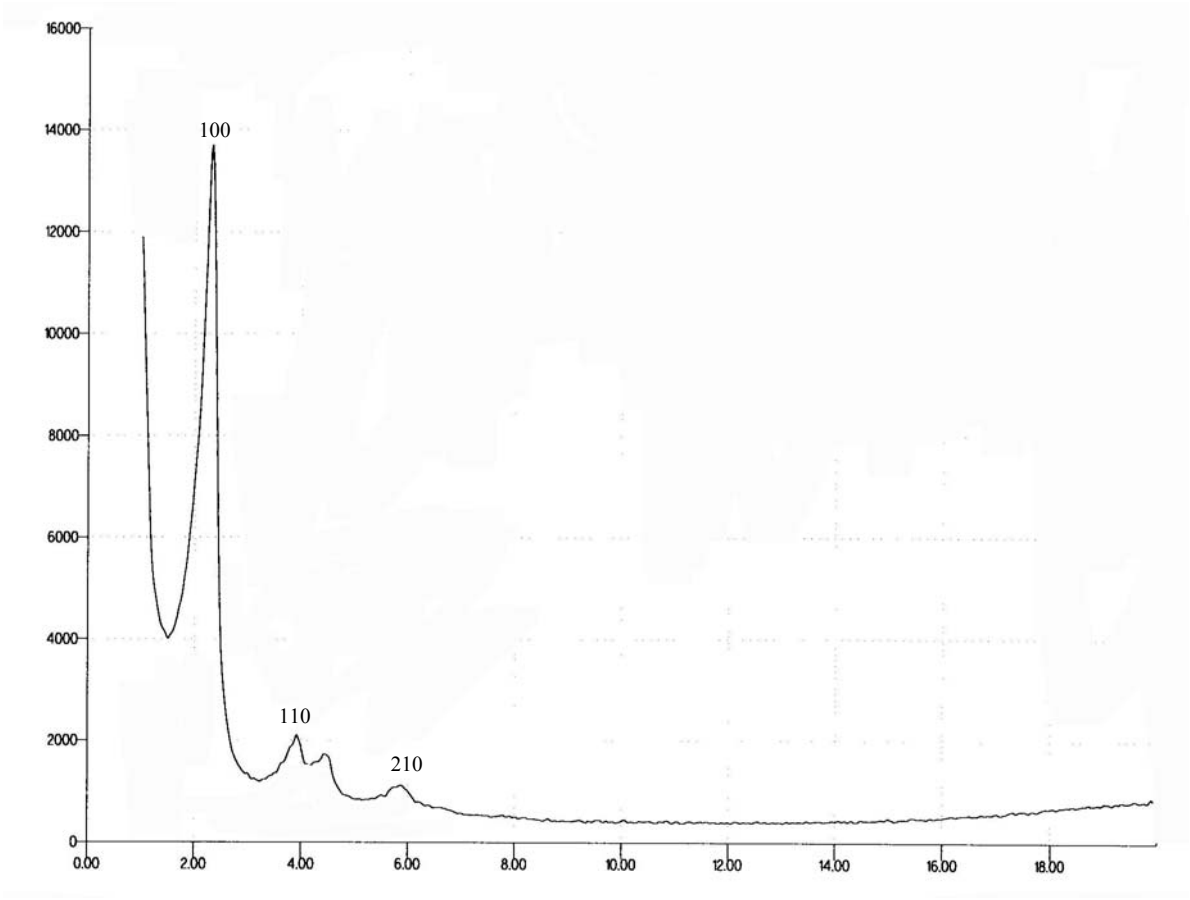

FIGURE 4-2 Typical XRD pattern for MCM-41

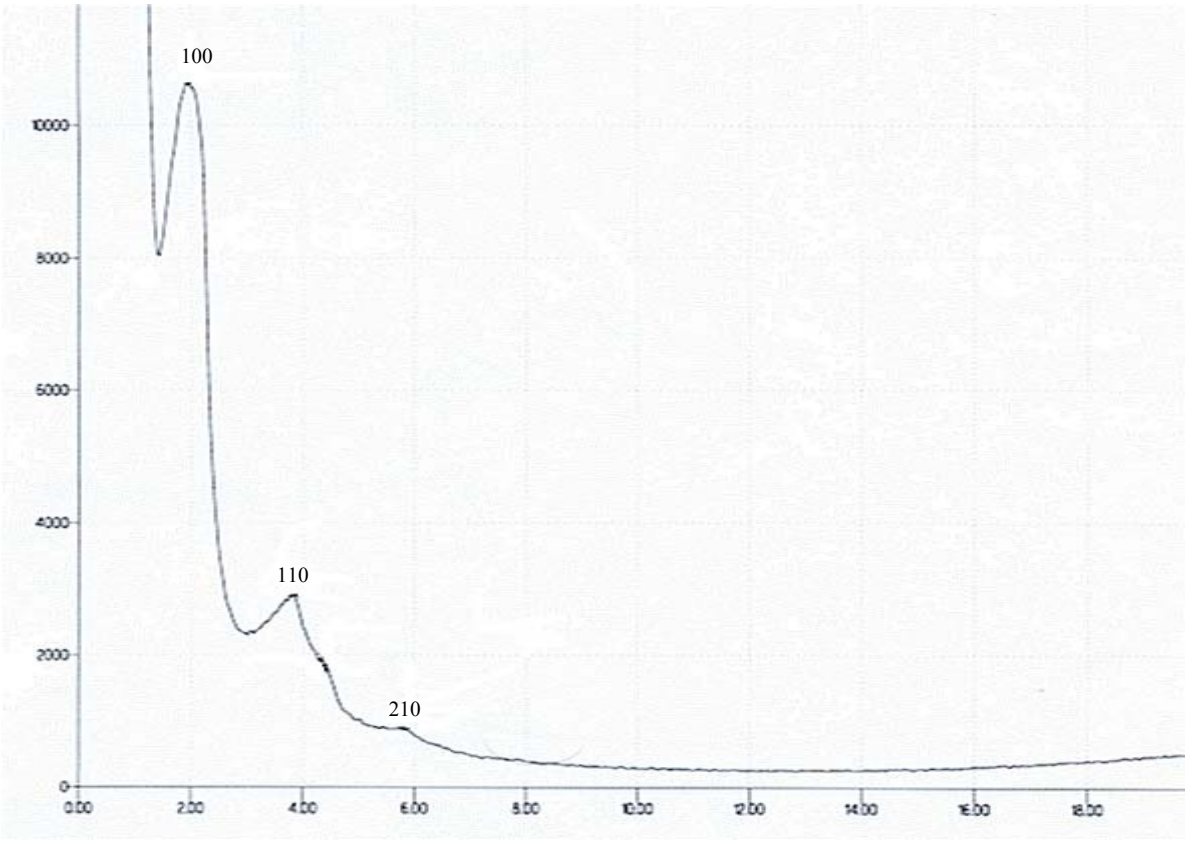

FIGURE 4-3 XRD pattern for the synthesized MCM-41

4.2 Gas Sorption Analyzer

4.2.1 Specific Surface Area

In comparing different catalysts or the effect of various treatments on catalytic activity, it is necessary to know the extent to which a change in activity is caused by a change in the area of a catalyst, in contrast to a change in intrinsic reactivity[28].

TABLE 4-1 prepared catalysts textural characteristics

Sample	BET Surface Area (m^2/g)	Pore Volume (cm^3/g)	Average Pore Diameter (A^0)
NiMo-ASA	186	0.33	36
NiMo-MCM-41	324	0.40	25
NiMo-β	313	0.41	26
NiMo-USY	300	0.35	23

Table 4-1 presents the textural characterization for the four prepared catalyst samples. It was observed that the amorphous NiMo-ASA catalyst has the lowest surface area as compared with other three zeolite based catalysts. In addition, NiMo-ASA catalyst exhibited the lowest pore volume and the highest average pore radius as compared with other catalysts. This is due to the fact that amorphous supports have more meso and macro-pores embedded in uniform structure which in turn reduces the overall surface area of the catalyst. In contrast, zeolites have well-ordered structure with the presence of micro-pores which provide large surface areas as high as 800 m^2/g [3].

It is worth mentioning that pure MCM-41 material has a surface area of 800 m^2/g while, β and USY zeolites have surface areas of 500 m^2/g. It was noticed that the surface area of the MCM-41, USY, and β materials has dropped to the range of 300 ~ 325 m^2/g when they were mixed with γ-alumina and impregnated with Nickel and Molybdenum metals. The explanation of this is that the incorporation of MCM-41, β, and USY materials into the γ-alumina matrix (30% zeolite mixed with 70% γ-alumina) produced surface areas decrease, due to the blockage of some of the zeolites pores. Similar finding was obtained by *J. Ramirez et. al*.[24]. Moreover, the impregnation of Nickel and Molybdenum metals into this support has further blocked more zeolite pores. This double blockage by γ-alumina and metals have reduced the surface areas of MCM-41, β, and USY materials by 60 %, 37 % and 40 % respectively.

4.2.2 Pore Size Distribution

The major application of this measurement is for the prediction of the effective diffusivity in a porous catalyst in conjunction with calculations of the ease of access of reactant molecules to the interior of a catalyst pellet by diffusion.

Figures 4-3, 4-4, 4-5, and 4-6, show the distribution of pore volumes along 10 ~ 300 A^0 pore radius for the four prepared catalysts. It is obvious that all catalysts have approximately the same peak positions but with different heights which represent different pore volumes.

Figure 4-3 shows that NiMo-ASA catalyst has wide distribution of pores. The curve peak is located in the meso-pore range with narrow pattern. The gentle drop of the curve indicates that NiMo-ASA includes considerable amount of macro-pores. In contrast, figure 4-4 presents NiMo-MCM-41 catalyst pore size distribution. It shows that it has lots of meso-

pores since the curve peak is wider at the mesoporous range. Moreover, the curve drop is drastic however it increases a bit at the tail end. This indicates the presence of some macro-pores in NiMo-MCM-41 catalyst.

In addition, figure 4-5 shows that NiMo-β catalyst has similar pattern to NiMo-MCM-41 catalyst with narrower but higher peak. However, the tail end of NiMo-β catalyst is higher than NiMo-MCM-41 catalyst indicating higher amount of macro-pores. On the other hand, figure 4-6 shows that NiMo-USY catalyst has micro-pores as well as meso-pores with narrow curve and lower tail end as compared with NiMo-MCM-41 and NiMo-β catalysts. This shows that NiMo-USY catalyst has lower amount of macro-pores than NiMo-MCM-41 and NiMo-β catalysts. The reason behind the existence of macro-pores in the prepared samples is due to crystals gathering and agglomerates formation. In addition, the incorporation of β and MCM-41 materials into the γ-alumina matrix as well as metal loading have plugged some of the micro-pores and generated meso and some macro-pores in the case of NiMo–β and NiMo-MCM-41 catalysts. Moreover, the dominance of γ-alumina structure into all prepared catalysts morphology is clear since the catalysts supports were prepared with 70 % γ-alumina. That is why NiMo-MCM-41 and NiMo-β catalysts have some macro-pores as shown in figures 4-4 and 4-5 respectively. Similar finding was obtained by *J. Ramirez et. al* [24].

In addition, it is very crucial to mention that with the conventional BET method that was used to measure the surface area and the pore size distribution for all catalysts, it is very difficult to exactly measure the micro-pores. Therefore, in the case of NiMo-USY and NiMo-β, the curves should be bimodal rather singular peaks. However, with existing capability, only mesoporous peaks can be detected.

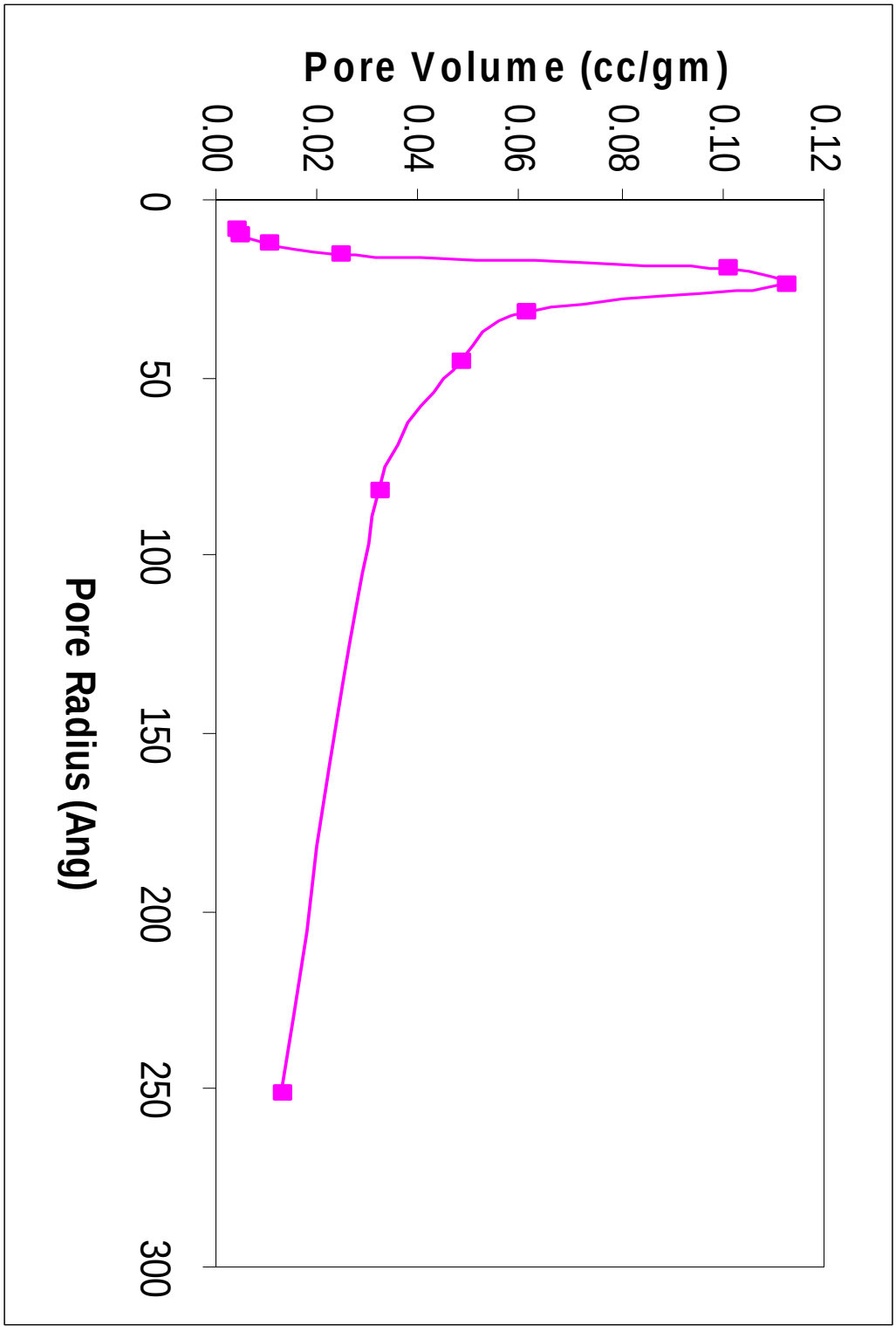

FIGURE 4-3 NiMo-ASA catalyst pore size distribution

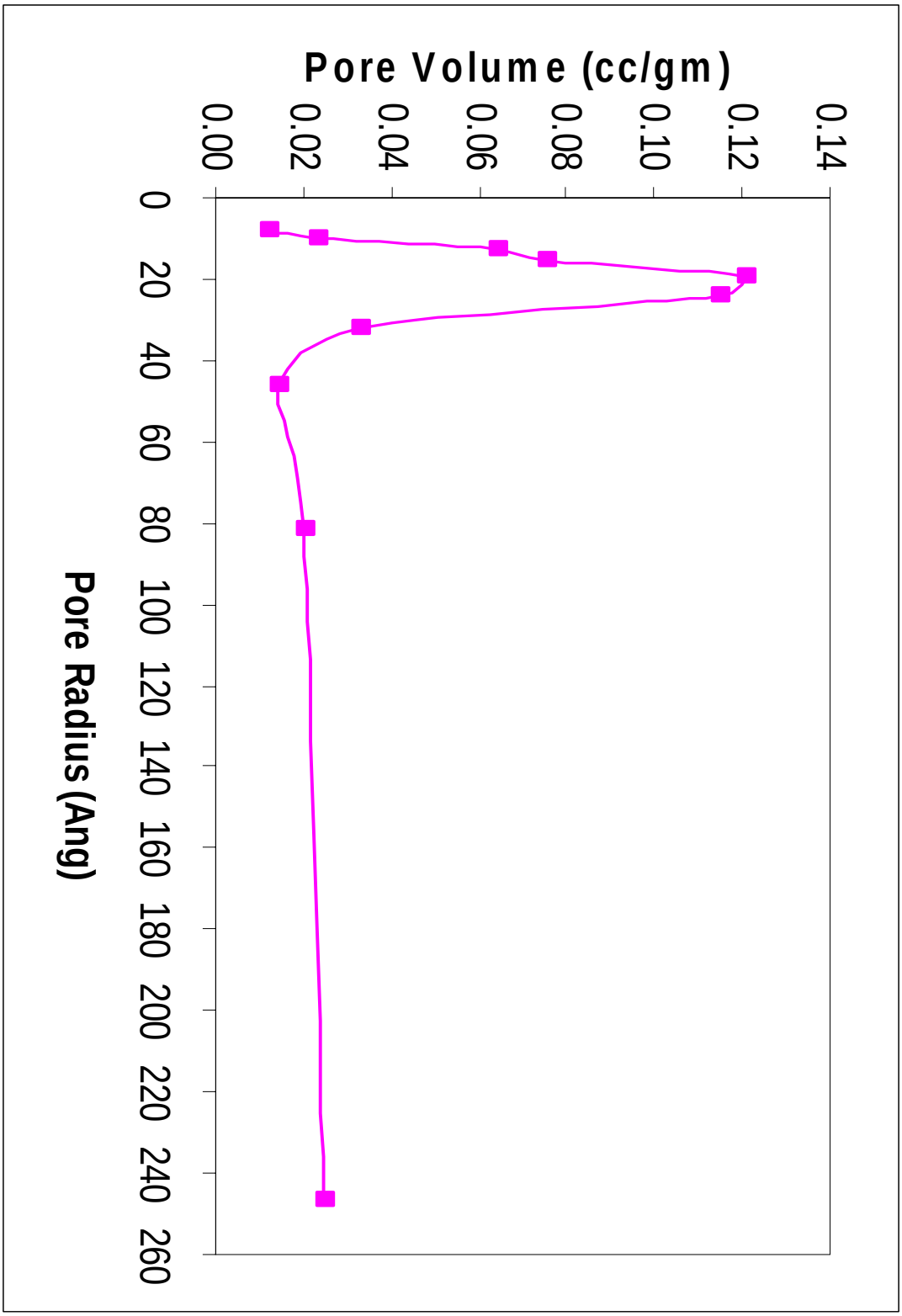

FIGURE 4-4 NiMo-MCM-41 catalyst pore size distribution

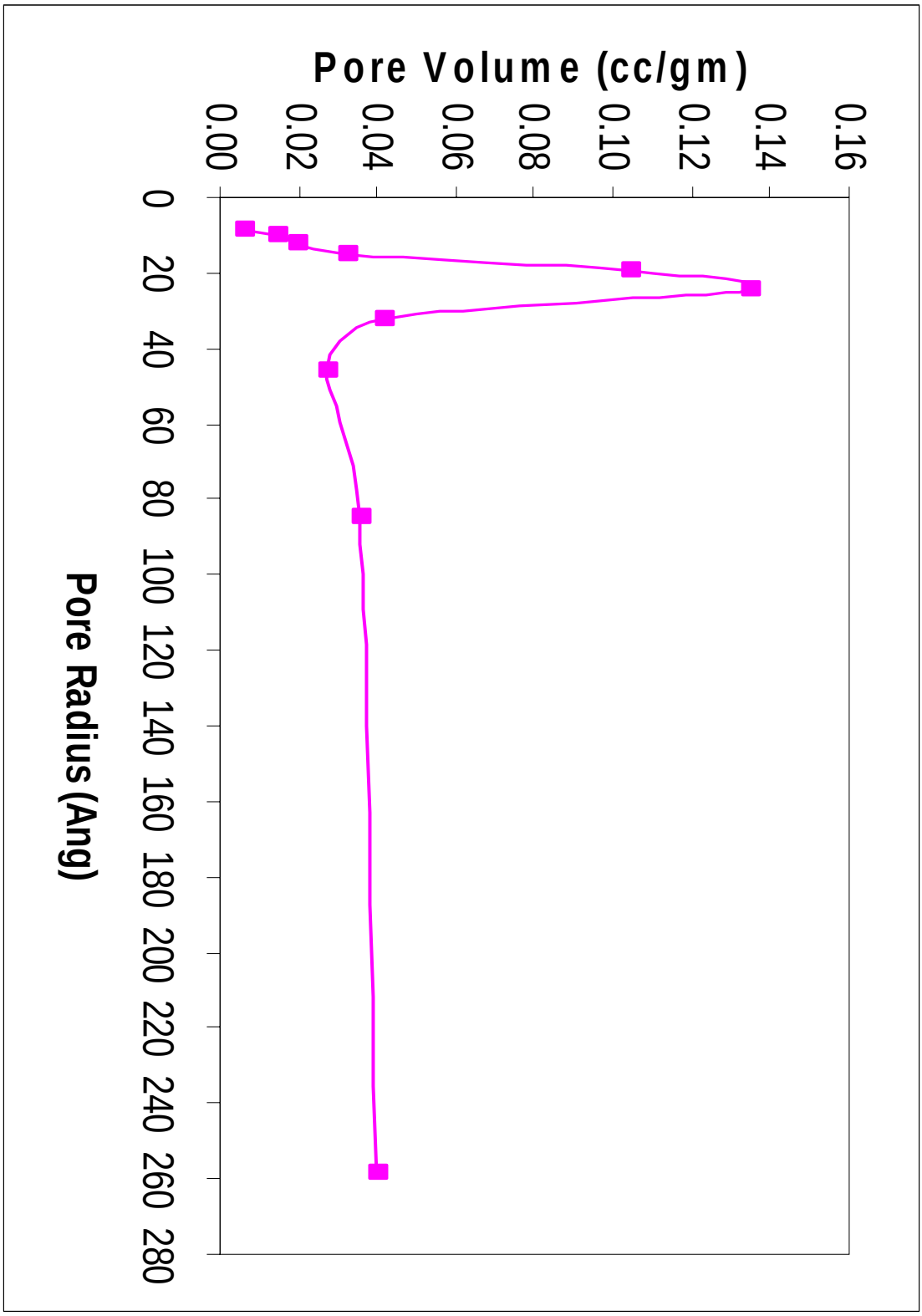

FIGURE 4-5 NiMo-β catalyst pore size distribution

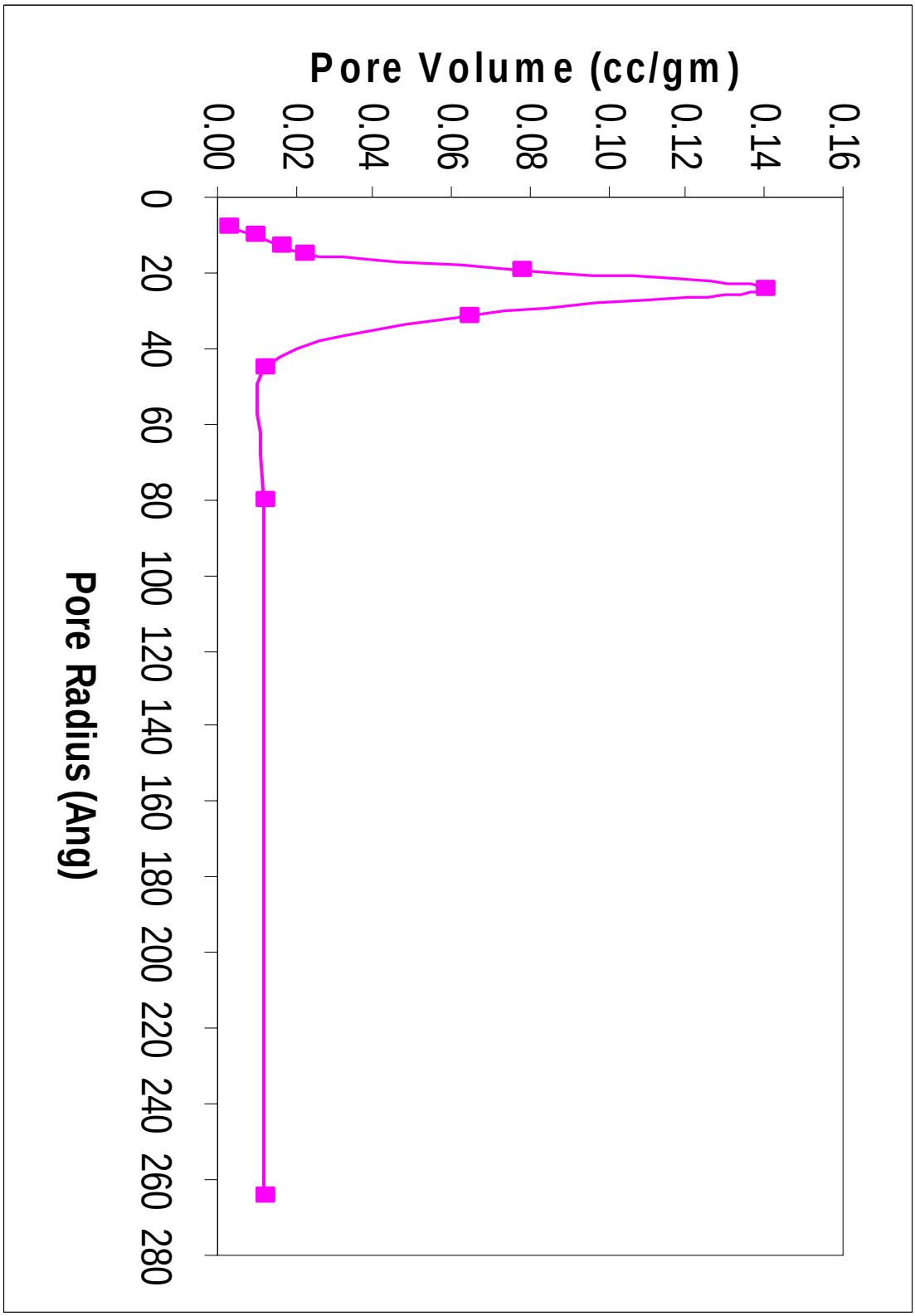

FIGURE 4-6 NiMo-USY catalyst pore size distribution

4.3 Temperature Programmed Reduction (TPR)

Temperature programmed reduction (TPR) has been widely used for the investigation and characterization of metal incorporated and metal supported catalysts. TPR peak area represents the amount of hydrogen consumption and peak temperature represents the reducibility of the metal oxide or oxides. Thus, TPR results can therefore be interpreted quantitatively as estimates of the distribution of various metal oxide phases as well as the metal support interaction for supported metal oxide catalysts[28].

TPR experiments were carried out in a system supplied by Ohkura Riken Co. Ltd. (Model TP-2000). The procedure for pretreatment and subsequent TPR experiments is as follows. At first, a 150 mg portion of catalyst sample (particle size: 600-212 μm) was placed in a quartz tube (8.0 mm o.d.) reactor and was held in the center by quartz wool plugs. The samples were pretreated in a flow of dry air. The temperature was raised to 400 ^{0}C for 2-h, and then cooled to ambient temperature. the air was purged by flowing dry Ar (30 cm^3/min) for 30-min at ambient temperature. The gas mixture used for reduction was 5 % H2 in Ar at a flow rate of 20 cm^3/min. The temperature of the reactor was increased linearly from room temperature to 1030 ^{0}C at a heating rate of 10 ^{0}C and then retained isothermally for 15 min. The moisture produced due to reduction or dehydration was trapped by a 5 A^0 molecular sieve. The hydrogen concentration was determined with a thermal conductivity detector (TCD). The TCD and molecular sieve trap were thermostated at 50 ± 0.1 ^{0}C. The temperature of the catalyst and the TCD current response were continuously monitored and recorded on a dedicated personal computer (NEX Model PC9821-Xe 10)[29].

Figures 4-7 through 4-10 present the TPR profiles of all prepared catalysts. All of the zeolite based catalysts showed double peak behavior while NiMo-ASA catalyst showed

triple peak behavior. This is because the metals are distributed into wide range of micro, meso, and macro-pores and it shows random distribution across the amorphous support as compared to the zeolitic supports.

The variation in the peak temperatures can be attributed to the differences in the metal support interactions and the multiple peak patterns might be due to the presence of nickel and molybdenum metals at different sites of the catalysts supports [30].

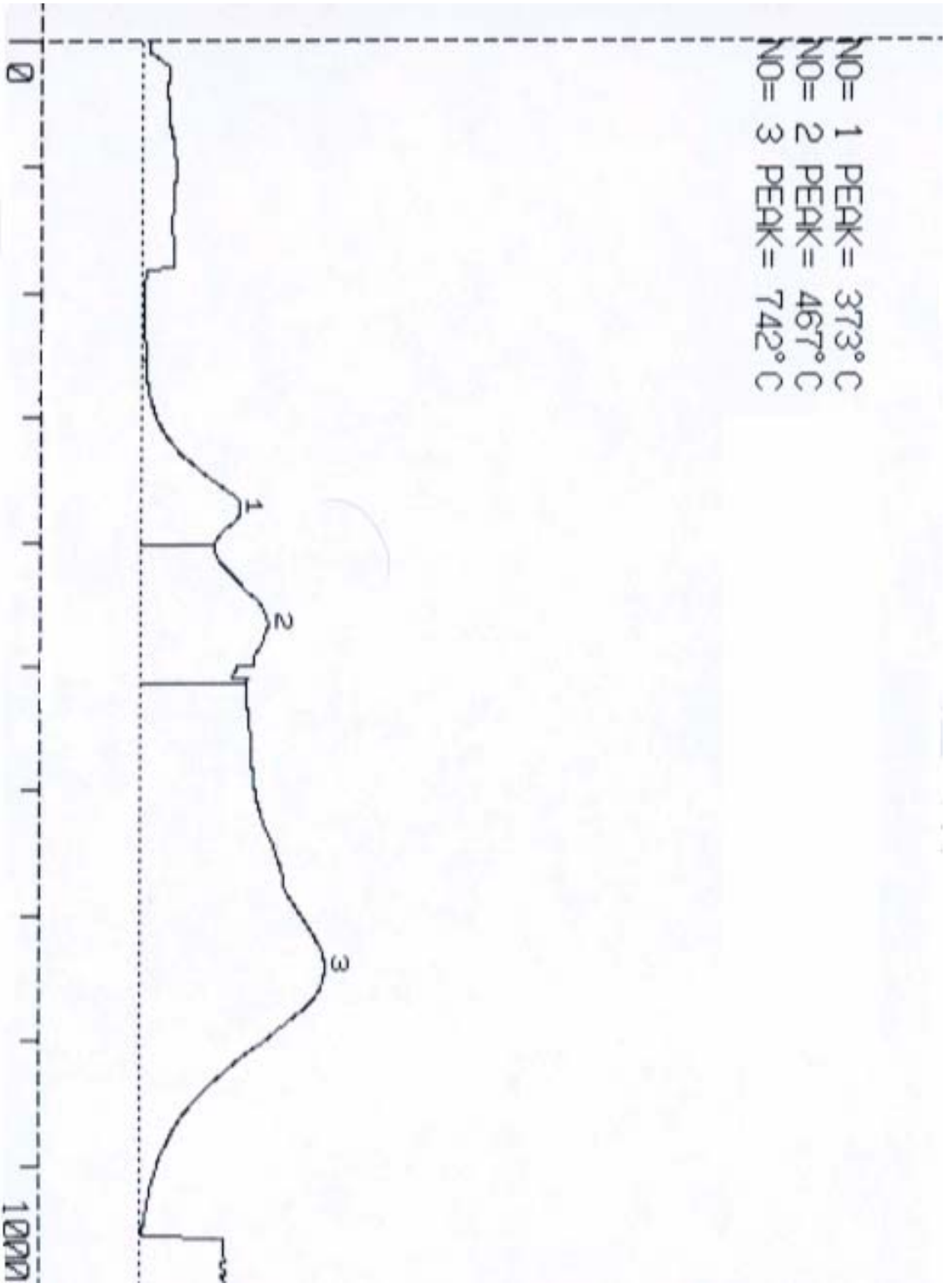

FIGURE 4-7 TPR pattern for NiMo-ASA catalyst

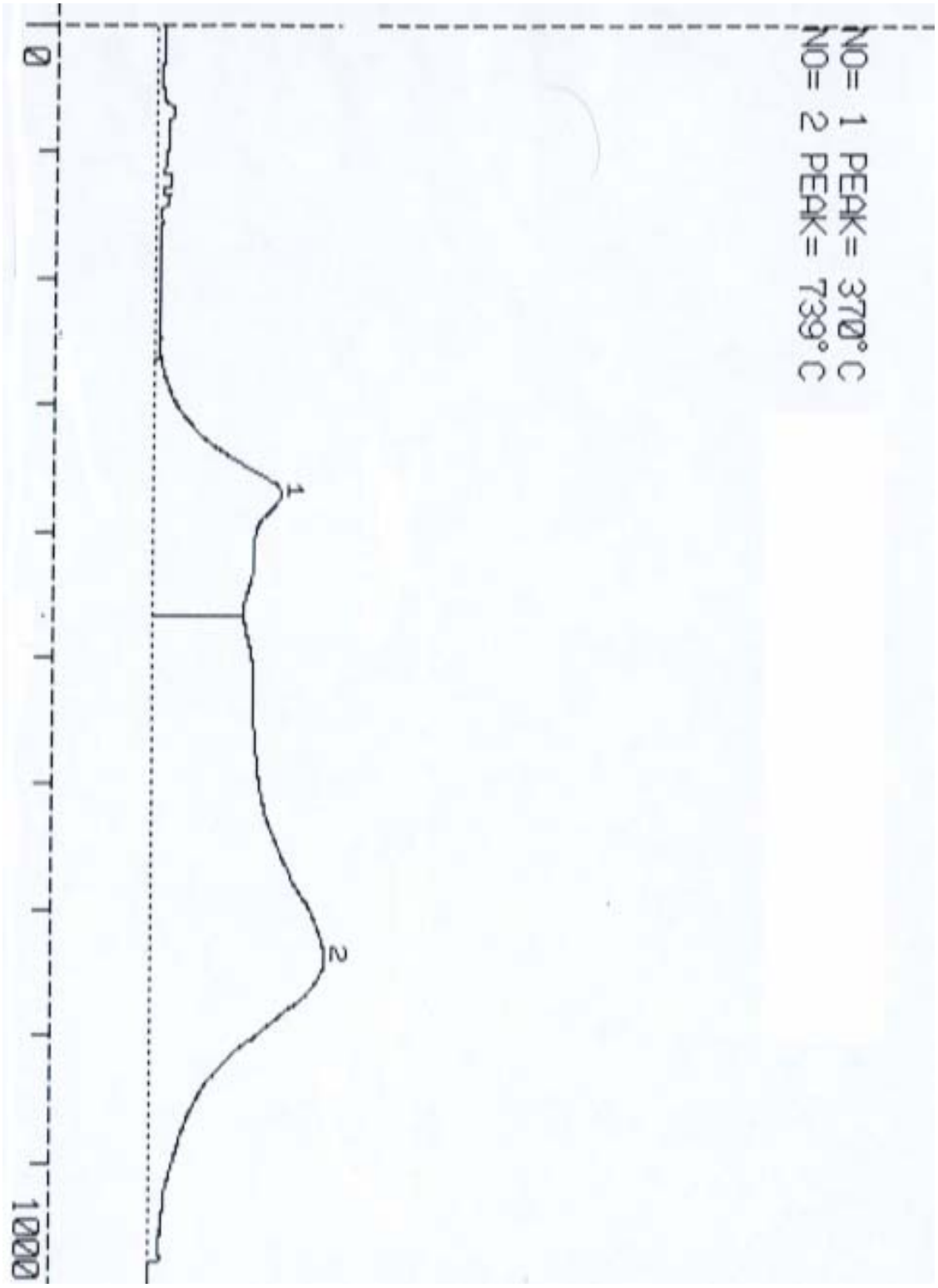

FIGURE 4-8 TPR pattern for NiMo-MCM-41 catalyst

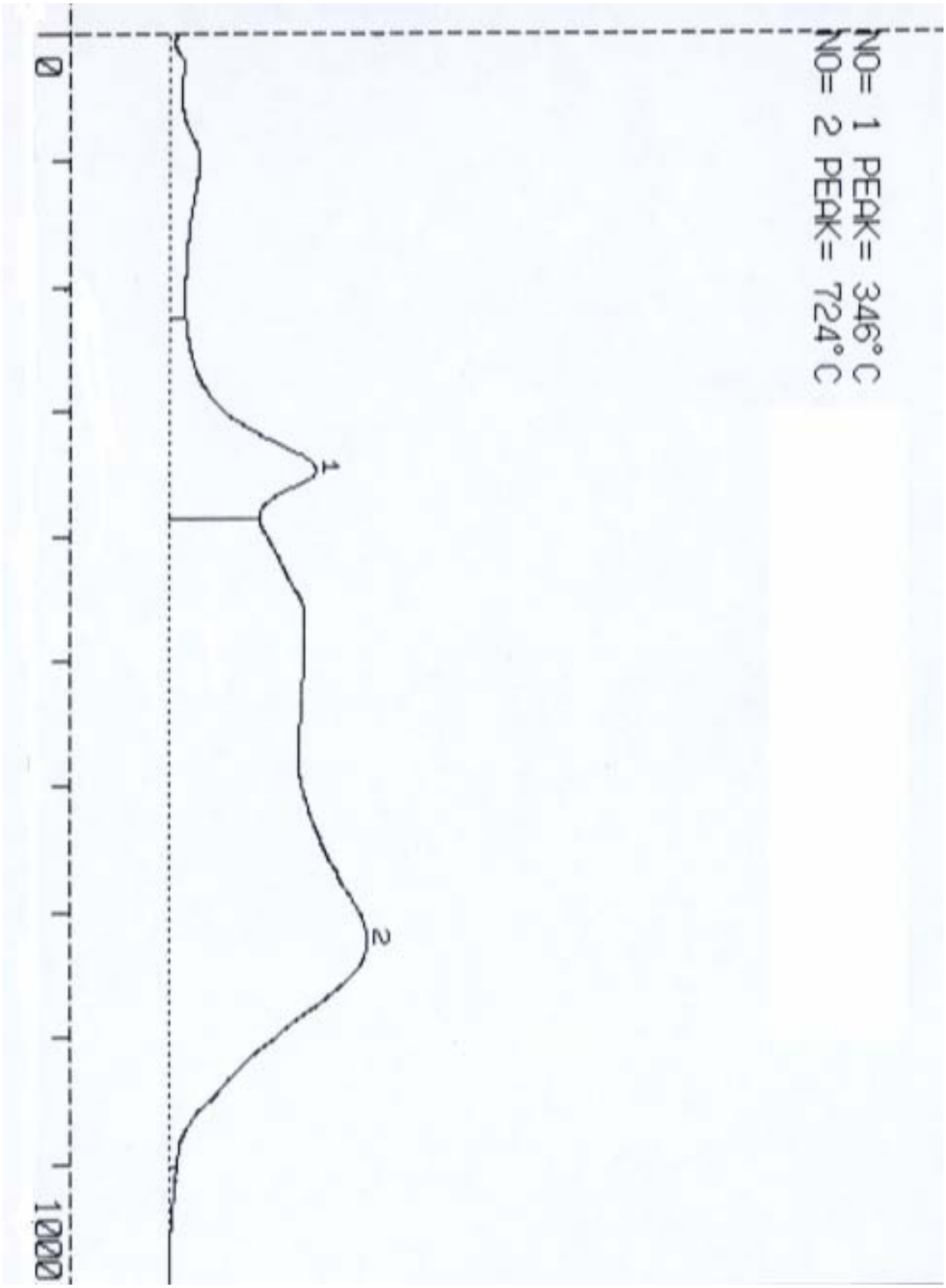

FIGURE 4-9 TPR pattern for NiMo-β catalyst

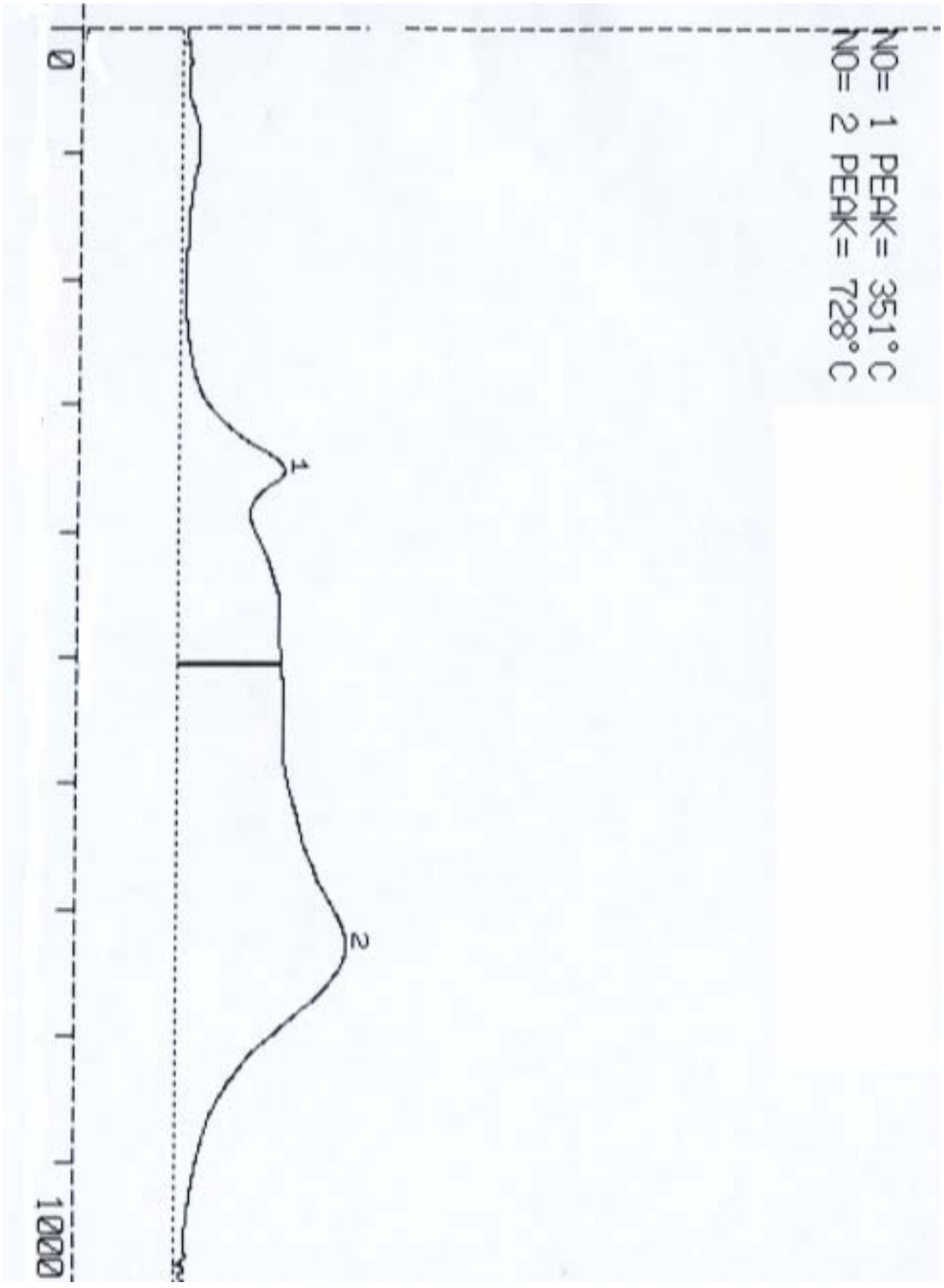

FIGURE 4-10 TPR pattern for NiMo-USY catalyst

4.4 Temperature Programmed Desorption (TPD)

The structures that give rise to acidity and indeed to catalytic activity are subject to some controversy. In the case of silica-alumina, the source of acidity may be rationalized in terms of a theory developed largely by Linus Pauling. If an aluminum ion, which is trivalent, is substituted isomorphously for a silicon ion, which is quadravalent, in a silica lattice comprising silica tetrahedral, the net negative charge must be stabilized by a nearby positive ion such as a proton. This positive ion can be produced by the dissociation of water, forming a hydroxyl group on the aluminum atom. The resulting structure, in which the aluminum and the silicon are both tetrahedrally coordinated, is a Bronsted acid. If this structure is heated, water of constitution is driven off and Bronsted acid sites are converted to Lewis acid sites[28].

The acid properties of the prepared four hydrocracking catalysts were determined by the TPD system (Model ATD 700) supplied Ohkura Riken CO. Ltd., Japan. The procedure of acidity measurement was as follows. First, 0.5 g of catalyst sample (particle size 22 – 212 μm) was placed in a quartz tube reactor (15 mm o.d.). the temperature was increased up to 400 ^{0}C for 2-h, then cooled to 100 ^{0}C. Ammonia (purity 99.9 %) was then introduced for 30-min at 100 Torr. After that, excessive ammonia was evacuated for 30-min at 100 ^{0}C under vacuum (10^{-3} Torr). Thermal desorption of ammonia was conducted at 100 Torr using He as a carrier gas up to 800 ^{0}C at a rate of 10 ^{0}C/min. The desorbed ammonia was monitored by TCD and Quadrupole detector (Massamate 200). This technique also enabled both the number of acid sites (Bronsted and Lewis) and acid strength distribution to be determined[31].

TABLE 4-2 TPD of ammonia for all prepared catalysts

Catalyst	Acidity (mmol/g)	Peak Temperature (^{0}C)
NiMo-MCM-41	0.33	264
NiMo-ASA	0.50	252
NiMo-β	0.56	233
NiMo-USY	0.59	238

Table 4-2 shows the TPD of ammonia for all of the prepared hydrocracking catalysts. The acidity of the prepared catalysts ranges from 0.33 mmol/g (NiMo-MCM-41) to 0.59 mmol/g (NiMo-USY). The lower acidity of NiMo-MCM-41 catalyst is expected since MCM-41 is a sililca based material and has low amount of alumina. Therefore, NiMo-MCM-41 catalyst has lower amount of γ-alumina than the other prepared catalysts. It is important to note that γ-alumina adds a lot to the total acidity of the catalysts. This is evident from the fact that even though NiMo-ASA (0.5 mmol/g) is amorphous catalyst but it has more acidity than NiMo-MCM-41 because it contains more γ-alumina than NiMo-MCM-41 catalyst. On the other hand, the variations in the TPD peak temperatures of all prepared catalysts, as shown in figure 4-11, indicate the strength of acidic sites. In case of NiMo-MCM-41, although it has lower acid quantities than the other catalysts, however, it has the highest peak temperature amongst the other catalysts. This indicates that NiMo-MCM-41 catalyst will offer more cracking activity and higher conversion.

In addition, NiMo-USY, NiMo-β, and NiMo-ASA catalysts contain almost the same total amount of acidity (0.5 ~ 0.59 mmol/g) with different peak temperatures. Therefore, their hydrocracking activity is expected to be similar.

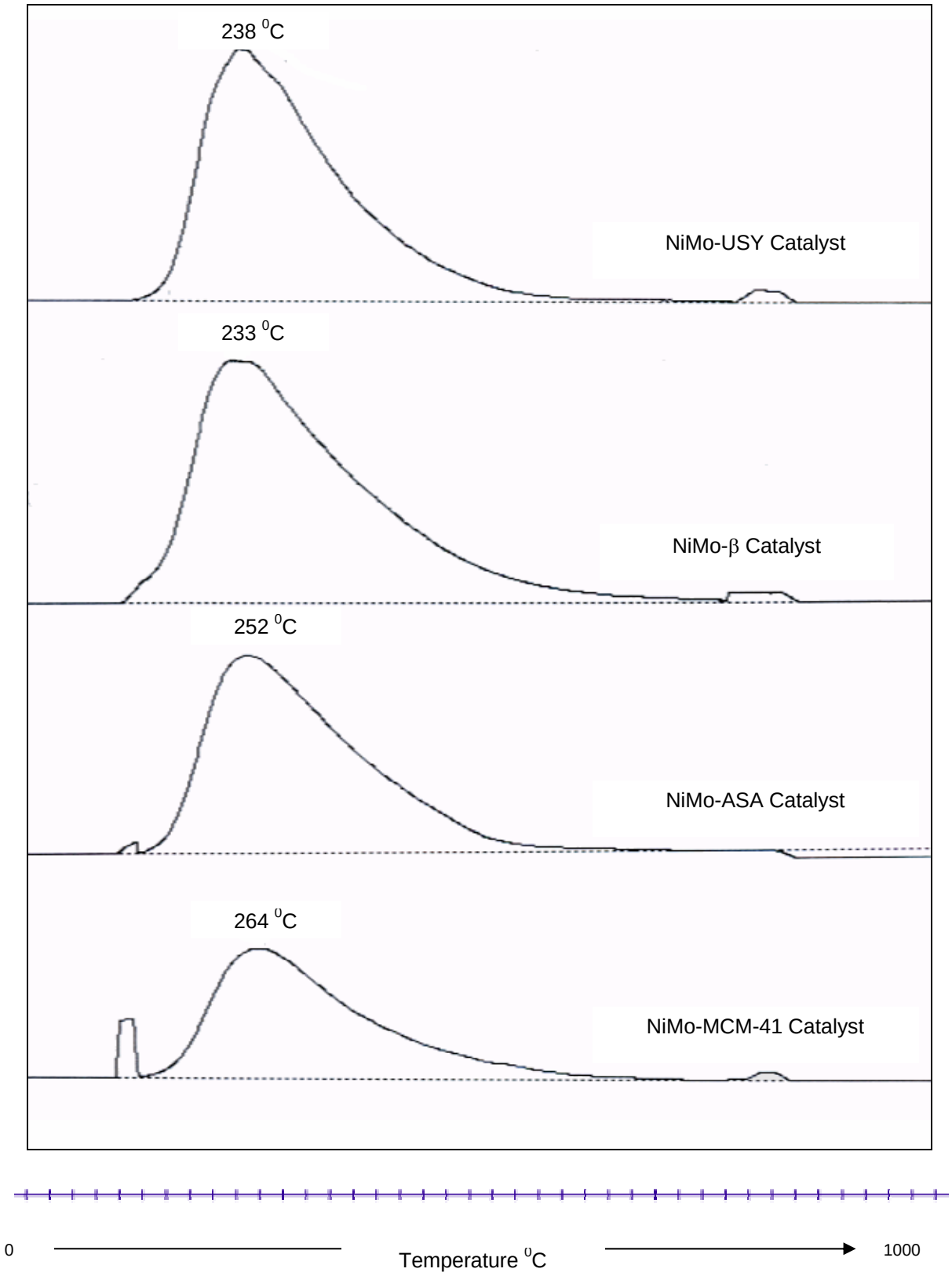

FIGURE 4-11 Superimposed graph showing TPD patterns for all prepared catalysts

4.5 Batch Reactor Evaluation

Batch reactors are closed systems in which measured quantities of reactant interact with a charge of catalyst which is usually maintained at a fixed temperature. The concentration of reactant diminishes with time as the reaction proceeds and this is utilized as the basis of experimental observation. Some of the early classic experiments on the kinetics of catalyzed gas reactions reported by Hinshelwood and by Rideal and Taylor were studied using batch reactors. Figure 4-12 shows a typical batch reactor with mixing [32].

The concept behind our study using this kind of reactor, is to contain the liquid VGO/DMO reactant in a vessel under hydrogen environment at high pressure as high as 150 kg/cm^2. The vessel is contained in an oven to progressively supply heat to the reactor. The reaction temperature was fixed at 410 ^0C for all tested catalysts. The liquid and gas mixture is very well mixed using a magnetic driven mixer in order to ensure an intimate contact between the reactants and the catalyst particles. As a result, the concentration and temperature of the contents of the reactor will be virtually constant. Moreover, the mixing has a great deal of importance. It reduces the interparticle resistances to minimum. Additionally, the interparticle diffusion resistance was further minimized by crushing the catalysts particles to small sizes. When the catalyst particles are sufficiently small, diffusion effects within the particle will be virtually absent and the measured rate will remain constant.

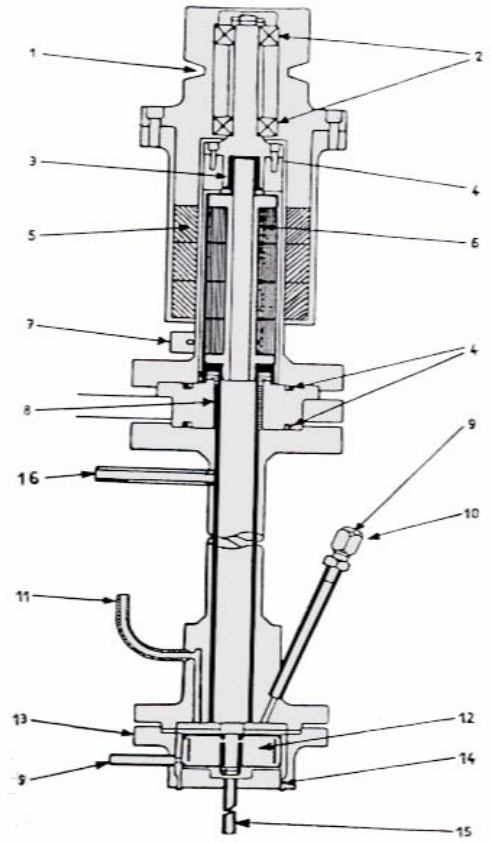

FIGURE 4-12 Details of autoclave batch reactor. 1, belt drive groove; 2, outer magnet bearings; 3, upper bearing; 4, O-ring seals; 5, outer magnet; 6, inner magnet; 7, reed relay; 8, lower bearing; 9, thermocouple entry; 10, pressure tapping; 11, gas inlet port; 12, catalyst basket; 13, reaction vessel; 14, baffles; 15, gas outlet port; 16, purge inlet port.

4.5.1 Effect of Mixing

In order to measure the effect of mixing in this particular experiment, two runs were conducted using the commercial catalyst at the same reaction conditions. One run was conducted with mixing and the other run was conducted without mixing during the reaction time. The major observation noticed was that the run with stirrer operating had better hydrodesulfurization function (44 % vs. 36 %) and hydrogenation function (10.3 % vs. 5.5 %). This is expected since mixing provides intimate contact between H_2, VGO/DMO feed and the catalyst. In the case of no mixing, more coke deposition is bound to occur since the cracked hydrocarbon will not necessarily meet H_2 compound to attach to it.

4.5.2 Commercial Catalyst Testing

Several runs utilizing the commercial catalyst were conducted in order to determine the maximum oven temperature and the resultant reaction temperature achievable. Table 4-3 shows the various runs conducted with their product analysis.

TABLE 4-3 Commercial catalyst different run conditions and product analysis

Run No.	Pressure (kg/cm^2)	Temperature (^0C)	Conversion %	Naphtha Yield %	Diesel Yield %
1	150	395	18.5	7.86	11.40
2	150	400	23.11	8.98	14.85
3	150	405	24.02	9.32	15.41
4	150	405	24.09	9.49	15.30
5	150	410	27.01	10.31	17.38

It is apparent that the first run did not provide very good conversion. Therefore, the temperature was increased 5 ^{0}C to test the catalyst response. As a result, run no. 2 gave better conversion and yield. When the temperature was increased 5 ^{0}C more, not much difference was observed in terms of conversion and yield. Thus, the temperature was increased to 410 ^{0}C. As a consequence, the conversion and yield were slightly increased. On this basis, it was decided to test the various prepared catalysts at 410 ^{0}C and use run no. 5 as our base line.

4.5.3 Experimental Repeatability/Reproducibility

In order to ensure the quality of our experiment procedure as well as our generated data, it is imperative to repeat the experiment several times to reproduce data. In reference to table 4-3, it is apparent that runs no. 3 & 4 were duplicated at the same reaction conditions and experiment procedure. The resulted conversion and yield were comparable and almost the same. On that basis, our experiment procedure was used throughout our study since the repeatability and reproducibility of data was achieved successfully.

4.5.4 Prepared Catalysts Testing

After checking the quality of the data produced by the batch reactor, the various prepared hydrocracking catalysts were tested at the pre-determined conditions (T = 410 ^{0}C & P = 150 kg/cm^2). The VGO/DMO feed blend (100 gm) was manually mixed with 3-gm crushed catalyst. The tested catalysts were crushed in order to mitigate the interparticle diffusion resistance. The mixture was loaded into the reactor vessel. The vessel was fixed into the experimental setup assembly and purged with H_2 during pressurizing. The reactor was pressurized to 150 kg/cm^2 and held at this pressure for around 30-min to make sure that the system is tight and can withhold this amount of pressure. After passing the pressure leak

test, the reactor pressure was dropped to 90 kg/cm^2 and the oven temperature program was started. Since the feed catalyst mixture solidifies at room temperature, the mixer was not started immediately in order to protect it from being damaged. The mixer was started after the reactor temperature reached 100 ^{0}C at which the feed catalyst mixture is at liquid state. After 2 1/2 hrs, the system pressure was adjusted to 150 kg/cm^2 and we started counting 1-hr reaction time. When 3 1/2 hr total time of the run was reached, the reaction was immediately stopped by switching off the oven program temperature and mixer rotation. After the reactor cooled down, gas sample was collected and the reactor system was depressurized. Then, the reactor vessel was opened and liquid products as well as catalyst samples were collected.

4.5.5 Products Analysis

Batch reactor products are categorized into gas, liquid and coke lay-down. The gas samples were analyzed using gas chromatography technique. While, the liquid samples were analyzed using the simulated distillation technique. Moreover, the catalyst samples were charged to the Elementar instrument to measure the amount of coke lay-down generated as a result of reaction. In addition, the liquid samples were analyzed for sulfur, carbon, and hydrogen components using Elementar instrument. This helped in calculating the hydrodesulfurization and hydrogenation activities of each individual catalyst.

4.5.5.1 Gas Chromatography

Gas samples from each run were introduced to the gas chromatography instrument which was initially calibrated using standard gas samples.

TABLE 4-4 Gas chromatography analysis

Compounds Vol. %	NiMo-ASA	NiMo-MCM-41	NiMo-Beta	NiMo-USY	Commercial Catalyst	Blank Run
CH4	0.97	0.24	1.56	1.31	0.07	2.51
C2	0.59	0.12	0.00	0.00	0.00	0.00
C2=	0.63	0.00	0.65	0.49	0.05	1.05
C3	0.00	0.11	0.00	0.00	0.00	0.00
C3=	0.00	0.00	0.00	0.00	0.00	0.00
i-C4	0.03	0.02	0.00	0.00	0.00	0.12
n-C4	0.00	0.04	0.00	0.00	0.00	0.00
t2-C4=	0.02	0.00	0.00	0.00	0.00	0.02
1-C4	0.00	0.00	0.00	0.00	0.00	0.00
i-C4=	0.00	0.00	0.00	0.00	0.00	0.00
c2-C4=	0.00	0.00	0.00	0.00	0.00	0.00
i-C5	0.03	0.00	0.00	0.00	0.00	0.04
n-C5	0.01	0.00	0.00	0.00	0.00	0.01
Hydrocarbon Gases	2.28	0.53	2.22	1.81	0.12	3.74

It is apparent from the above table, that the commercial catalyst has produced the least amount of gases as compared to the four prepared catalysts. The second least gases were produced by the NiMo-MCM-41 mesoporous catalyst. It is almost 4 times the commercial catalyst. The lower gas make is attributed to the lower acidity of NiMo-MCM-41 catalyst as shown in figure 4-13. On the other hand, the more acidic catalysts namely NiMo-β, NiMo-USY, and NiMo-ASA, have produced much more gases than both the commercial and the NiMo-MCM-41 catalysts. The gases produced from the acidic catalysts are approximately 20 times the commercial catalyst. The higher acidity resulted into over-cracking at the acidic sites and more gas make and as a result, peaks of olefinic gases (e.g. C2=) were

detected in the case of the acidic catalysts as shown in table 4-4. However, NiMo-MCM-41 along with the commercial catalyst had very minute amount of olefinic gases.

In the case of blank run, thermal cracking has resulted into tremendous amount of gases and produced the highest amount of olefinic gases as compared to the catalytic reactions results. This clearly indicates the actual benefits of catalytic reactions over thermal reactions.

TABLE 4-5 Gas make against catalyst acidity

	NiMo-MCM-41	NiMo-β	NiMo-ASA	NiMo-USY
Gas Make, Vol.%	0.53	2.22	2.28	1.81
Acidity, mmol/gm	0.33	0.56	0.5	0.59

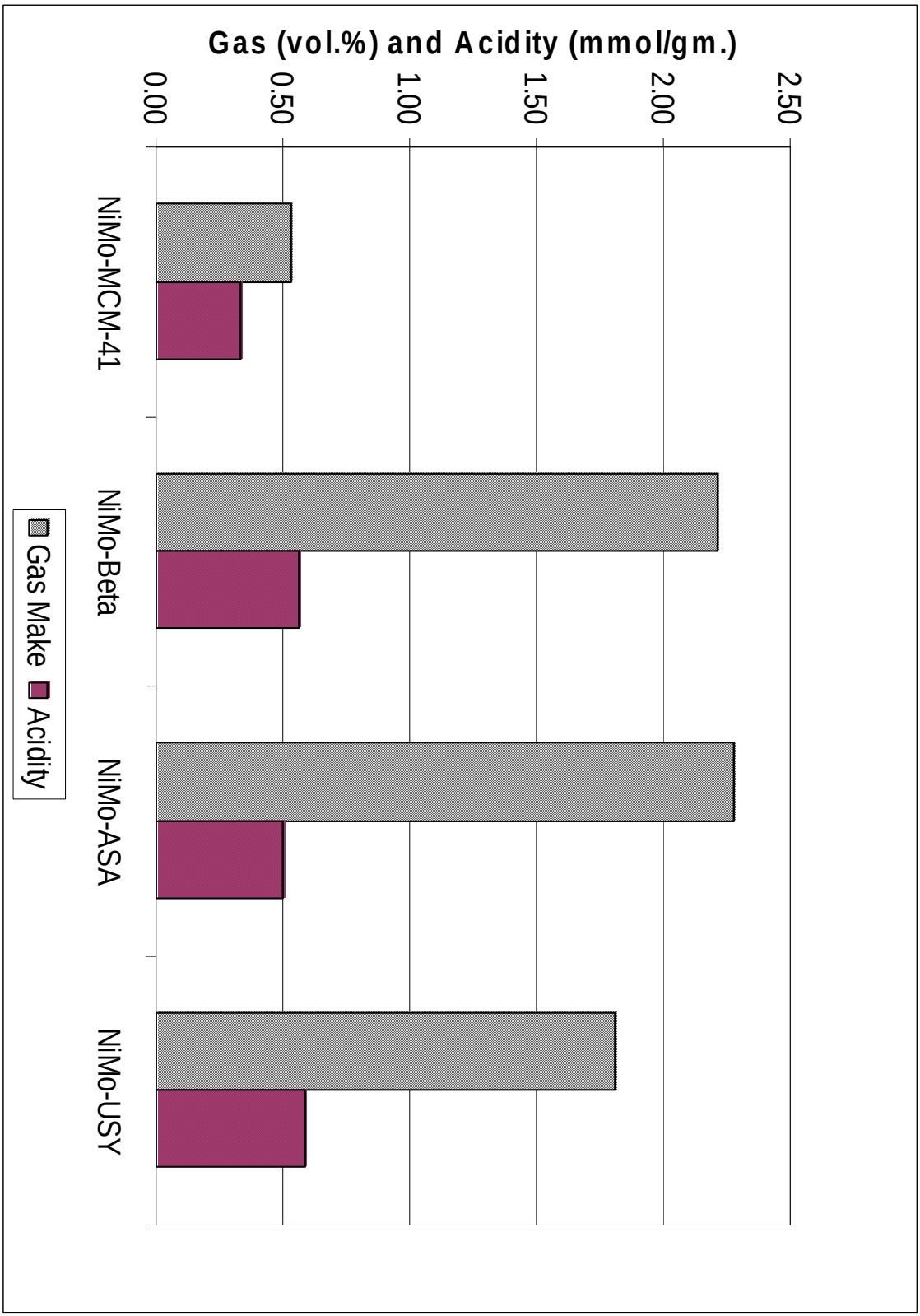

FIGURE 4-13 Acidity and gas make of prepared catalysts

In practice, refiners who are interested in more diesel and naphtha and less gas make would like to load the less acidic catalyst to avoid excessive gas production. Therefore, NiMo-MCM-41 catalyst would be a good candidate for this purpose and is very much comparable to the commercial catalyst. However, refiners who are integrated with petrochemical industry would prefer to produce more gases to boost their profitability.

4.5.5.2 Catalyst Selectivity

TABLE 4-6 Tested catalysts selectivity

Product %	VGO/DMO Feed 85% / 15%	Comm.	NiMo-MCM-41	NiMo-β	NiMo-ASA	NiMo-USY
Naphtha (IBP-400 ^{0}F)	0.21	10.31	10.1	9.27	9.55	9.55
Distillate (400-700 ^{0}F)	0.72	17.38	20.52	18.41	18.6	18.8
Residue (800-900 ^{0}F)	37.43	32.42	30.23	30.85	31.52	31.8
Residue (900-1050 ^{0}F)	61.65	39.89	39.25	41.46	40.34	39.65
Total	100	100	100	100	100	100

Table 4-6 shows that all prepared catalysts have yielded almost the same naphtha yield and more diesel yield than the commercial catalyst. However, NiMo-MCM-41 catalyst has produced the highest diesel yield and the lowest gas make amongst all tested catalysts. This can be attributed to the main feature of this catalyst being mesoporous and having lower acidity. This result makes NiMo-MCM-41 catalyst very attractive to be considered as a hydrocracking catalyst for VGO/DMO blend feed.

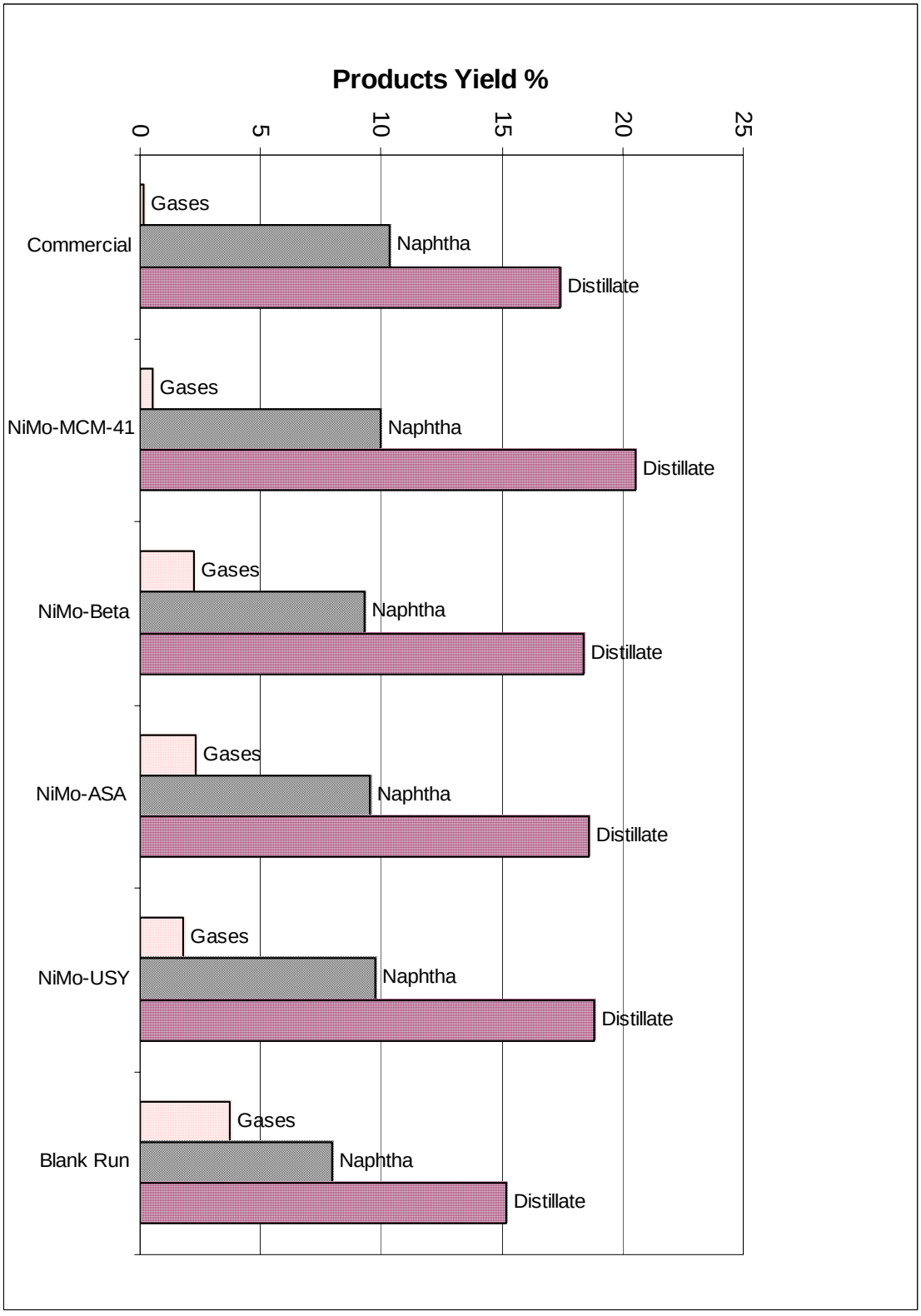

FIGURE 4-14 Tested catalysts selectivity

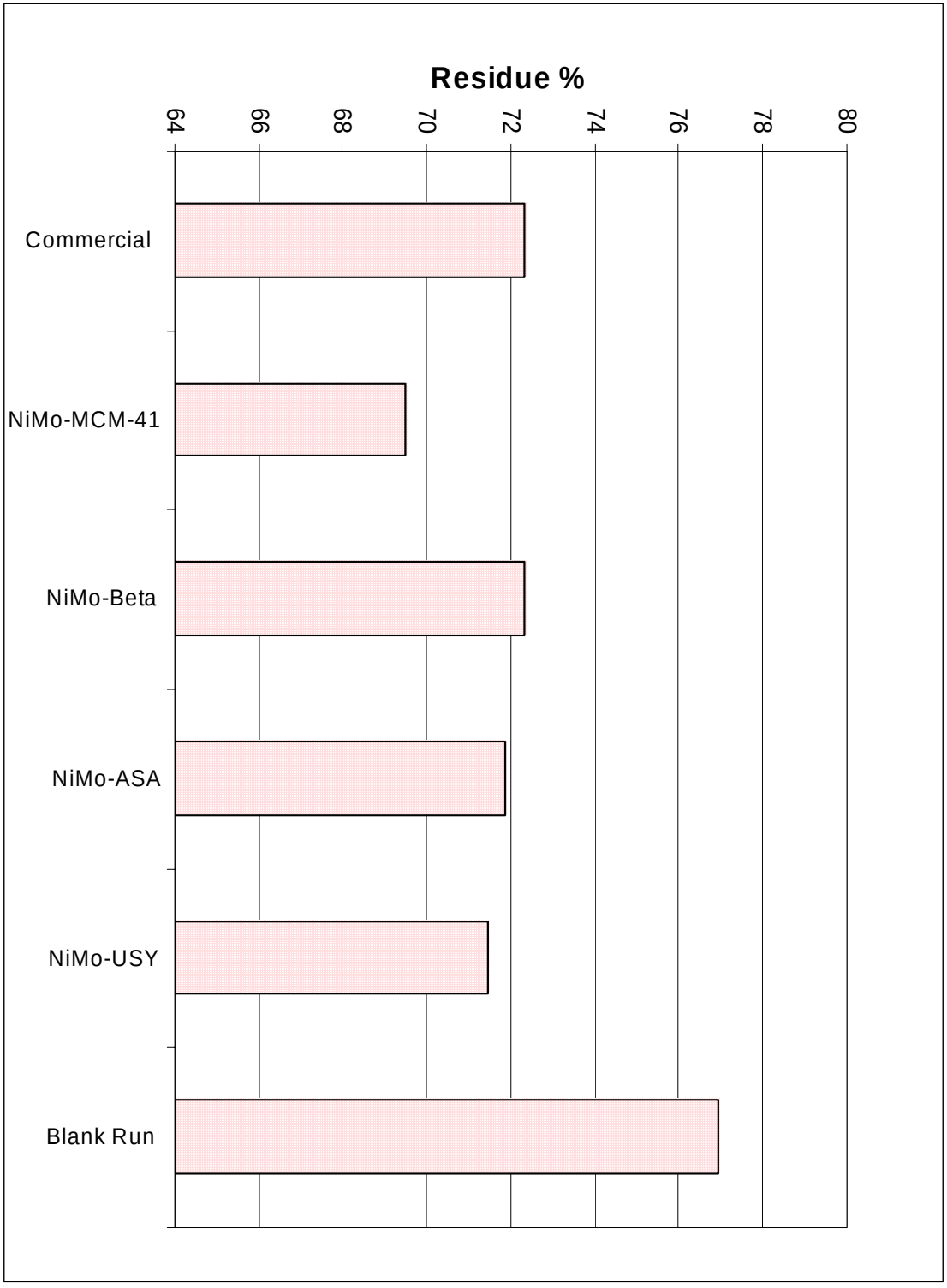

FIGURE 4-15 Tested catalysts unconverted material (residue)

On the other hand, as shown in figure 4-14, all tested catalysts including the commercial catalyst have the tendency to produce more diesel than naphtha. Therefore, all of the tested catalysts can be tagged as diesel selective catalyst or diesel mode catalyst.

Additionally, figure 4-15 shows that NiMo-MCM-41 catalyst has lower residue yield than the commercial and other prepared catalysts. The other three prepared catalysts namely NiMo-ASA, NiMo-β, and NiMo-USY had almost similar residue to the commercial catalyst. The lower residue make of NiMo-MCM-41 catalyst indicates higher conversion as will be discussed later.

On the contrary, thermal cracking run has produced the least naphtha and diesel yields and the highest residue and gas make. This again shows the advantage of catalytic reactions over thermal reactions.

4.5.5.3 Catalyst Activity

Figure 4-16 shows that the VGO/DMO blended feed does not contain hydrocarbons in the range of n-C5 to n-C20. The peaks in figure 4-16 indicate that the feed contains material in the range of n-C24 ~ n-C40. In practice, this type of feed is considered very heavy and has high tendency for coke lay down during reactions. Figure 4-17 shows the product curve of the commercial catalyst reaction. Unlike the feed curve, the front end of the curve shows high peaks indicating conversion of the heavy hydrocarbon molecules to smaller molecules. Moreover, figure 4-18 shows that the product of NiMo-MCM-41 catalyst has higher peaks at the front end of the curve than the commercial catalyst indicating higher conversion. In the case of NiMo-ASA, NiMo-β, NiMo-USY catalysts, they have almost similar peaks to the commercial catalyst which denotes that they have relatively similar conversion. If the feed and the products curves were superimposed, one can notice a slight shift in the feed

curve peak to the left towards the lower molecular weights hydrocarbon which indicates lower density product as compared to feed.

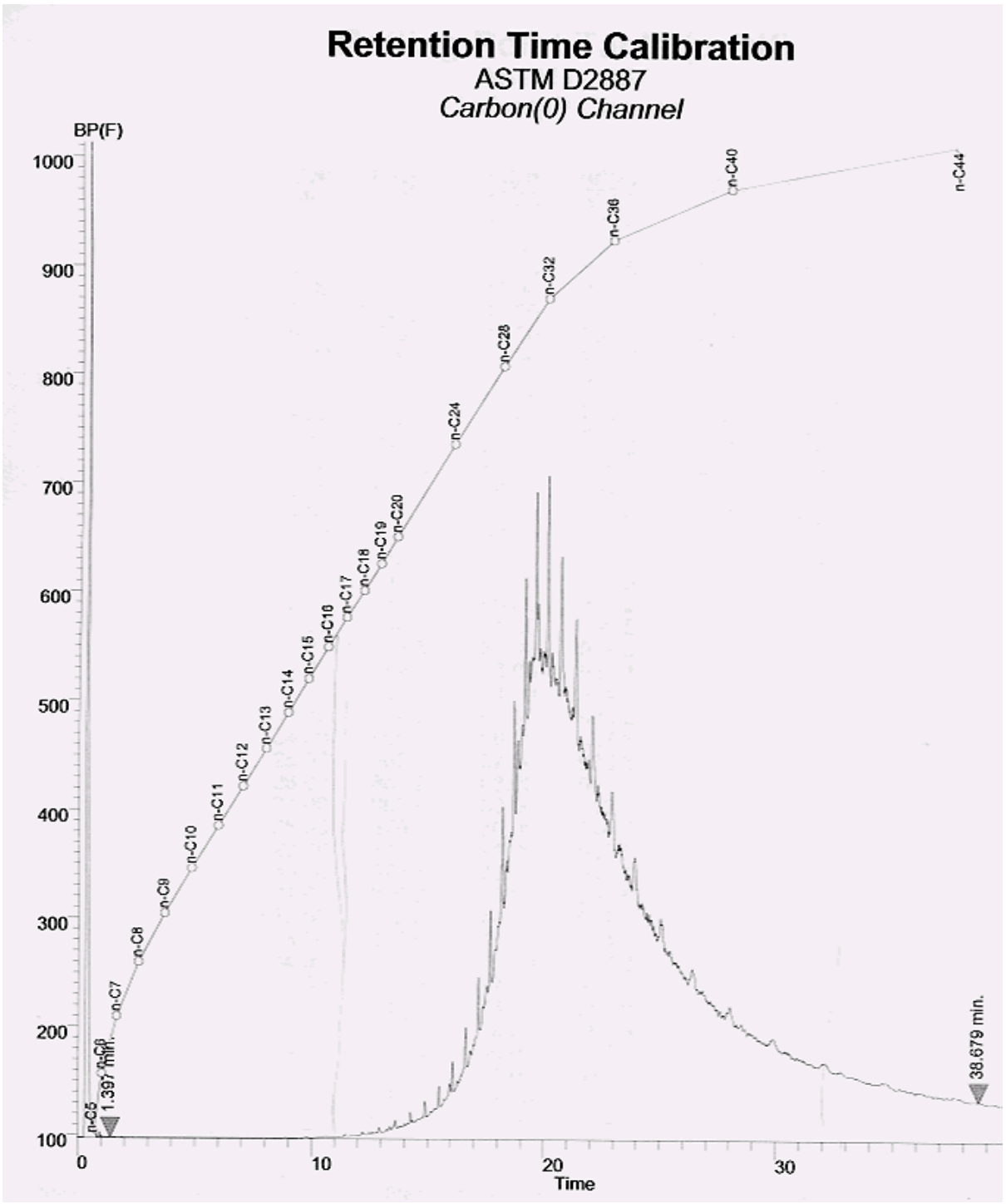

FIGURE 4-16 Simulated distillation curve for VGO/DMO blended feedstock

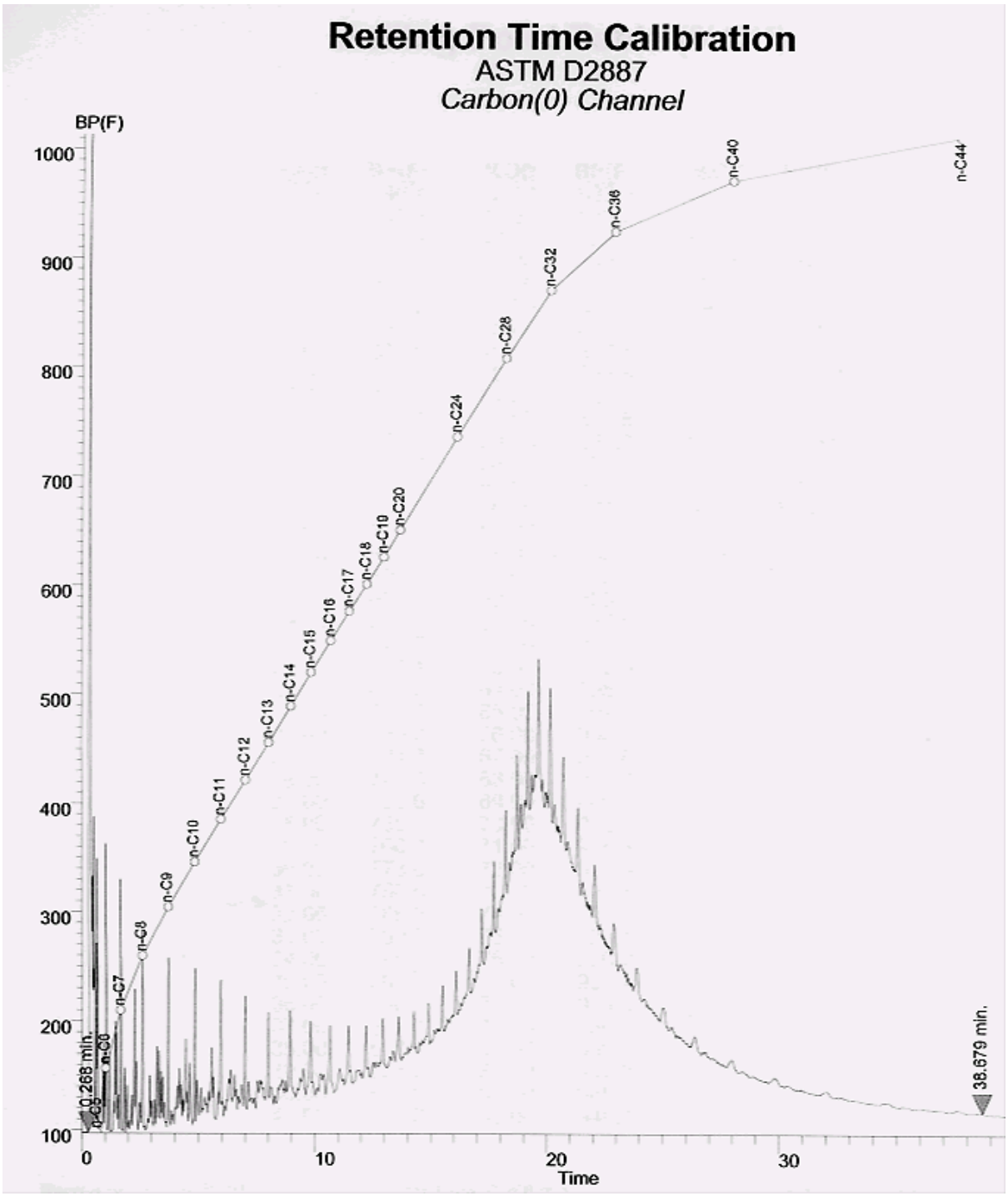

FIGURE 4-17 Simulated distillation curve for commercial catalyst product

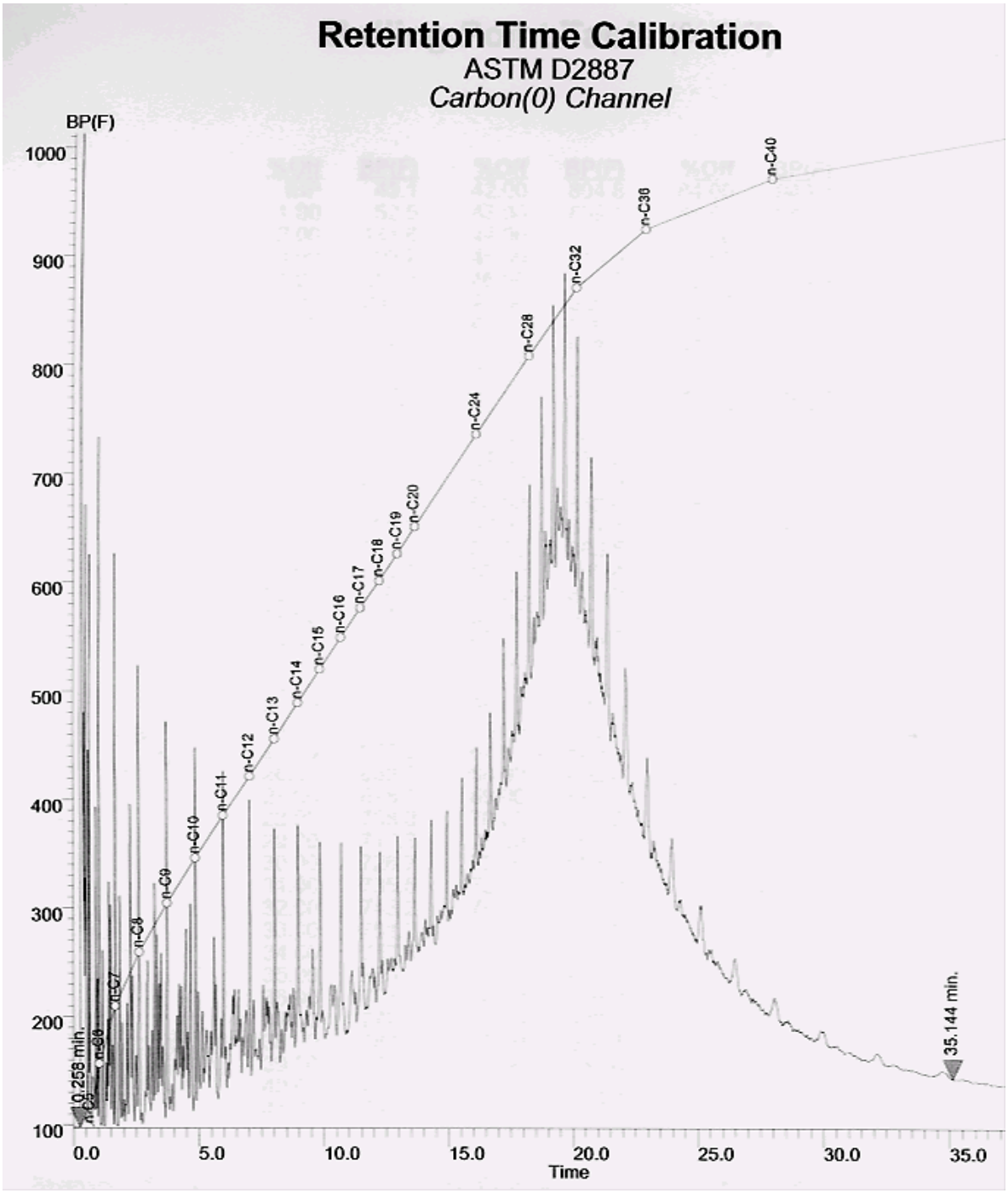

FIGURE 4-18 Simulated distillation curve for NiMo-MCM-41 catalyst product

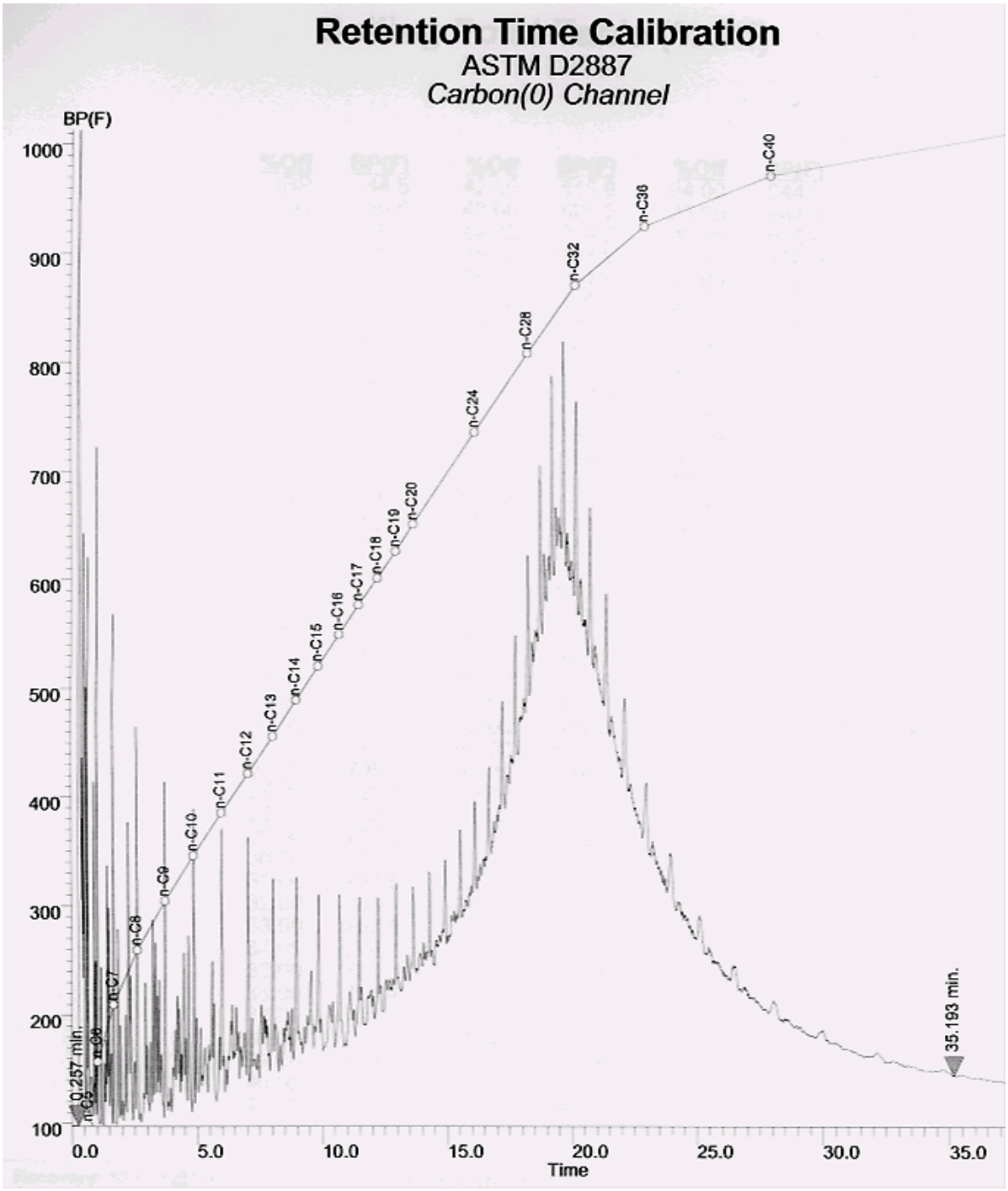

FIGURE 4-19 Simulated distillation curve for NiMo-β catalyst product

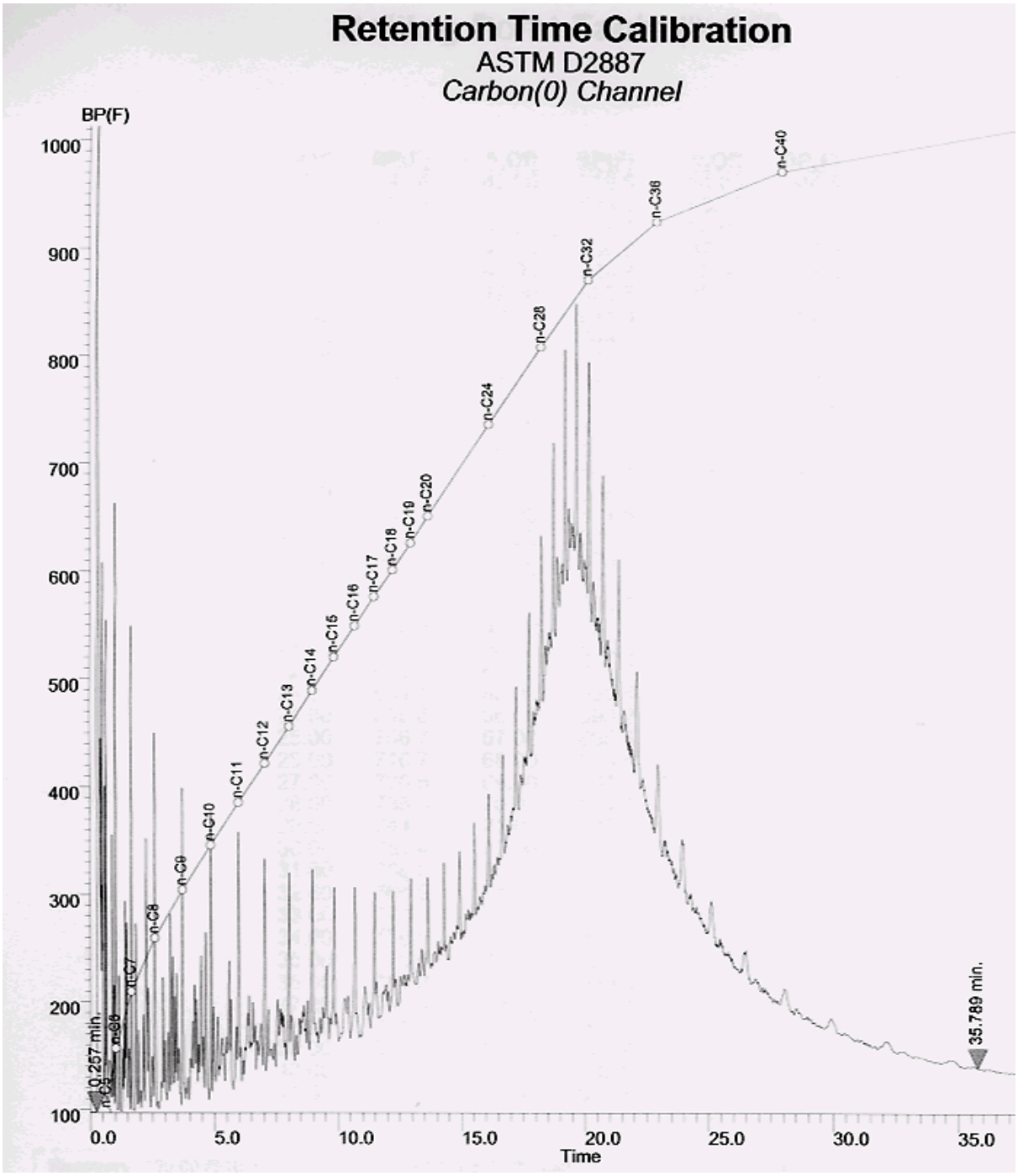

FIGURE 4-20 Simulated distillation curve for NiMo-ASA catalyst product

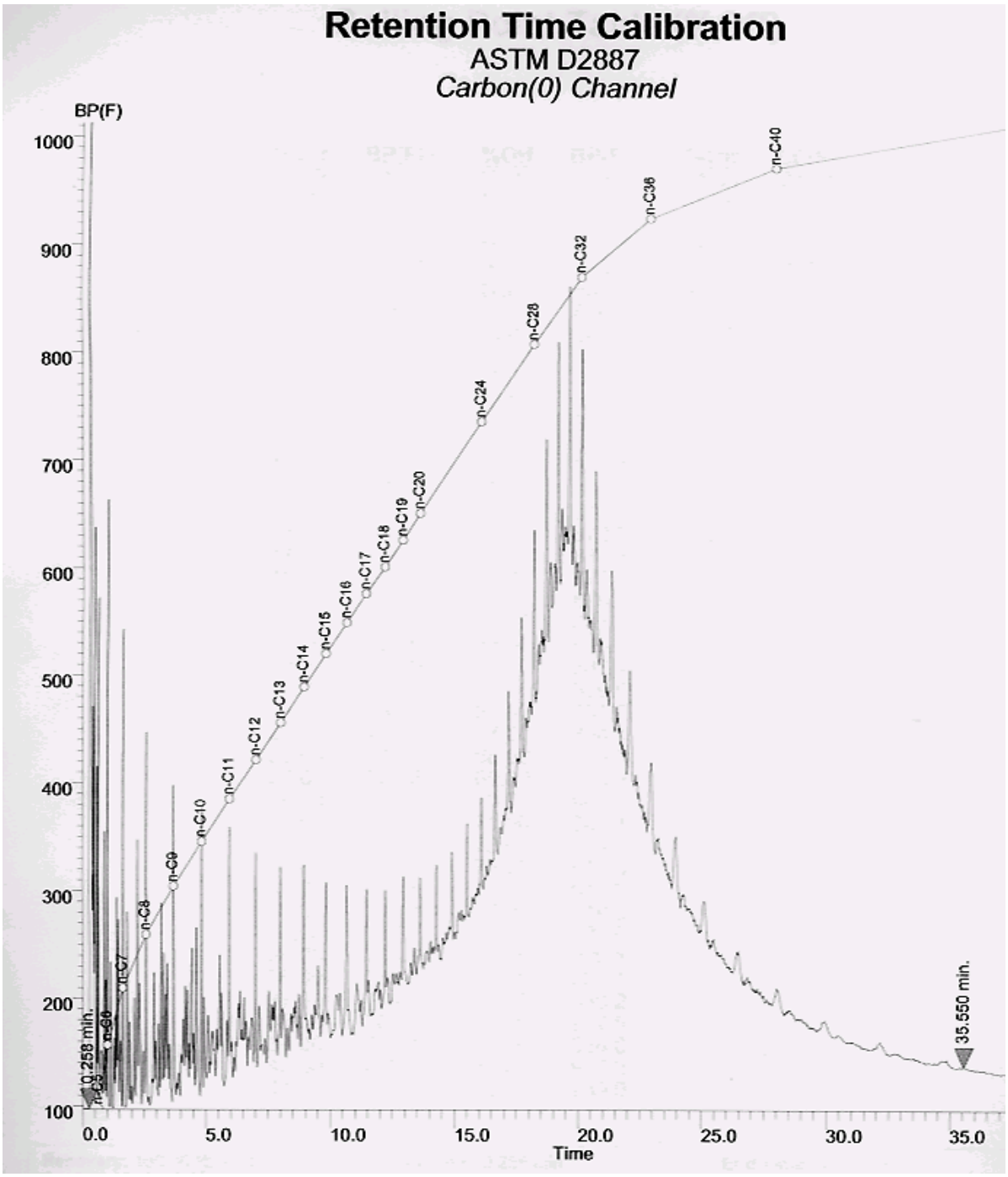

FIGURE 4-21 Simulated distillation curve for NiMo-USY catalyst product

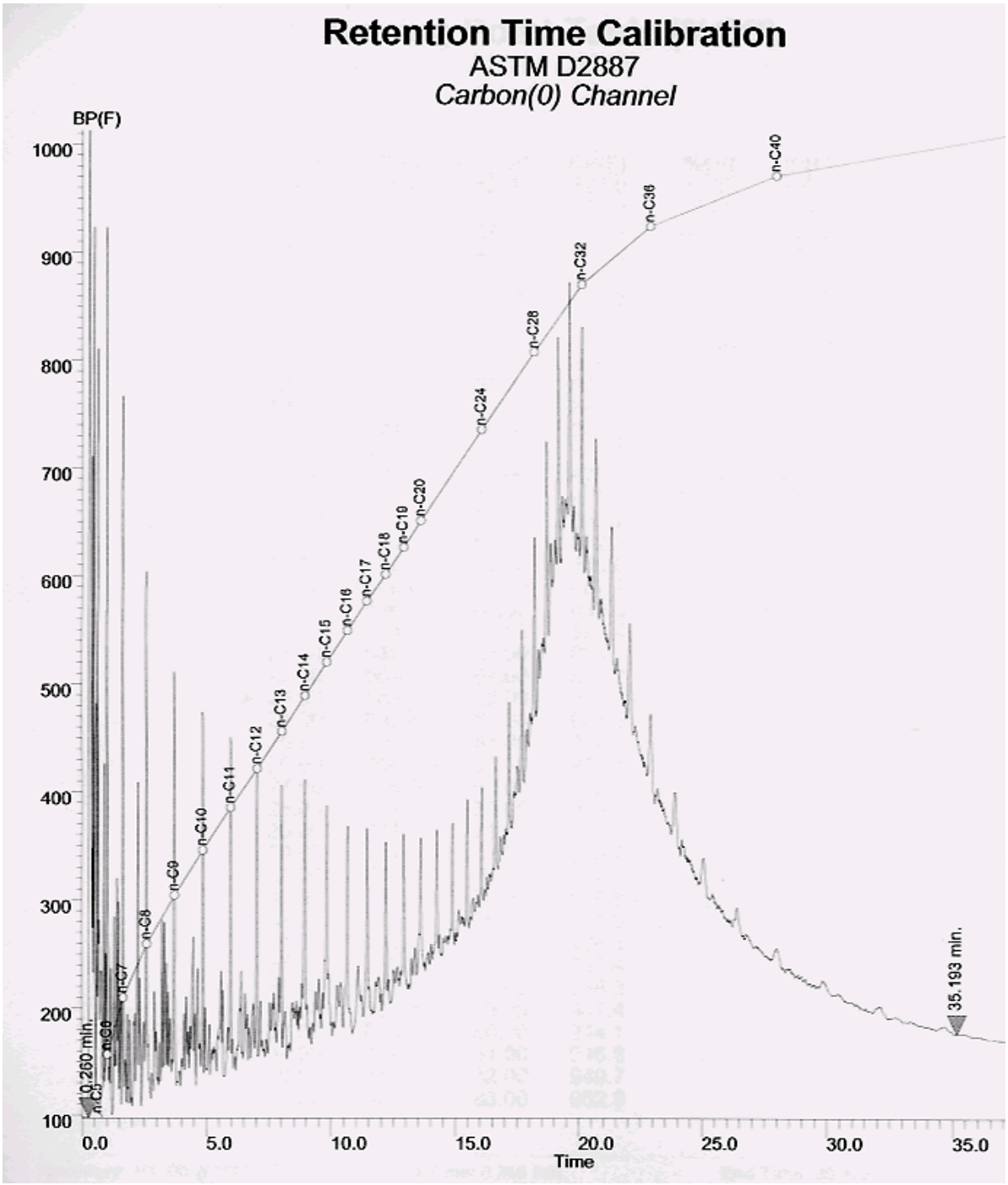

FIGURE 4-22 Simulated distillation curve for the blank run product

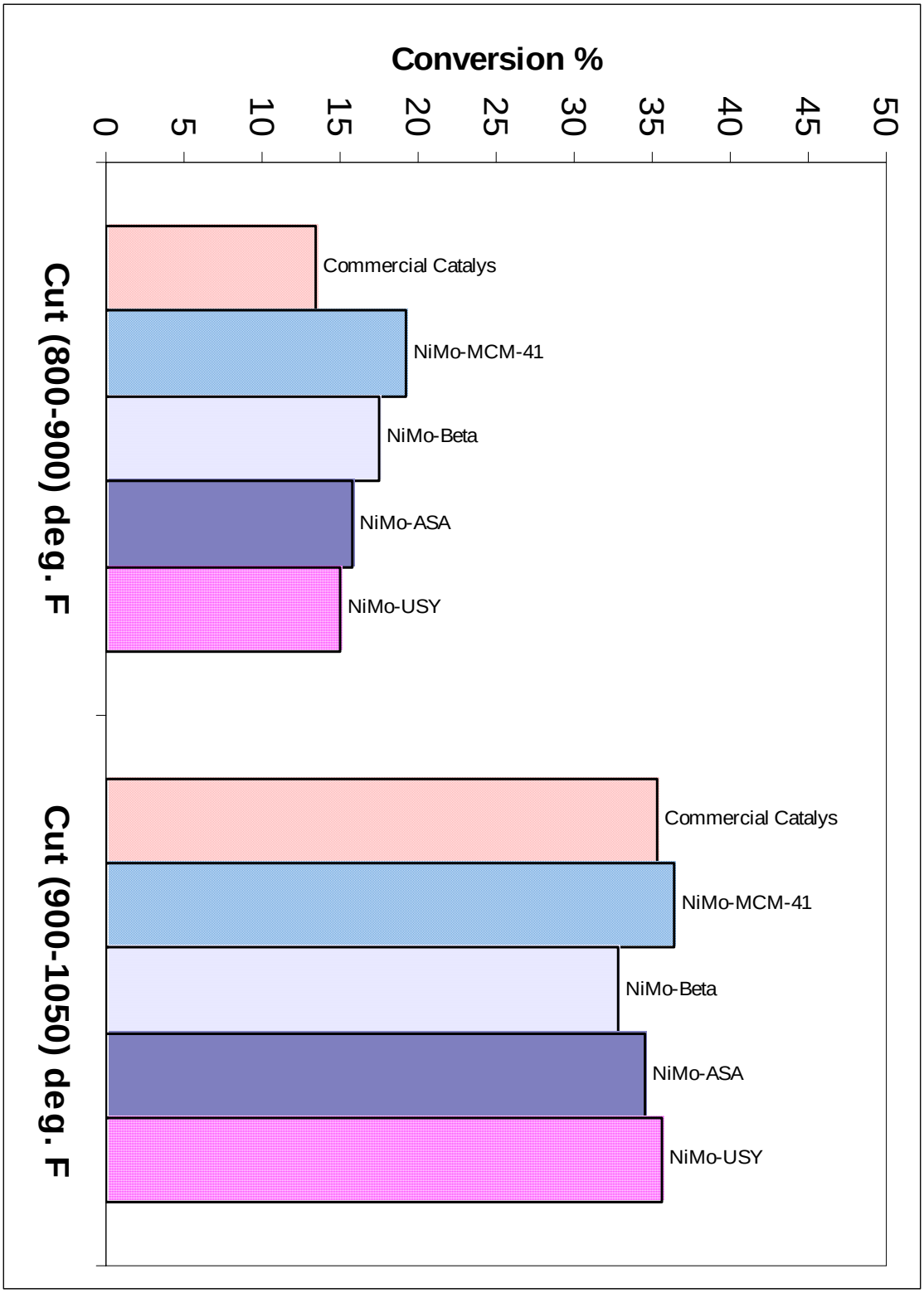

FIGURE 4-23 Tested catalysts conversion for 800 - 900 ^{0}F cut and 900 - 1050 ^{0}F cut

Figure 4-23 and table 4-7 show that NiMo-MCM-41 was able to convert hydrocarbons contained in the 800 ^{0}F – 900 ^{0}F cut better than the commercial and the other prepared catalysts. However, in the heavier cut (900 ^{0}F – 1050 ^{0}F) all tested catalysts had relatively similar conversion. It is imperative to mention that the heavier cut was easier to crack and convert than the lighter cut. That is evident from the fact that even thermal cracking achieved good conversion as the catalytic cracking in the case of heavier cut. However, in the case of lighter cut (800 0F – 900 0F), thermal cracking did not achieve comparable conversion. Thus, this is one of the advantages of NiMo-MCM-41 being able to accommodate both cuts and achieve very good conversion in both of them unlike other tested catalysts.

TABLE 4-7 Tested catalysts conversion for 800 - 900 ^{0}F cut and 900 - 1050 ^{0}F cut

	[1]Conversion %				
Cut Range, ^{0}F	Commercial	NiMo-MCM-41	NiMo-β	NiMo-ASA	NiMo-USY
800 - 900	13.37	19.23	17.57	15.78	15.04
900 - 1050	35.29	36.33	32.74	34.56	35.69
Overall	27.01	29.97	27.01	27.47	27.89

As shown in table 4-7, NiMo-MCM-41 had the highest overall conversion compared with the commercial and other prepared catalysts. This can be attributed to the fact that NiMo-MCM-41 catalyst had more surface area (324 m^2/g) and total pore volume (0.4 cm^3/g) than the other catalysts. On the contrary, NiMo-USY (S.A. 300 m2/g) and NiMo-β (S.A. 313 m2/g) catalysts had lower conversion than NiMo-MCM-41 even though they have relatively similar surface areas to NiMo-MCM-41 catalyst. That is because they have micro-pores that are very small (7.3 A^0) to accommodate large molecules present in the

[1] *Conversion = (700$^+$ in feed – 700$^+$ in product) / 700$^+$ in feed * 100*

feed. Therefore, it is very much possible that some of these micro-pores were moth-plugged by the large molecules causing them to be inactive. Moreover, their higher acidity generated more gases than Naphtha and Diesel which in turn reduced their conversion a little.

4.5.5.4 Catalyst Hydrodesulfurization (HDS) Activity

Sulfur is the most abundant heteroatom in crude oils. Sulfur exits in the form of thiols (mercaptants), sulfides, disulfides, thiophene and thiophene derivatives. The process of removing sulfur is called hydrodesulfurization. Reference to our prepared catalysts in this research, hydrodesulfurization is carried out over sulfides of molybdenum and promoted with nickel. Hydrodesulfurization represents a number of different reactions, which are discussed in previous sections.

Figure 4-24 shows the inter-relation between the content of sulfur in the products and the HDS activity of the prepared catalysts as compared with the commercial catalyst. It is obvious that all of the prepared catalysts offered much better HDS activity than the commercial catalyst. Table 4-8 shows that the HDS activity of the prepared catalysts ranges between 72 % ~ 80 % as compared to 56 % HDS activity obtained by the commercial catalyst. In addition, it is apparent that the blank run did not achieve any sulfur reduction which is expected since no catalyst was there to enhance the HDS reactions. This finding is very important since low sulfur products are always the target of refiners.

TABLE 4-8 Sulfur content of the products and catalyst HDS activity

Catalyst	Feed	Commercial	NiMo-MCM-41	NiMo-β	NiMo-ASA	NiMo-USY	Blank Run
Sulfur wt%.	2.5	1.107	0.564	0.508	0.589	0.695	2.5
[2]HDS	-	56	77	80	76	72	0

[2] *HDS% =(Sulfur in feed – Sulfur in product) / Sulfur in feed * 100*

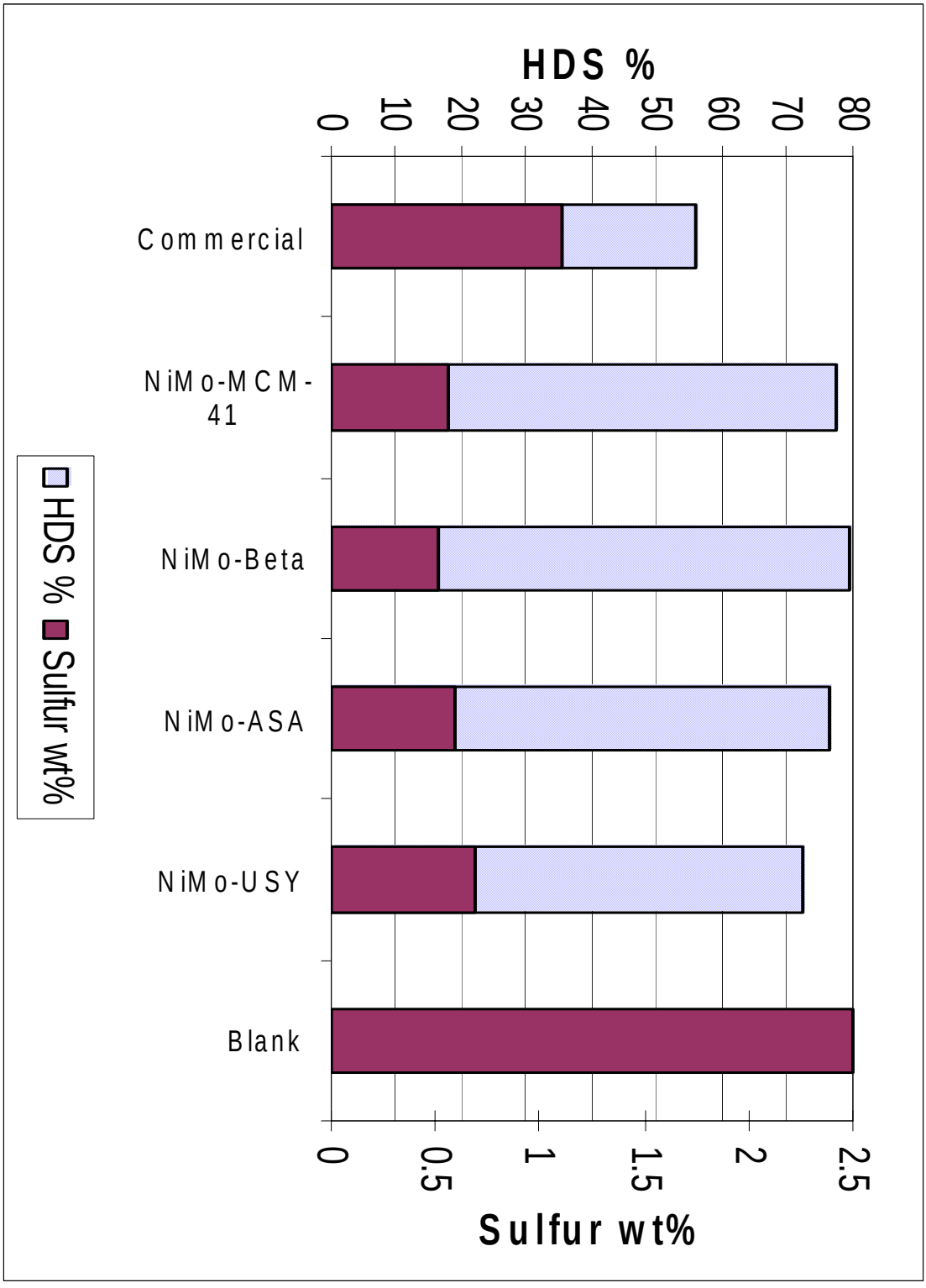

FIGURE 4-24 Content of sulfur in the products and the HDS activity of the tested catalysts

The sulfur content of petroleum fractions must be reduced for a variety of reasons:

a. The maximum acceptable sulfur content in the feed to a catalytic reformer is determined by the nature of the catalyst. Bimetallic reforming catalysts are especially sensitive, and the sulfur content must be limited to the vicinity of 1 ppm or less.
b. Air pollution control standards require removal of, in most cases 80 percent or more of the sulfur otherwise present in various oils.
c. Much of the sulfur in a gas oil fed to a catalytic cracker may be deposited in the form of coke, the sulfur content of which is converted to sulfur dioxide in the regenerator and emitted to the atmosphere from the combustion chamber. To limit air pollution from this source, the sulfur content of the gas oil may be reduced before being fed to the catalytic cracking unit.
d. The organosulfur content of the feed to a Hydrocracker must be reduced to avoid poisoning of the hydrocracking catalyst.
e. Reduction of sulfur content reduces corrosion during refining and handling and improves the odor of the products.

4.5.5.5 Catalyst Hydrogenation Activity

A great variety of hydrogenation reactions are carried out industrially. These range from large scale, continuous catalytic operations in petroleum refineries dealing with streams of complex compositions to small scale batch operations. The most common catalyst is Nickel promoted catalyst. Nickel readily absorbs hydrogen into the interstices between metal atoms which facilitates hydrogenation reactions.

It is clear from figure 4-25 that NiMo-MCM-41, NiMo-β, and NiMo-USY catalysts, which are nickel promoted, had higher hydrogenation activity as compared to the commercial

catalyst. However, NiMo-ASA, which has the lowest surface area, had lower hydrogenation activity than the commercial catalyst. This indicates that the prepared zeolitic catalysts along with NiMo-MCM-41 have better metals dispersion than the amorphous catalysts (Commercial and NiMo-ASA) which resulted in better hydrogenation activity. On the other hand, NiMo-MCM-41 catalyst showed the best hydrogenation activity which is almost double the activity of the commercial catalyst catalysts. It seem that NiMo-MCM-41 have very good tendency to utilize hydrogen in saturating the unsaturated hydrocarbons resulted from cracking reactions. On the other hand, no hydrogenation took place in the case of blank run.

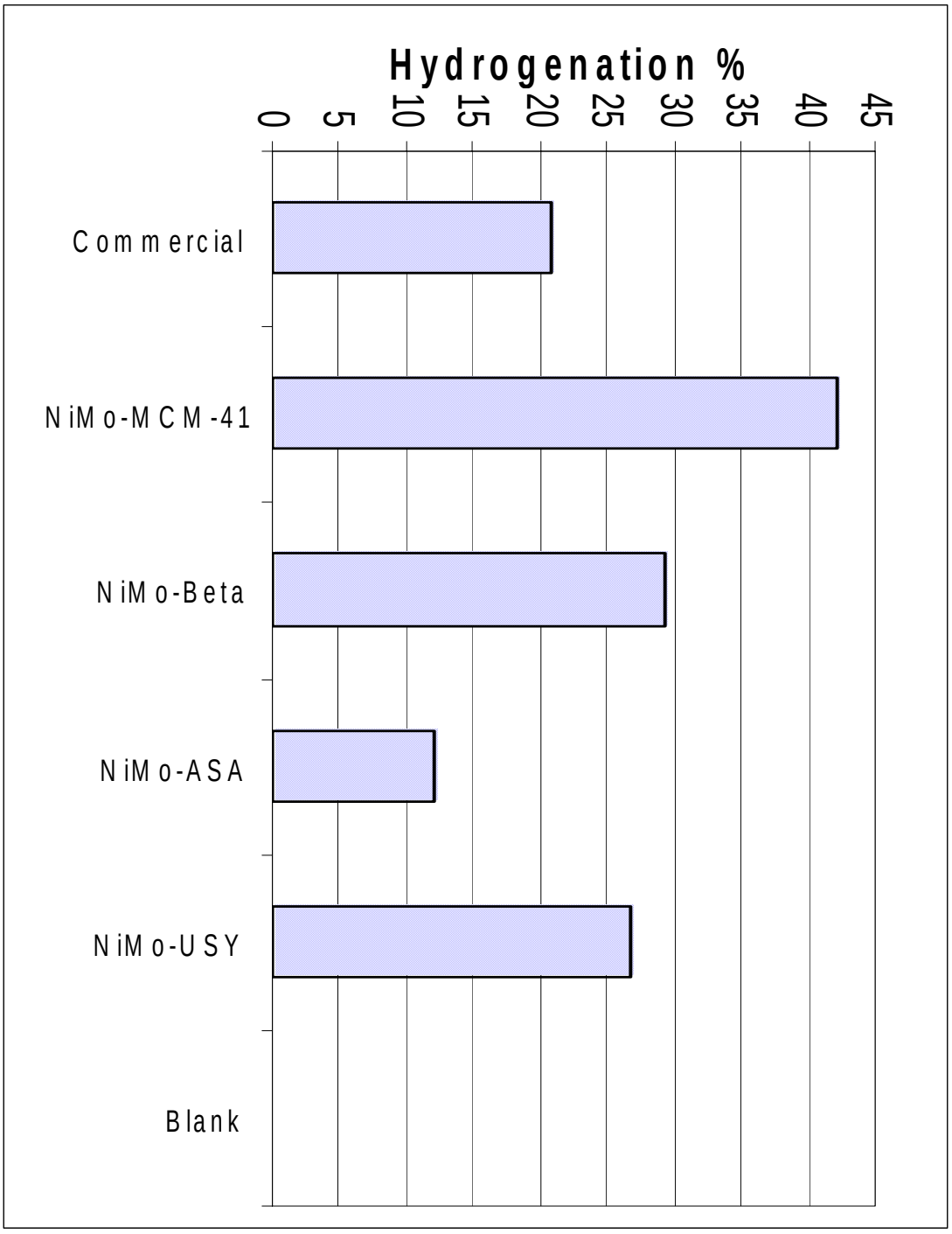

FIGURE 4-25 Hydrogenation activity

4.5.5.6 Carbon Formation Tendency

Carbon formation deposits (coke) can be formed on catalysts under a wide variety of conditions in a reducing environment. The factors involved on nonmetallic substances such as acid catalysts are substantially different from those with metals. On nonmetallic catalysts the deposits may contain considerable hydrogen, represented by an empirical formula CH_x in which *x* may vary between 0.5 and 1. Carbon deposits on metallic catalysts generally contain little or no hydrogen.

Since all of the tested catalysts contain metals, elemental analysis was utilized to measure the extent of carbon (element) deposits on the catalysts at the end of each individual experiment. It is evident from figure 4-26 that zeolitic catalysts, represented by NiMo-MCM-41, NiMo-β, and NiMo-USY, produced more carbon deposits than the amorphous catalysts (Commercial and NiMo-ASA). This is due to the fact that zeolitic catalysts are acidic and have more surface area for reactants to over-crack. This in turn results in more carbon deposits formation specially, when the cracked reactants are not immediately hydrogenated on a metal site. Coke formation have a direct effect on the catalyst stability however, this can not be measured by the means of batch reactor. It can rather be measured by a flow reactor which can be run for longer period of time to roughly quantify the catalyst run length.

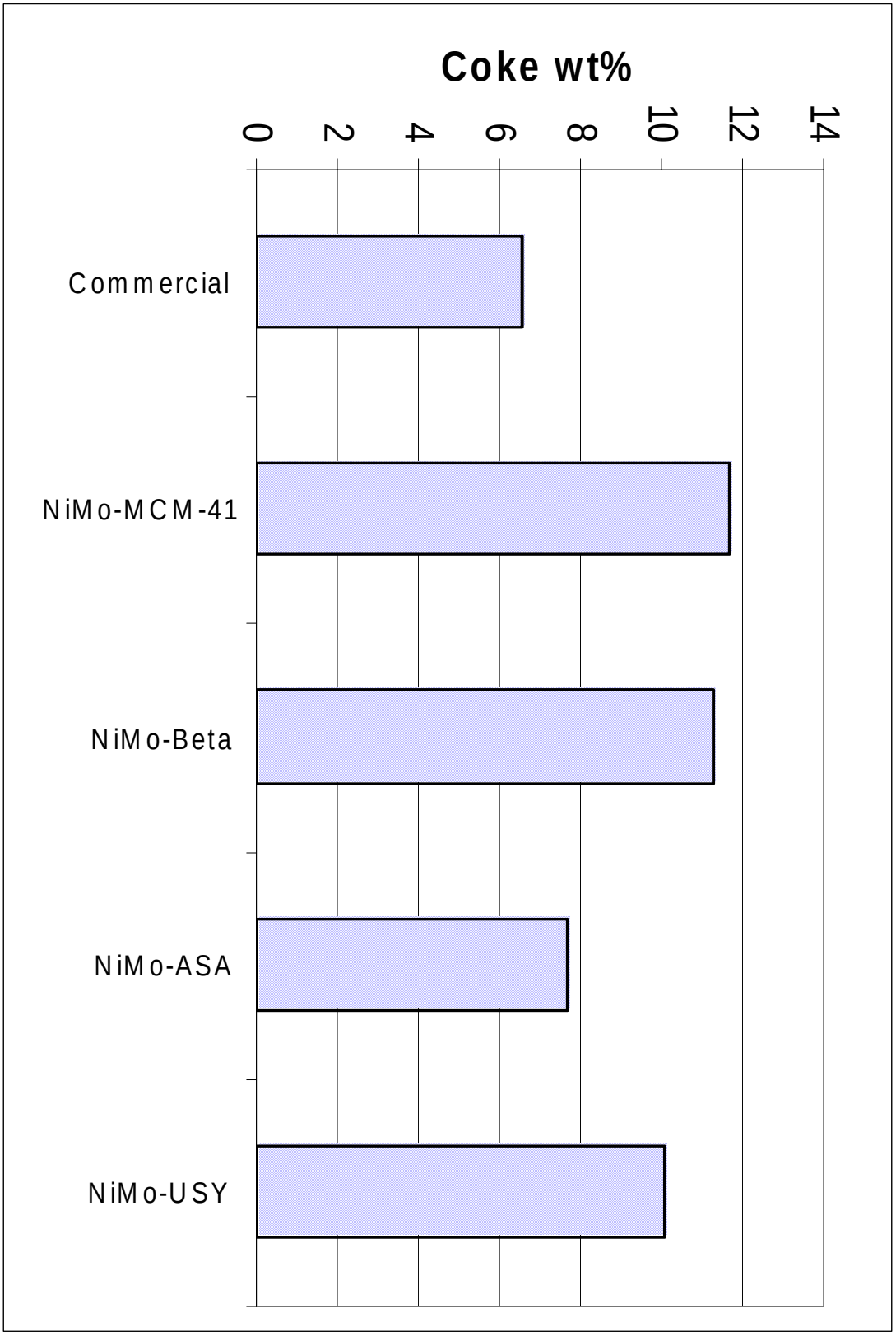

FIGURE 4-26 Coke deposits on tested catalysts

5

Conclusions and Recommendations

5.1 Conclusions

1. All prepared catalysts showed better hydrodesulfurization activity than the commercial catalyst. All prepared catalysts were impregnated with Nickel and Molybdenum which were very effective in reducing the sulfur in the product. Khorasheh et. al. [21] had similar conclusion where NiMo catalyst was very active material for most performance indices.
2. NiMo-MCM-41 achieved the highest hydrogenation activity amongst all tested catalysts. It had almost double the hydrogenation activity of the commercial catalyst. In contrast, NiMo-ASA had the lowest hydrogenation activity.
3. The prepared catalysts had relatively similar activity to the commercial catalyst. However, NiMo-MCM-41 catalyst was the most active by achieving 30% overall conversion as compared to 27% achieved by the commercial catalyst.
4. NiMo-MCM-41 catalyst was able to convert hydrocarbons contained in the 800 ^{0}F – 900 ^{0}F cut better than the commercial catalyst and the other prepared catalysts. However, in the heavier cut (900 ^{0}F – 1050 ^{0}F), all tested catalysts had relatively similar conversion. This indicates that NiMo-MCM-41 catalyst is able to accommodate both cuts and achieve very good conversion in both of them unlike other tested catalysts.
5. All tested catalysts were diesel selective catalyst with slight variations. The tested catalysts produced similar naphtha yield. However, in the case of diesel,

the prepared catalysts produced more diesel than the commercial catalyst specially NiMo-MCM-41 which yielded 21% diesel as compared to 17% diesel yield produced by commercial catalyst.

6. The commercial catalyst produced the least amount of gases as compared to the other prepared catalysts. The second least gases were produced by NiMo-MCM-41 mesoporous catalyst. On the other hand, NiMo-USY, NiMo-β, and NiMo-ASA catalysts have produced much more gases than both the commercial and NiMo-MCM-41 catalysts because they are more acidic.

7. The higher acidity of NiMo-USY, NiMo-β, and NiMo-ASA catalysts resulted into over-cracking at the acidic sites and more gas make. As a result, peaks of olefinic gases (e.g. C2=) were detected. However, NiMo-MCM-41 and the commercial catalysts had very minute amount of olefinic gases.

8. NiMo-USY, NiMo-β, and NiMo-MCM-41 catalysts had higher surface area and pore volume than NiMo-ASA amorphous catalyst.

9. NiMo-ASA catalyst had higher average pore diameter than the other prepared catalysts. This is expected since it contains wide distribution of pores as compared to the zeolitic catalysts which mainly contain meso-pores.

10. NiMo-USY, NiMo-β, and NiMo-MCM-41 catalysts showed double TPR peaks while NiMo-ASA showed triple peak behavior. This is attributed to metals being distributed into wide range of micro, meso, and macro-pores and it shows random distribution across amorphous support as compared to the zeolitic supports.

11. Using TPD method, NiMo-MCM-41 had the lowest acidity as compared to other prepared catalysts. This is attributed to the fact that MCM-41 is a silica based material and has low amount of alumina. This is one of the advantages of MCM-41 being mesoporous and having low acidity as compared to β and USY zeolites. The mesoporous feature along with the lower acidity was the main reasons for NiMo-MCM-41 catalyst to achieve the highest conversion and the lowest gas make as compared with the other prepared catalysts.
12. In batch reactor evaluation, the importance of mixing was observed. The run with mixing achieved better HDS and hydrogenation activities than the run without mixing.

5.2 Recommendations

1. All prepared catalysts, specially, NiMo-MCM-41 should be further studied using flow reactor with the same feed blend of VGO/DMO. This will measure the catalyst stability.
2. Different metals loading of Ni and Mo should be tried to further enhance the HDS and hydrogenation functions of the catalysts.
3. Different metals combinations (e.g. NiW, CoMo, etc.) should be impregnated into the catalysts supports to enhance the HDS and hydrogenation activities.
4. The γ-alumina and zeolite ratio should be varied until higher surface area is achieved and optimum acidity is obtained.
5. More sophisticated gas sorption method should be utilized to determine the distribution of micro-pores in the catalyst.

APPENDIX A

RECIPE FOR MCM-41 MATERIAL SYNTHESIS

Components:

Silica sources: Ludox (40 wt% silica, **[Alfa]**)

Aluminum sources: Aluminum sulfate **[Alfa]**

Metal source: e.g. Nickel nitrate **[Fisher Scientific Company]**

Metal source: e.g. Hexa-Ammonium Heptamolybdate **[Mallim Ckrodt]**

Organic Template: 25 wt% aqueous solution of cetyl tri methyl ammonium bromide (CTABr, **[Aldrich]**)

Solution A:

1. Take 12.5 gm of CTABr and dissolve it in 38 gm of deionized water.
2. Keep on stirring in PP bottle applying gentle heat. In case it gets thick then add solution of NaOH so as to make gel.

Solution B:

1. Take 1 gm NaOH and dissolved it in 13.5 gm water.
2. Add 1.55 gm $NaAlO_2$ to the solution and stir it for long time till it gets dissolved.

Solution C:

1. Dissolve 3.83 gm NaOH in 100gm water.
2. Add 33.5gm ludox HS-40 and heat for ½ hour with continuous stirring till clear solution is obtained.

PROCEDURE:

1. Add solution A and solution B at room temperature.
2. Cool C to RT & Mix C to solution obtained from step 1 and stir it ½ hour.
3. Adjust pH with 30% acetic acid to 10.5.
4. Allow to cool the solution for 1 hour and again adjust pH to 10.5.
5. After every 24 hour pH was adjusted to 10.5 and allowed to react for 4 days at 373 K in reactor bottle.
6. After 4 days, product was filtered and washed with ethanol and dried overnight at 323^{o}C.

APPENDIX B

RECIPE FOR CATALYST PREPARATION

B.1 NIMO-USY CATALYST

MATERIALS:

1. USY Zeolite = 6 grams.
2. AP1 Cataloid (71% γ-alumina) = 19.72 gram (14 gram γ-alumina).
3. Ammonium Heptamolybdate (AHM) = 1.425 gram.
4. Nickel Nitrate (NiNo3) = 0.973 gram.

PROCEDURE:

Support Preparation:

1. Physically and thoroughly mix USY zeolite with AP1 Cataloid for 30 minutes.
2. Slowly add diluted water until a dough is formed.
3. Put the dough in a non-adhesive bag and roll it.
4. Load the rolled dough into the extruder to make extrudate.
5. Dry the extrudate support for 1 hr @ 60 ^{0}C.
6. When the support is dry, crush it into smaller sizes and keep it overnight @ 110 ^{0}C.
7. Take the support from the oven and calcine it.

Support Impregnation:

1. Check the incipient volume of the support by adding diluted water to 0.5 gram of the support until it is absorbed. The resulted incipient volume for USY support was 0.725 ml / g support.
2. Use 8.55 gram of support. Based on the incipient volume measured, the required impregnation solution for the USY support was 6.2 ml.
3. Dissolve AHM first with diluted water and continuously stir and heat until the solution is clear. Then add nickel nitrate powder and continue stirring and stop heating to avoid precipitation.
4. After few minutes of stirring, pour the solution thoroughly onto the catalyst support (extrudate) and keep mixing in a pan until all the solution is absorbed.
5. Cover the pan and wait for 30minutes for soaking.
6. Put the pan in the oven overnight @ 60 ^{0}C to dry.
7. Calcine the impregnated catalyst into the calciner.

B.2 NIMO-MCM-41 CATALYST

MATERIALS:

1. MCM-41 = 6 grams.
2. AP1 Cataloid (71% γ-alumina) = 19.72 gram (14 gram γ-alumina).
3. Ammonium Heptamolybdate (AHM) = 1.425 gram.
4. Nickel Nitrate (NiNo3) = 0.973 gram.

PROCEDURE:

Support Preparation:

1. Physically and thoroughly mix MCM-41 zeolite with AP1 Cataloid for 30 minutes.
2. Slowly add diluted water until a dough is formed.
3. Put the dough in a non-adhesive bag and roll it.
4. Load the rolled dough into the extruder to make extrudate.
5. Dry the extrudate support for 1 hr @ 60 ^{0}C.
6. When the support is dry, crush it into smaller sizes and keep it overnight @ 110 ^{0}C.
7. Take the support from the oven and calcine it.

Support Impregnation:

1. Check the incipient volume of the support by adding diluted water to 0.5 gram of the support until it is absorbed. The resulted incipient volume for MCM-41 support was 0.82 ml / g support.
2. Use 8.55 gram of support. Based on the incipient volume measured, the required impregnation solution for the MCM-41 support was 7.01 ml.

3. Dissolve AHM first with diluted water and continuously stir and heat until the solution is clear. Then add nickel nitrate powder and continue stirring and stop heating to avoid precipitation.
4. After few minutes of stirring, pour the solution thoroughly onto the catalyst support (extrudate) and keep mixing in a pan until all the solution is absorbed.
5. Cover the pan and wait for 30minutes for soaking.
6. Put the pan in the oven overnight @ 60 ^{0}C to dry.
7. Calcine the impregnated catalyst into the calciner.

B.3 NIMO-β CATALYST

MATERIALS:

1. β Zeolite = 6 grams.
2. AP1 Cataloid (71% γ-alumina) = 19.72 gram (14 gram γ-alumina).
3. Ammonium Heptamolybdate (AHM) = 1.425 gram.
4. Nickel Nitrate (NiNo3) = 0.973 gram.

PROCEDURE:

Support Preparation:

1. Physically and thoroughly mix β zeolite with AP1 Cataloid for 30 minutes.
2. Slowly add diluted water until a dough is formed.
3. Put the dough in a non-adhesive bag and roll it.
4. Load the rolled dough into the extruder to make extrudate.
5. Dry the extrudate support for 1 hr @ 60 ^{0}C.
6. When the support is dry, crush it into smaller sizes and keep it overnight @ 110 ^{0}C.
7. Take the support from the oven and calcine it.

Support Impregnation:

1. Check the incipient volume of the support by adding diluted water to 0.5 gram of the support until it is absorbed. The resulted incipient volume for β support was 0.73 ml / g support.
2. Use 8.55 gram of support. Based on the incipient volume measured, the required impregnation solution for the β support was 6.5 ml.

3. Dissolve AHM first with diluted water and continuously stir and heat until the solution is clear. Then add nickel nitrate powder and continue stirring and stop heating to avoid precipitation.
4. After few minutes of stirring, pour the solution thoroughly onto the catalyst support (extrudate) and keep mixing in a pan until all the solution is absorbed.
5. Cover the pan and wait for 30minutes for soaking.
6. Put the pan in the oven overnight @ 60 ^{0}C to dry.
7. Calcine the impregnated catalyst into the calciner.

B.4 NIMO-ASA CATALYST

MATERIALS:

1. Silica Alumina (ASA) = 6 grams.
2. AP1 Cataloid (71% γ-alumina) = 19.72 gram (14 gram γ-alumina).
3. Ammonium Heptamolybdate (AHM) = 1.425 gram.
4. Nickel Nitrate (NiNo3) = 0.973 gram.

PROCEDURE:

Support Preparation:

1. Physically and thoroughly mix ASA zeolite with AP1 Cataloid for 30 minutes.
2. Slowly add diluted water until a dough is formed.
3. Put the dough in a non-adhesive bag and roll it.
4. Load the rolled dough into the extruder to make extrudate.
5. Dry the extrudate support for 1 hr @ 60 ^{0}C.
6. When the support is dry, crush it into smaller sizes and keep it overnight @ 110 ^{0}C.
7. Take the support from the oven and calcine it.

Support Impregnation:

1. Check the incipient volume of the support by adding diluted water to 0.5 gram of the support until it is absorbed. The resulted incipient volume for ASA support was 0.66 ml / g support.
2. Use 8.55 gram of support. Based on the incipient volume measured, the required impregnation solution for the ASA support was 5.64 ml.

3. Dissolve AHM first with diluted water and continuously stir and heat until the solution is clear. Then add nickel nitrate powder and continue stirring and stop heating to avoid precipitation.
4. After few minutes of stirring, pour the solution thoroughly onto the catalyst support (extrudate) and keep mixing in a pan until all the solution is absorbed.
5. Cover the pan and wait for 30minutes for soaking.
6. Put the pan in the oven overnight @ 60 ^{0}C to dry.
7. Calcine the impregnated catalyst into the calciner.

APPENDIX C

CALCINATION PROCEDURE

Program the claciner as follows:

1. Room temperature → 110 ^{0}C @ 2 ^{0}C / min.
2. 30 minutes soaking.
3. 110 ^{0}C → 250 ^{0}C @ 5 ^{0}C / min.
4. 30 minutes soaking.
5. 250 ^{0}C → 550 ^{0}C @ 10 ^{0}C / min.
6. 240 minutes soaking.
7. Take the sample and cool it into the dissicator for 15 minutes.
8. Load the sample into an air tight bottle and label it.

APPENDIX D

SAMPLE CALCULATIONS

Conversion = (700^+ in feed – 700^+ in product) / 700^+ in feed * 100

Yield = Distillate produced / Total reactant * 100

HDS% = (Sulfur in feed – Sulfur in product) / Sulfur in feed * 100

H/C = (H/1) / (C/12)

Hydrogenation%= (H/C of feed – H/C of product) / (H/C of feed) * 100

Required impregnation solution for MCM-41 support =

0.82 ml / g support * 8.55 support = 7.01 ml solution

LITERATURE CITED

1. R. A. Khan; *Metal Incorporation in MCM-41 for HDS*; M. S. Thesis, King Fahd University of Petroleum and Minerals 2001-2002.
2. H. S. Fogler, *Elements of Chemical Reaction Engineering 3rd edition*, Prentice Hall PTR 1999.
3. J. Scherzer, A. J. Gruia; *Hydrocracking Science and Technology*; 1996 by Marcel Dekker Inc.
4. S. Qader and G. R. Hill, *Ind. Eng. Chem. Proc. Des. Dev. 8(1): 98* (1969).
5. F. Y. A. El-Kady, *Ind. J. Tech. 17:*176 (1979).
6. A. S. Nasution, *Proc. 5th Int. Semin. New Dev. Engine Oils, Ind. Oils, Fuels Addit.,* 1985.
7. B. E. Stangeland, *Ind. Eng. Chem. Proc. Des. Dev. 13:*71 (1974).
8. D. Duayne Whitehurst, Takaaki Isoda, and Isao Mochida, *Advances in Catalysis*, **42**, 345-467 (1998).
9. Knudsen K.G., B. H. Cooper, and H. Topsoe, *Applied Catalysis A: General*, **189**, 205 (1999).
10. D. Chadwick, and M. Breysse, *Journal of Catalysis*, **71**, 226 (1981).
11. J. Lipsch, A. Schuit, *Journal of Catalysis,* **15**, 179 (1969).
12. F. Massoth, *Journal of Catalysis,* **36**, 164 (1975).

13. R. Voorhoeve and J. Stuiver, *Journal of Catalysis,* **23**, 243 (1971).

14. H. Topsoe, B. Ckausen, R. Candia, C. Wivel and S. Morup, *Journal of Catalysis,* **68**, 433 (1981).

15. C. Wivel, R. Candia, B. Clausen, S. Morup and H. Topsoe, *Journal of Catalysis,* **68**, 453 (1981).

16. H. Topose, B. Clausen and F. Massoth, *Hydrotreating Catalysis: Science and Technology,* Berlin (1996).

17. E. Hensen, J. Lardinois, H. de Beer, V. H. J., J. Veen and V. Santen, *J. Catal,* **187,** 95 (1999).

18. M. Nagi, H. Koyama, S. Sakamoto and S. Omi, *Stud. Surf. Science. Catal,* **127**, 195 (1999).

19. S. Ahmed, A. Hassan, K. Alam, M. A. Al-Shalabi, and T. Inui; *Preparation and Characterization of Zeolite-Based Hydrocracking catalysts*; Pakistan Journal of Applied Sciences 2002.

20. J. P. Franck, J. F. Le Page; Catalysts for the hydrocracking of heavy gas oils into middle distillates, *Institute Francais du Petrole*.

21. M. R. Gray, F. Khorasheh, and S. E. Wanke; *The role of catalyst in hydrocracking of residues from Alberta bitumens*, Department of Chemical Engineering, University of Alberta T6G 2G6.

22. A. Hassn, S. Ahmed, M. A. Ali, H. Hamid, and T. Inui; *A comparison between β-and USY zeolite-based hydrocracking catalysts*; Applied Catalysis A: General 220 (2001) 59-68.

23. M. A. Ali, T. Tatsumi, and T. Masuda; Development of heavy oil hydrocracking catalysts using amorphous sililca-alumina and zeolites as catalyst supports; Applied Catalysis A: General 233 (2002) 77-90.

24. J. Ramirez, R. Contreras, P. Castillo, T. Klimova, R. Zarate, and R. Luna; *Characterization and Catalytic activity of CoMo HDS catalysts supported on alumina-MCM-41*, Applied Catalysis A: General 197 (2000) 69-78.

25. Y. Hashimoto, T. Enomoto, K. Honna, H. Aizono, H. Ueki, N. Ohshilo, M. Yoshimoto, and H. Shimada; *Development of Zeolite-Based catalyst for resid hydrocracking*; JCCP catalysts research laboratory , KSP D12F-1237,3-2-1; Petroleum Chemistry Division Preprints 2002, 47(4), 351.

26. X. Zhao, Q. (Max) Lu, and Graeme Millar; *Advances in Mesoporous Molecular Sieve MCM-41*; Ind. Eng. Chem. Res. 1996, 35, 2075-2090.

27. M. Campanati, G. Fornasari, and V. Vaccari; *Fundamentals in preparation of heterogeneous catalysts*; Catalysis Today 77 (2003) 299-314.

28. C. N. Satterfield, *Heterogeneous catalysis in industrial practice*, Vol. 2, McGraw-Hill International Editions, 1993.

29. S. Ahmed, S. Ali, K. Alam, S. Hamid; *Characterization of Commercial Hydrocracking Catalysts By Temperature Programmed Methods: TPR/TPS/TPD*; Arabian Journal for Science and Engineering, Vol. 24, Number 1C, June 1999.

30. S. Ahmed, S. Ali, H. Hamid, and K. Honna; *Preparation, Characterization, and Catalytic Evaluation of First Stage Hydrocracking Catalyst*; Science and Technology in Catalysis 2002.

31. S. Ahmed, K. Alam, and H. Al-Suaibi; *Characterization of Hydrocracking Catalyst: Metal-Acidity Balance*; Center for refining and Petrochemicals, The Research Institute, King Fahd University of Petroleum and Minerals, 2002.

32. J. M. Thomas, W. J. Thomas; *Principles and Practice of Heterogeneous Catalysis*; Weinheim (Federal Republic of Germany) 1997.

VITA

Name	Walid A. Al-Naeem
Date & Place of Birth	July 1, 1973, Dammam
Nationality	Saudi
Religion	Islam
Marital Status	Married
Educational qualifications	Bachelor of Science in Chemical Engineering from Tulsa University, Oklahoma, USA (Aug. 1991 - May 1995). M. Sc. in Chemical Engineering from King Fahd University of Petroleum & Minerals, Dhahran, Saudi Arabia (2002-todate).